

## **UC Irvine**

### **UC Irvine Electronic Theses and Dissertations**

#### **Title**

Microglial Contributions to Alzheimer's Disease Pathogenesis

#### **Permalink**

<https://escholarship.org/uc/item/8mj2145s>

#### **Author**

Dominguez, Elizabeth

#### **Publication Date**

2019

Peer reviewed|Thesis/dissertation

UNIVERSITY OF CALIFORNIA,  
IRVINE

Microglial Contributions to Alzheimer's Disease Pathogenesis

DISSERTATION

submitted in partial satisfaction of the requirements  
for the degree of

DOCTOR OF PHILOSOPHY

in Biological Sciences

by

Elizabeth Erin Dominguez

Dissertation Committee:  
Associate Professor Kim Green, Chair  
Associate Professor Mathew Blurton-Jones  
Professor Andrea Tenner

2019

Figure 1 from Introduction reused from The Journal of Clinical Investigation, 127 (9), Sarlus, H and Heneka, M.T, *Microglia in Alzheimer's disease*, Page 3241, © 2017 American Society for Clinical Investigation.

Figure 3 from Introduction reused from Neuron, 82 (2), Elmore *et al.*, *Colony-stimulating factor 1 receptor signaling is necessary for microglia viability, unmasking a microglia progenitor cell in the adult brain*, Page 384, © 2014 Elsevier.

Figure 4 from Introduction reused from Brain, 139 (4), Spangenberg *et al.*, *Eliminating microglia in Alzheimer's mice prevents neuronal loss without modulating amyloid- $\beta$  pathology*, Page 1269, © 2016 Oxford University Press.

Chapter 1 reused from Brain, 139 (4), Spangenberg *et al.*, *Eliminating microglia in Alzheimer's mice prevents neuronal loss without modulating amyloid- $\beta$  pathology*, Page 1269, © 2016 Oxford University Press.

All other materials © 2019 Elizabeth Erin Dominguez

## **DEDICATION**

I dedicate this dissertation to my friends and family who have offered unwavering support and encouragement during the past five years of my doctoral journey.

# TABLE OF CONTENTS

	Page
LIST OF FIGURES	iv
LIST OF ABBREVIATIONS	vi
ACKNOWLEDGMENTS	viii
CURRICULUM VITAE	ix
ABSTRACT OF THE DISSERTATION	xi
INTRODUCTION	1
A. Alzheimer's disease pathophysiology	1
B. Microglial roles under homeostatic conditions	2
C. Microglial dysfunction in Alzheimer's disease	6
D. Microglial elimination via administration of CSF1R inhibitors	16
CHAPTER 1: Establishing the roles of chronically activated microglia in aged Alzheimer's disease mice	22
CHAPTER 2: Ascertaining microglial functions in Alzheimer's disease onset and progression	50
CHAPTER 3: Evaluating microglial ApoE as a contributor to plaque formation	94
DISSERTATION CONCLUDING REMARKS	102
REFERENCES	106

## LIST OF FIGURES

		Page
Figure 1	Acute versus chronic activation of microglia in AD	9
Figure 2	Chemical structure of CSF1R inhibitors PLX3397 and PLX5622	18
Figure 3	CSF1R inhibition eliminates microglia from the healthy, adult mouse brain	19
Figure 4	Treatment with the CSF1R inhibitor PLX3397 eliminated microglia in Rosa-YFP mice	20
Figure 1.1	Chronically activated microglia in 5xfAD mice are dependent on CSF1R signaling for their survival	30
Figure 1.2	Surviving IBA1 <sup>+</sup> cells are of microglial identity	32
Figure 1.3	Elimination of microglia does not modulate A $\beta$ levels or plaque load	34
Figure 1.4	Microglial elimination in young 5xfAD mice does not affect A $\beta$ pathology	35
Figure 1.5	Elimination of microglia with PLX5622	37
Figure 1.6	Modest changes in Alzheimer's disease-related genes with microglial elimination	39
Figure 1.7	Microglial elimination reduces neuroinflammatory signaling	40
Figure 1.8	Astrocyte numbers are not affected by microglial elimination	42
Figure 1.9	Microglia modulate dendritic spine number in the CA1 and prevent neuronal loss in the subiculum of 5xfAD mice	44

Figure 2.1	Plaque-distal microglia contain aggregated A $\beta$	59
Figure 2.2	Long-term elimination of microglia with PLX5622 treatment does not induce peripheral leukocyte or behavioral abnormalities	61
Figure 2.3	Long-term elimination of microglia in 5xfAD mice reduces plaque number and volume and is accompanied by cerebral amyloid angiopathy (CAA) onset	64
Figure 2.4	No detectable alterations in A $\beta$ levels or APP processing with microglia elimination in 5xfAD mice	67
Figure 2.5	Microglia facilitate plaque formation and compaction	70
Figure 2.6	Microglia deposit available A $\beta$ into dense-core plaques	73
Figure 2.7	Administration of an analogous CSF1R inhibitor, PLX3397 (75 and 600 ppm), to 5xfAD mice	75
Figure 2.8	Principal component analysis of RNA-seq data	77
Figure 2.9	Remaining plaque-forming microglia in the microdissected hippocampus exhibit a DAM expression profile	78
Figure 2.10	Microglia mediate downregulation of neuronal/plasticity genes in the hippocampus in response to AD pathology	81
Figure 2.11	Microglia seed plaques	85
Figure 3.1	ApoE immunoreactivity is absent from plaques and microglia with PLX5622 treatment	97
Figure 3.2	Microglial ApoE facilitates plaque formation	99

## LIST OF ABBREVIATIONS

6E10	Amyloid- $\beta$ 1–16
ABCA7	ATP-binding cassette transporter A7
ACE	Angiotensin-converting enzyme
AD	Alzheimer's disease
Aldh1L1	Aldehyde dehydrogenase family 1 member L1
ApoE	Apolipoprotein E
APP	Amyloid precursor protein
ASC	Apoptosis-associated speck-like protein containing a CARD
ATG7	Autophagy related 7 homolog
A $\beta$	Beta-amyloid
BACE1	beta-secretase 1
BBB	Blood brain barrier
BDNF	Brain-derived neurotrophic factor
C3	Complement 3
CCL2	C-C chemokine ligand 2
CD33	CD33 molecule
CLU	Clusterin molecule
CNS	Central nervous system
COX	Cyclooxygenase
CR3	Complement receptor 3, <i>aka</i> ITGAM, <i>aka</i> CD11b
CSF1	Colony-stimulating factor 1
CSF1R	Colony-stimulating factor 1 receptor
CX3CR1	Fractalkine receptor
CX3CR1-DTR	CX3CR1-diphtheria toxin receptor
DAM	Disease-associated microglia
DAMPs	Damage-associated molecular patterns
EPHA1	EPH Receptor A1
GFAP	Glial fibrillary protein
GWAS	Genome wide association studies
IBA1	Ionized calcium-binding adapter molecule 1
IDE	Insulin degrading enzyme
IGF-1	Insulin-like growth factor-1
IL	Interleukin
INPP5D	Inositol Polyphosphate-5-Phosphatase D
LAMP1	Lysosomal associated membrane protein 1
LDL	Low density lipoprotein
LPS	Lipopolysaccharide
LRP1	lipoprotein receptor related protein 1
MCI	Mild cognitive impairment
MHC	Major histocompatibility complex
MIP	Macrophage inflammatory proteins
MMPs	Matrix metalloproteases
NEP	Nepriylsin

NGF	Nerve growth factor
NLRP3	NACHT-, LRR-, and pyrin-domain-containing protein 3
NO	Nitrous oxide
p3GluA $\beta$	$\beta$ -amyloid [pyroglutamate-3]
PBS	Phosphate buffered saline
PEN2	Presenilin enhancer 2
PFA	Paraformaldehyde
PGE2	Prostaglandin E2
PI	Propidium iodide
PK	Pharmacokinetics
PSEN1	Presenilin 1
PSEN2	Presenilin 2
PVNS	Pigmented Villonodular Synovitus
RAGE	Receptor for advanced glycation end products
ROS	Reactive oxygen species
SEM	Standard error of the mean
SNPs	Single nucleotide polymorphisms
TGF- $\beta$	Transforming-growth factor-beta
Thio-S	Thioflavin-S.
TNF- $\alpha$	Tumor necrosis factor-alpha
TREM2	Triggering receptor expressed on myeloid cells 2
UPS	Ubiquitin proteasome system
WT	Wild-type

## **ACKNOWLEDGMENTS**

I am forever grateful for the teachings and support of my mentor, Dr. Kim N. Green. His brilliance is rivaled only by his enthusiasm.

I would like to thank my annual advisory committee members, Professor Andrea Tenner and Associate Professor Mathew Blurton-Jones for their expertise and advice over the years. Additionally, I would like to thank my advancement committee members, Professor Carl Cotman, Associate Professor Masashi Kitazawa, and Associate Professor Joshua Grill for providing helpful suggestions and critique.

Special thanks to Dr. Rachel Rice who took me under her wing, providing me with not only the fundamentals of wet laboratory techniques but the ability to critically evaluate my own and others' research.

I thank Dr. Allison Najafi and Dr. Lindsay Hohsfield for their mentorship and guidance throughout my graduate career.

I would also like to thank Miguel Arreola, Joshua Crapser, Nicole Phan, Jasmine Hsu, and Darian Perez for their technical assistance over the years.

This work was supported by NINDS R01NS083801 to KNG, NIA F31AG059367 and NIA T32AG00096 to EES, American Federation for Aging Research to KNG, Whitehall Foundation to KNG, and Alzheimer's Association to KNG. I thank Elsevier, Oxford University Press, and American Society for Clinical Investigation for permission to include copyrighted figures and text as part of my dissertation.

## CURRICULUM VITAE

### Elizabeth Erin (Spangenberg) Dominguez

- 2013 B.S. in Biological Sciences, University of California, Irvine
- 2017 M.S. in Biological Sciences, University of California, Irvine  
Dr. Kim N. Green
- 2019 Ph.D. in Biological Sciences, University of California, Irvine  
Dr. Kim N. Green

## HONORS AND AWARDS

- 2013 Excellence in Research – Dean’s Award, University of California, Irvine
- 2016 William F. Holcomb Scholarship, University of California, Irvine
- 2017 NIH Training Grant recipient in the Neurobiology of Aging, University of California, Irvine
- 2017 First place predoctoral “Elevator Pitch” competition, Convergent Science Training Grants Retreat, University of California, Irvine
- 2018 NIA National Research Service Award

## PUBLICATIONS

### Original Reports

**Spangenberg EE**, Severson PL, Hohsfield LA, Crapser JD, Zhang J, Burton EA, Zhang Y, Spevak W, Lin J, Phan NY, Habets G, Rymar A, Tsang G, Walters J, Nespi M, Singh P, Broome S, Ibrahim P, Zhang C, Bollag G, West BL, Green KN. Synthesis of a specific CSF1R inhibitor for sustained microglial depletion reveals crucial roles of microglia in plaque development and transcriptional alterations in Alzheimer’s disease. *Under review*.

Elmore MRP, Hohsfield LA, Kramar EA, Soreq L, Lee RJ, Pham ST, Najafi AR, **Spangenberg EE**, Wood MA, West BL, Green KN (2018). Replacement of microglia in the aged brain reverses cognitive, synaptic, and neuronal deficits in mice. *Aging Cell*. 17(6):e12832.

Caccamo A, Branca C, Piras IS, Ferreira E, Huentelman MJ, Liang WS, Readhead B, Dudley JT, **Spangenberg EE**, Green KN, Belfiore R, Winslow W & Oddo S (2017). Necroptosis activation in Alzheimer’s disease. *Nat Neurosci*. 20(9):1236-1246.

**Spangenberg EE**, Green KN (2016). Inflammation in Alzheimer's disease: Lessons learned from microglia-depletion models. *Brain Behav Immun.* S0889-1591(16):30197-0.

**Spangenberg EE**, Lee RJ, Najafi AR, Rice RA, Elmore MRP, Blurton-Jones M, West BL, Green KN (2015). Eliminating microglia in Alzheimer's mice prevents neuronal loss without modulating A $\beta$  pathology. *Brain.* 139(Pt 4):1265-81.

Rice RA, **Spangenberg EE**, Yamate-Morgan H, Lee RJ, Arora RP, Hernandez MX, Tenner AJ, West BL, Green KN (2015) Elimination of microglia improves functional outcomes following extensive neuronal loss in the hippocampus. *J Neurosci.* 35(27):9977-89.

Elmore, MRP\*, Najafi AR\*, Koike MA, Dagher NN, **Spangenberg EE**, Rice RA, Kitazawa M, Matusow B, Nguyen H, West BL, Green KN (2014) Colony-stimulating factor 1 receptor signaling is necessary for microglia viability, unmasking a microglial progenitor cell in the adult brain. *Neuron.* 82(2):380-397.

#### Abstracts and Posters

"Microglia facilitate parenchymal plaque formation in 5xfAD mice." **Spangenberg EE**, Severson PL, Hohsfield LA, Green KN. Alzheimer's and Parkinson's Diseases Congress 2019, Lisbon, Portugal.

"Microglial modulation of astrogliosis and A $\beta$  plaque compaction in 5xfAD mice." **Spangenberg EE**, West BL, Green KN. Alzheimer's Association International Conference 2018, London, UK.

"Microglia facilitate parenchymal plaque formation and compaction." **Spangenberg EE**, West BL, Green KN. REMIND Emerging Scientist Symposium 2017, Irvine, CA.

"Elimination of microglia prevents neuronal loss without modulating A $\beta$  pathology in a mouse model of Alzheimer's disease." **Spangenberg EE**, Lee R, West BL, Green KN. Institute for Clinical and Translational Science 2016, Irvine, CA.

#### TEACHING

2014	Bio 93: From DNA to Organisms
2015	Bio 37: Brain Dysfunction
2017	Bio 37: Brain Dysfunction

# **ABSTRACT OF THE DISSERTATION**

Microglial Contributions to Alzheimer's Disease Pathogenesis

By

Elizabeth Erin Dominguez

Doctor of Philosophy in Biological Sciences

University of California, Irvine, 2019

Associate Professor Kim Green, Chair

Microglia are the primary central nervous system (CNS) immune cell and carry out a variety of important functions in the brain, including immune defense, regulation of synaptic formation and maintenance, promotion of proper brain connectivity, calcium homeostasis, and trophic support for neurons. Increasing evidence points to a loss of microglial homeostatic functioning in disease conditions, including Alzheimer's disease (AD), leading to the hypothesis that a failure in immune-related mechanisms contributes to disease progression. Additionally, genome-wide association studies (GWAS) identify variants in myeloid-associated genes as a substantial contributor to AD risk, highlighting the significance of myeloid biology in the development of AD. Thus, intense focus has recently been placed on microglia to identify their roles in AD onset and progression. Importantly, the development of compounds and genetic models to ablate the microglial compartment have emerged as effective tools to further our understanding of microglial function in AD. Previously, we reported that administration of colony-stimulating factor 1 receptor (CSF1R) inhibitors eliminate >99% of microglia brain-wide in the healthy adult murine brain. As an extension of these findings, the goal of my dissertation is to utilize

CSF1R inhibitors in mouse models of Alzheimer's disease to ascertain the various function(s) of microglia in AD pathogenesis. As demonstrated in the first chapter of my dissertation, I administered CSF1R inhibitors to mice to ablate the microglial compartment for one month during advanced stages of pathology in 5xfAD mice, of which 12% of plaque-distal microglia survived CSF1R inhibitor treatment whereas 50% of plaque-associated microglia remained. With this paradigm, I observed improvements in contextual fear memory, normalized brain-wide inflammatory signaling, the regeneration of lost dendritic spine densities, and additionally, the absence of microglia prevented neuronal loss. These data indicate that, during the later stages of disease, primarily plaque-distal microglia mount a detrimental and non-resolving inflammatory response in the AD brain that damages synapses and neurons, ultimately impairing cognitive function, whereas plaque-associated microglia exert neuroprotective effects. Importantly, microglial ablation in advanced pathology AD mice did not modulate  $\beta$ -amyloid ( $A\beta$ ) burden in the brain, possibly due to a loss of microglial  $A\beta$  clearance capabilities during advanced stages of AD. As previously stated, myeloid biology is heavily implicated in the development of AD, via GWAS; thus, I next sought to explore the contributions of microglia in disease onset. To that end, I eliminated microglia prior to the onset of pathology, as well as throughout the course of disease in chapter two. As microglia are phagocytic cells, if the degradation of  $A\beta$  by microglia in early AD protects against  $A\beta$  accumulation and deposition, perturbing this process while microglia are functional phagocytes should dramatically elevate  $A\beta$  pathology. Contrary to expectations, I found that lifelong ablation of microglia prevented parenchymal plaque burden, except in areas where microglia survived CSF1R inhibition, indicating that

microglia are facilitate plaque formation. In chapter three of the dissertation, I expanded upon these findings and identify microglial Apolipoprotein E (ApoE) as a contributor to plaque formation in 5xfAD mice. Collectively, these results highlight a spectrum of microglial functional states, dependent on disease stage (i.e., A $\beta$  pathology onset and disease severity) and proximity to A $\beta$  plaques, and demonstrate that microglia act as critical and causative agents in the onset and development of AD pathology.

# INTRODUCTION

## A. Alzheimer's disease pathophysiology

Sporadic AD is an age-related, neurodegenerative disease characterized by the extracellular deposition of A $\beta$  plaques and intraneuronal tau neurofibrillary tangles. It is one of the most common forms of dementia, affecting roughly 10% of the population aged 65, and up to 50% of people aged 85 and over<sup>1</sup>, with the number of cases expected to triple by 2050<sup>2</sup>. Therefore, understanding the mechanistic changes in the human brain leading to pathophysiology of the disease is essential to produce effective therapies. According to the amyloid cascade hypothesis, the triggering factor for the disease is the accumulation of amyloid aggregates composed of A $\beta$  peptides<sup>3</sup>. A critical role of A $\beta$  in AD manifestation is supported by mutations in  $\beta$ -amyloid precursor protein (APP) and presenilin 1 (PSEN1) and presenilin 2 (PSEN2) that lead to increased A $\beta$  production and deposition in familial AD<sup>4</sup>. In sporadic AD, A $\beta$  may have an initiating role and is implicated in a complex network of pathological processes, including sustained chronic neuroinflammation, tau hyperphosphorylation, synapse degeneration and neuronal loss. These processes may converge over time, until neurodegeneration prevails and clinical symptoms manifest<sup>5</sup>. This progression has been divided into three stages: preclinical, mild cognitive impairment (MCI), and dementia<sup>6</sup>. Following amyloid deposition, the presence of intraneuronal neurofibrillary tangles comprised of hyperphosphorylated tau is observed, which correlates more strongly with cognitive status, and neurodegeneration, than amyloid pathology<sup>7</sup>.

Due to the general acceptance of the amyloid cascade hypothesis since its conception, the field of AD has historically been driven toward developing A $\beta$ -modulating

therapeutics. Indeed, amyloid deposits in humans present decades before the cognitive deficits associated with this disorder are evident<sup>8</sup>. However, to date, all therapies designed to modulate A $\beta$  production in the AD brain have failed in the clinic, as well as the vast majority of non-A $\beta$ -targeting therapies<sup>9</sup>. Thus, AD has one of the highest failure rates of any disease at 99.5-99.6%<sup>9</sup>. These failures were presumably due to attempts to intervene at later stages in the disease process when substantial neuronal loss has already occurred, suggesting that treatments during the prodromal or MCI stages of AD may be beneficial. However, A $\beta$ -targeting therapeutics administered during these phases have proved ineffective, as evidenced by the recent failure of Biogen's Phase III clinical trials of aducanumab, administered during the early symptomatic phase of AD (unpublished results from ADPD Conference, 2019). Thus, a reevaluation of the precise roles of various pathologies in AD is required and highlights a need for AD treatments to extend beyond the realm of A $\beta$  modulation.

## **B. Microglial roles under homeostatic conditions**

Microglia are the brain's resident immune cells, comprising approximately 10-15% of all cells found in the brain<sup>10</sup>, whereby they function as the first line of defense to protect the CNS from injury and invading pathogens. In this surveying state, microglia exhibit a ramified morphology and support the health and functioning of neurons. Upon detection of an insult, microglia respond by becoming activated, developing an amoeboid morphology, and migrating to, and proliferating at, the site of the insult. In acute inflammatory events, the pro-inflammatory response resolves and microglia continue their surveillance of the brain parenchyma and maintenance of synaptic and neural

circuitry. In the following sections, I will briefly outline the various roles of microglia in the healthy brain, highlighting specifically their roles in immune surveillance, pathogen recognition and injury response, and synaptic and circuit sculpting.

### *CNS maintenance and immune surveillance*

Disturbances in homeostasis result in an immune response mediated by microglia, distinguished by dramatic morphological, functional, and transcriptional alterations of these cells<sup>11-13</sup>. This state of microglial activation coincides with a reorganization of surface receptors to facilitate interactions between extracellular molecules and neighboring cells and release of soluble factors that act as pro- or anti-inflammatory mediators. Activated microglia produce and secrete several proinflammatory mediators, including tumor necrosis factor- $\alpha$  (TNF $\alpha$ ), interleukin (IL)-6, and nitric oxide (NO), all of which play a role in cellular debris and pathogen clearance<sup>14</sup>. Neuroimmune regulatory proteins modulate the immune response and facilitate the resolution of inflammatory processes<sup>15</sup>, which subsequently leads to the activation of neurotrophic signaling pathways that promote tissue repair, including insulin-like growth factor 1 (IGF-1), brain-derived neurotrophic factor (BDNF), transforming-growth factor- $\beta$  (TGF- $\beta$ ), and nerve growth factor (NGF)<sup>16</sup>. The resolution of the inflammatory response is essential for CNS homeostasis, with failures in normal inflammation resolution mechanisms leading to a chronic neuroinflammatory state and progression of neurodegenerative changes<sup>17</sup>.

### *Injury response and pathogen detection*

While in a quiescent state, microglia are continually active and surveying the brain environment, extending and retracting their processes without disturbing the fragile

neural circuitry<sup>18</sup>. However, following minimal alterations to brain homeostasis, microglia readily undergo activation-related processes<sup>19</sup>. This can involve phagocytic processes, whereby microglia utilize their highly developed lysosomal compartment that bears critical protease activity to remove tissue detritus or damaged cells<sup>20-24</sup>. Microglia constitutively express several families of receptors that facilitate the removal of aged, necrotic tissues, and toxic molecules from the circulation and their surroundings. Among these receptors are scavenger receptors (e.g., CD36, SR1)<sup>25,26</sup>, low-density lipoprotein (LDL) receptor family members (e.g., LDLR, ApoER2, and VLDL)<sup>25,26</sup>, and three receptor tyrosine kinases (i.e., the TAM receptors Tyro3, Axl, and Mertk)<sup>27</sup>. In addition, microglia capture and endocytose immune complexes and complement-opsonized protein complexes through Fc receptors<sup>28</sup> and complement receptors<sup>24,29</sup>, including CR1 (CD35), CR2 (CD21), CR3 (CD11b, CD18), CR4 (CD11c, CD18), and C5aR (CD88, C5L2). To regulate migration and positioning of microglia in the CNS and to enhance their phagocytic functioning, microglia also express chemokine receptors<sup>30</sup>, such as CX3CR1 and CXCR4 and integrins (e.g., CD11b and CD11c). As stated earlier, microglia return to a quiescent state to continue homeostatic maintenance functions following stimulus removal from the brain.

### *Synaptic sculpting and cognition*

In addition to clearance of cellular debris and pathogens, microglia are involved in the removal of synapses from neuronal cell bodies via synaptic stripping. This phenomenon was first observed in a model of facial nerve injury in rats<sup>31</sup>, in which microglial localization to the site of injury and interaction with facial motor neurons resulted in the

removal of synaptic contacts. In the developing brain, microglia form brief, repetitive contacts with synapses, eliminating any weak or unnecessary synaptic structures, a process which is modulated by sensory experiences<sup>22</sup>. Knockout of the microglial purinergic receptor P2Y12, which mediates process motility during injury response, also disrupts plasticity in the visual system<sup>32</sup>. While the exact mechanism behind microglia-mediated synaptic elimination (whether it be by phagocytosis or the secretion of various factors) has yet to be elucidated, it is evident that the interaction between microglia and synapses is crucial for activity-dependent plasticity in the developing brain. Accumulating evidence points to neuron-microglia crosstalk as an essential mechanism for proper synapse and network maintenance. One pathway implicated in this crosstalk involves CX3CR1 expressed on microglia and its ligand CX3CL1, released by neurons. Knockout of CX3CR1 during development produces deficits in synaptic pruning, characterized by an excess of dendritic spines and immature synapses, resulting in weakened synaptic transmission and decreased functional brain connectivity<sup>20</sup>. Behaviorally, loss of CX3CR1 manifests in impaired social interactions reminiscent of autism spectrum disorder and other neuropsychiatric disorders<sup>20</sup>. While increasing evidence points to critical roles of microglia in synaptic maintenance, investigations into the functional significance of these events were scarce. Using electrophysiological approaches, it was demonstrated that a reduction in synapses restricted the frequency of glutamatergic synaptic currents<sup>33</sup>, suggesting that microglia influence neuronal communication and function. Furthermore, disruption of signaling between complement 3 (C3), which is localized to synaptically-enriched regions, and its receptor, complement receptor 3 (CR3), impairs microglial phagocytosis of synaptic inputs, leading to

sustained deficits in brain wiring<sup>34</sup>. Collectively, these studies underscore the role of microglia as regulators of the synaptic landscape in the developing brain, implicating neuron-microglia crosstalk as a crucial process for proper brain development.

The role of microglia in synaptic sculpting during development is well-described, and we previously reported that the absence of microglia in the healthy adult mouse brain increases total dendritic spine density and intensity of immunolabeling for the synaptic surrogates PSD95 and synaptophysin<sup>35,36</sup>, indicating that microglia continue to regulate the synaptic landscape in adulthood. Collectively, these studies point to microglia as critical mediators of synaptic sculpting in the developing and adult brain, providing a vital function in shaping and modulating neuronal circuitry to maintain normal brain connectivity.

### **C. Microglial dysfunction in Alzheimer's disease**

#### *GWAS and myeloid biology in AD*

The hypothesis of compromised microglial function as a contributor to AD pathogenesis gained momentum following the publication of recent GWAS results. These studies identified several single nucleotide polymorphisms (SNPs) that convey risk of developing AD, with many of these SNPs associated with or related to microglial function including triggering receptor expressed on myeloid cells 2 (*TREM2*), CD33 molecule (*CD33*), complement receptor type 1 (*CR1*), clusterin (*CLU*), EPH Receptor A1 (*EPHA1*), ATP-binding cassette transporter A7 (*ABCA7*), *SPI1*, and inositol Polyphosphate-5-Phosphatase D (*INPP5D*)<sup>37-39</sup>, indicating that microglia play a critical role in the development of AD. The generation of knockout mice for various immune-associated GWAS genes have allowed for *in vivo* investigations into the contribution of

these genes in AD pathogenesis. Inactivation of CD33 in APP/PS1 mice reduced A $\beta$  accumulation and plaque burden<sup>40</sup>, whereas ABCA7 deficiency in APP/PS1 and TgCRND8 mice exacerbated A $\beta$  load<sup>41,42</sup>, highlighting the importance of these genes in regulating A $\beta$  pathology. Additionally, reports of TREM2 deficiency in AD mice found worsening<sup>43</sup> and mitigation<sup>44</sup> of A $\beta$  pathology. This discrepancy in plaque observations was later found to be related to disease progression, whereby TREM2 deficiency ameliorates plaque burden in early AD and exacerbates plaque pathology in later stages<sup>45</sup>. However, a common thread throughout all TREM2-knockout studies is the prevention of the association of myeloid cells – whether it be microglia or monocytes – with plaques, indicating that TREM2 signaling regulates myeloid cell responses to A $\beta$  in AD.

#### *Immune activation in plaque formation processes*

In addition to the general functions of these cells in AD, the timing of neuroinflammation in the progression of AD is also crucial to our understanding of the disease – reports indicate that inflammatory changes precede the appearance of amyloid plaques<sup>46-48</sup>. In line with observations in humans, early immune activation in AD mice can trigger disease pathogenesis. Specifically, systemic immune stimulation in prenatal mice with a viral mimetic (*i.e.*, double stranded RNA) followed by immune challenge later in adulthood, was sufficient to induce the development of sporadic-like AD, characterized by deposition of A $\beta$  and tau, impairments in working memory, as well as chronic microglial activation<sup>49</sup>. Interestingly, this study provides evidence for immune activation early in life as a sufficient factor to induce AD onset. In support of immune mechanisms

driving disease initiation, it was recently demonstrated that microglia release apoptosis-associated speck-like protein containing a CARD (ASC) specks in an age-dependent manner through the activation of the NACHT-, LRR-, and pyrin-domain-containing protein 3 (NLRP3) inflammasome in AD<sup>50</sup>. *In vivo*, ASC specks form in response to A $\beta$  and their release following microglial activation enhanced A $\beta$  seeding and spreading<sup>50</sup>, suggesting a mechanism by which physiological microglial activity contributes to plaque formation. However, PET imaging with the second generation TPSO ligand DPA-714 in early stage and prodromal AD patients showed that patients with increased ligand binding exhibited slowed cognitive decline, suggesting that microglial activation is protective in the early stages of the disease<sup>51</sup>. Collectively, these studies – in addition to the TREM2 studies discussed earlier – highlight the importance of inflammation-targeted therapeutic approaches for treating AD, but caution that the timing of intervention may be crucial.

### *Neuroinflammation in AD*

Within the CNS, immune-related responses are encompassed by the term neuroinflammation, which influences both cellular and tissue homeostasis and supports neuronal functioning<sup>52</sup>. Under normal physiological conditions/non-disease states, neuroinflammatory processes are self-limiting, resolving once the detected stimulus is cleared from the brain. This acute form of neuroinflammation is in stark contrast to the chronic form observed in AD (Fig. 1), which is hypothesized to result from a failure in immune clearance mechanisms<sup>53,54</sup>. Neuroinflammation is a complex process that

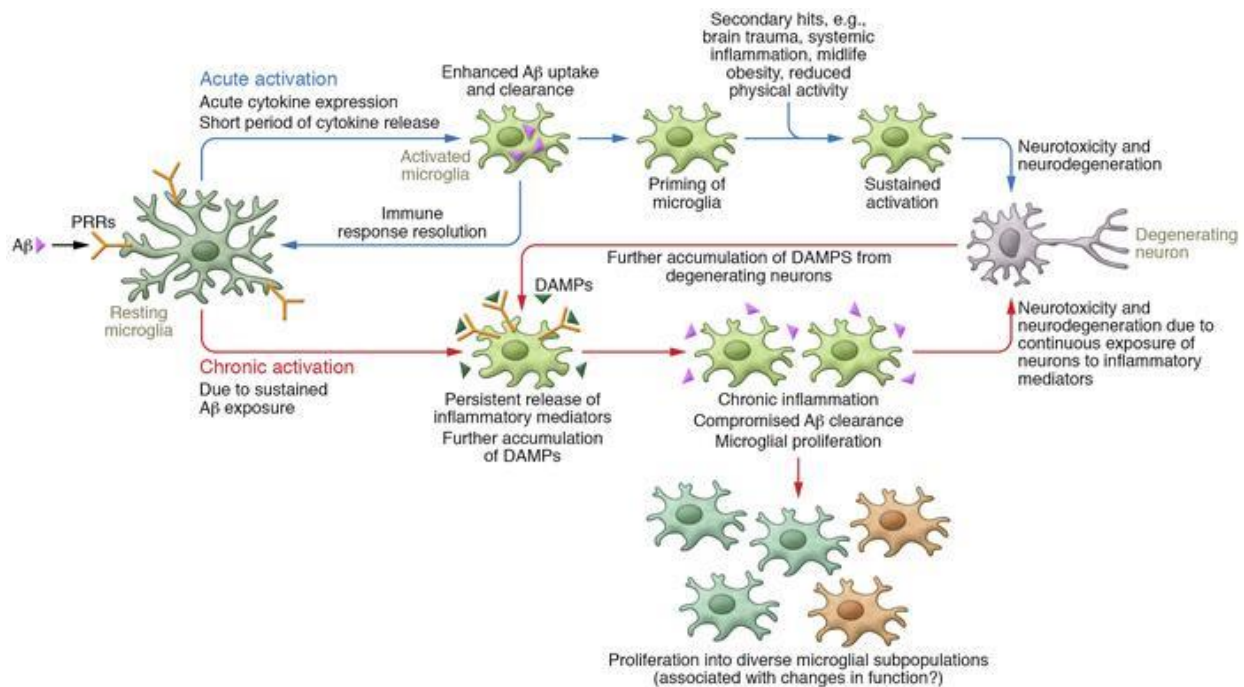


**Figure 1 Acute versus chronic activation of microglia in AD.** A $\beta$  binds to PRRs, leading to activation of resting microglia. Acutely activated microglia express cytokines, which drive enhanced phagocytosis, uptake, and clearance of A $\beta$ . Long-term activation of microglia drives proliferation as well as a chronic inflammatory state that causes neurotoxicity and neurodegeneration. Sustained activation of microglia, induced by brain trauma, systemic inflammation, obesity, and reduced physical activity, also drives neurotoxicity and neurodegeneration. DAMPs that arise from these processes further activate microglia, leading to compromised A $\beta$  phagocytosis and propagating chronic inflammation. Chronic inflammation and accumulation of A $\beta$  are well-established clinical features of AD.

involves various cell-cell interactions within the CNS<sup>55</sup>. Microglia and astrocytes are the two types of glial cells with distinct etiologies that contribute to the initiation of the inflammatory cascade<sup>56,57</sup>. The perception of pathological triggers, such as A $\beta$  in AD, is mediated by receptors originally designed to recognize danger- or pathogen-associated molecular patterns (DAMPs/PAMPs)<sup>58-60</sup>. Following stimulus recognition, glial cells produce and secrete various proinflammatory cytokines, as well as a number of chemokines that facilitate the recruitment of additional glial cells<sup>14</sup>. Indeed, exposing microglia to A $\beta$  induces the production and release of pro-inflammatory cytokines, including IL-1 $\beta$ , IL-6, TNF $\alpha$ , TGF- $\beta$ , as well as chemokines, such as macrophage

inflammatory proteins (MIP)-1a, 1b, -2, and C-C motif chemokine ligand 2 (CCL2)<sup>14</sup>, presumably in an attempt to facilitate the clearance of A $\beta$ . Collectively, the production of these pro-inflammatory mediators can promote the neurodegeneration of otherwise healthy neighboring neuronal populations<sup>14</sup>. While undergoing cellular death, these neurons release their cellular contents and secrete DAMPS, amplifying and perpetuating the inflammatory response<sup>61,62</sup>. Many of the highly upregulated neurotoxic factors in the AD brain are evidenced to be microglia-derived, including TNF- $\alpha$ , NO, IL-1 $\beta$ , and reactive oxygen species (ROS)<sup>63</sup>. Moreover, the secretion of IL-1, TNF- $\alpha$ , and C1q by microglia was demonstrated to induce astrocyte reactivity, which in turn promoted the death of neurons and oligodendrocytes<sup>64</sup>, further emphasizing the detrimental effects of factors secreted by chronically-activated microglia. Additionally, knockout of *Nlrp3* – a critical component in the inflammasome pathway and major contributor to neuroinflammatory insult in the CNS – mitigated inflammatory signaling, decreased deposition of A $\beta$ , restored synaptic plasticity, and improved cognitive function in APP/PS1 mice<sup>65</sup>. Importantly, the formation and secretion of the NLRP3 inflammasome is restricted to the microglial compartment in the mouse brain<sup>66</sup>, which together with the *Nlrp3* knockout data, indicates that dysfunctional regulation of microglial NLRP3 signaling may contribute to plaque onset in AD.

In AD, neuroinflammation is considered a chronic and detrimental process<sup>67</sup>. Post-mortem examination of AD brains consistently demonstrates elevated numbers of microglia and astrocytes surrounding A $\beta$  deposits<sup>68</sup>. This observation is accompanied by overall increases in inflammatory cytokine and chemokine production<sup>68</sup>. Additionally, the extent of gliosis correlates strongly with disease progression and cognitive

impairments<sup>69,70</sup> with data suggesting that microglia are the critical cell type contributing to this neuroinflammatory environment in AD<sup>71</sup>, leading to increased interest in understanding the function of microglia-mediated neuroinflammation in AD.

### *Microglial phagocytosis and clearance of aggregated A $\beta$*

Since microglia are the primary immune cell in the brain and A $\beta$  accumulation has been implicated as a causative factor in AD, intense focus has been placed on the regulation of A $\beta$  dynamics by glial cells. The clearance of A $\beta$  by glial cells is carried out through the following primary mechanisms: 1) production of various A $\beta$ -degrading proteases 2) activation of glial proteasomal and autophagic pathways, 3) glial internalization/degradation of A $\beta$ , and 4) secretion of extracellular chaperones that facilitate the exit of A $\beta$  to the periphery. For the production of A $\beta$ -degrading proteases, glial cells are responsible for the expression of the vast majority of these factors<sup>72</sup>. The metalloendopeptidases neprilysin and insulin degrading enzyme (IDE) degrade primarily monomeric A $\beta$  species<sup>73,74</sup>, whereas plasminogen activators and angiotensin-converting enzyme (ACE) are more effective at degrading aggregated A $\beta$ . Matrix metalloproteases (MMPs) are involved in the degradation of both monomeric and fibrillar forms of A $\beta$ . Lastly, lysosomal peptidases including Cathepsin B are involved in the degradation of A $\beta$  following its phagocytosis by microglia, in part by reducing longer forms of A $\beta$  into shorter, less toxic species, such as A $\beta$ <sub>1-38</sub><sup>75</sup>. In the ubiquitin proteasome system (UPS), individual target proteins, including damaged, short-lived, or misfolded proteins are selectively targeted by the conjugation of ubiquitin<sup>76</sup>, which is performed by several enzymes (E1-3). Indeed, the UPS is capable of cleaving A $\beta$  in a dose-dependent

manner<sup>77</sup> and E3 ligases play a crucial role in the degradation of A $\beta$ . In the autophagy pathway, it is proposed that defective clearance of A $\beta$ -generating autophagic vacuoles creates a favorable environment for the accumulation of A $\beta$  in AD. In support of this, increasing autophagic processes via rapamycin reduces amyloid burden *in vivo*<sup>78</sup>. Additionally, extracellular chaperones play a pivotal role in the clearance of A $\beta$  through their modulation of A $\beta$  fibrils and mediation of interactions between A $\beta$  and lipoprotein receptor related protein 1 (LRP1) receptors on astrocytes. Genetically, the E4 allele of the apolipoprotein E gene is the strongest risk factor for sporadic AD, with the presence of one allele sufficient to increase an individual's risk for developing AD ~3-4 fold<sup>79</sup>. Thus, ApoE is easily the most studied of the extracellular chaperones. While predominantly expressed by astrocytes, ApoE expression can be induced under disease conditions in microglia<sup>80,81</sup> and is highly enriched in plaque-associated microglia<sup>82,83</sup>. As a chaperone, ApoE binds A $\beta$  in an isoform-dependent manner, with reduced A $\beta$ -ApoE binding in the presence of the ApoE4 isoform<sup>84</sup>, leading to increased seeding of fibrillar A $\beta$  and transport of soluble A $\beta$ . Another important mechanism of A $\beta$  clearance is its internalization by microglial cells. A $\beta$  can be internalized and cleared by microglia through fluid phase pinocytosis<sup>85</sup>, phagocytosis, particularly when bound by the C3b complement system<sup>86</sup>, and receptor-mediated endocytosis via action of Scavenger receptors<sup>58,87</sup>, Toll-Like receptors<sup>88</sup>, Receptor for Advanced Glycation End Products (RAGE)<sup>89</sup>, Fc Receptors<sup>90</sup>, TREM2<sup>43,91</sup>, and LRP1<sup>92</sup>. Thus, microglia regulate A $\beta$  clearance through a variety of mechanisms, many of which go awry in AD. Traditionally, it was believed that microglia respond to the presence of A $\beta$  deposits by clearing them from the brain via phagocytosis of A $\beta$ -fibrils<sup>93</sup>. *In vitro* studies show

accumulating evidence that microglia internalize and degrade A $\beta$  aggregates<sup>94-98</sup>. However, there has been no clear consensus *in vivo* as to whether microglia are capable of phagocytosing and degrading A $\beta$ , as some studies show internalization of A $\beta$  within the microglial lysosome<sup>99</sup> whereas others observe no A $\beta$  plaque clearance by these cells<sup>100,101</sup>. To directly assess the roles of microglia in A $\beta$  clearance and plaque dynamics, several methods for *in vivo* microglial ablation have been developed, allowing researchers to probe the contribution of microglia to pathophysiology. For example, clodronate liposomes induce apoptosis in phagocytizing macrophages<sup>102</sup>. Using this method in P0 5xfAD mouse organotypic hippocampal slice cultures, microglial depletion leads to the rapid accumulation of A $\beta$  deposits, showing that microglia in development and/or in slice cultures actively clear A $\beta$ <sup>94</sup>. However, upon replenishment with juvenile microglia, A $\beta$  clearance is restored resulting in fewer A $\beta$  deposits. Notably, replenishment with adult 5xfAD microglia does not reduce plaque deposits, indicating that the phagocytic ability of microglia is quickly lost with age, somewhere between 1 and 6 months of age. In CD11b-HSVTK mice, the thymidine kinase of herpes simplex virus is expressed under the CD11b promoter. Thymidine kinase converts ganciclovir into cytotoxic kinases, leading to cell death of CD11b-expressing cells (i.e., microglia in the CNS) and can maintain ablation for up to four weeks<sup>103</sup>. In these investigations, researchers crossed CD11b-HSVTK and AD mice to assess alterations in plaque dynamics with the elimination of microglia and found no changes in plaque load, A $\beta$  levels, or dystrophic neuritic structures near plaques, in either young or aged animals<sup>104</sup>. As the absence of microglia had no impact on A $\beta$  dynamics, these data suggest that aged microglia may not be actively involved in phagocytosing and/or clearing plaques in

the AD brain. Collectively, it appears that microglia in AD are ineffective A $\beta$  phagocytes, as evidenced by the continued presence of plaques surrounded by activated microglia in the AD brain, contributing to the enduring chronic neuroinflammatory environment for the duration of the disease.

Recent evidence suggests that plaque-associated microglia *in vivo* are in a suppressed phagocytic state due to the overproduction of IL-10<sup>105</sup>, prostaglandin E2 (PGE2)<sup>106</sup>, and arginase-1<sup>107</sup>. Indeed, subsequent exposure of microglia to certain stimuli, including lipopolysaccharide (LPS)<sup>108</sup>, IL-1 $\beta$ <sup>109</sup>, IL-33<sup>110</sup>, as well as the retinoid X receptor agonist bexarotene<sup>111</sup>, 40Hz light stimulation<sup>112</sup>, ultrasound<sup>113</sup>, and 40 Hz auditory stimulation<sup>114</sup> are sufficient to induce microglial degradation of A $\beta$ . Together, these studies indicate that microglia are fully capable of A $\beta$  phagocytosis, given a favorable environment in which to do so. Additionally, in a transgenic model of A $\beta$  arrest, switching off the APP transgene halted the progression of A $\beta$  pathology, but did not induce the breakdown or clearance of plaques<sup>115</sup>, providing further evidence that microglia are not responsible for regulating A $\beta$  dynamics in the AD brain.

#### *Neuroprotective functions of microglia in AD*

Although the evidence implicating microglial association with plaques is pervasive in different murine models of AD, as well as AD patients, the function of this association is still under investigation. Through examination of the role of microglia in regulating plaque dynamics, it was discovered that microglia constitute a barrier surrounding amyloid deposits, serving to limit the outward expansion of A $\beta$  deposition<sup>91,116-118</sup>. Moreover, plaque-associated microglia limited the toxic effects of A $\beta$ 42 hotspots on

nearby neurons<sup>117</sup>. As smaller (and presumably newer) plaques were most restricted in size, these data provide evidence for a neuroprotective role of microglia early in the disease in shielding neurons from toxic species of A $\beta$  and suggests that this method of plaque restriction is lost with age. Indeed, recent evidence describes a specific expression profile of plaque-associated microglia in the AD brain, identified as disease-associated microglia (DAM)<sup>83</sup>, which are neuroprotective and switched on during disease. This neurodegenerative phenotypic switch is triggered by TREM2, leading to activation of APOE signaling and subsequent suppression of homeostatic microglial phenotype<sup>83,119</sup>. DAM cells express *Spp1*, *Itgax*, *Axl*, *Lilrb4*, *Clec7a*, *Csf1*, and *ApoE* and are highly enriched in microglia surrounding plaques<sup>83,119</sup>. Because of their association with plaques and increased intake of A $\beta$  particles, it is postulated that DAM cells are a more phagocytic subset of microglia. In support of this, knockout of *Trem2*<sup>91</sup> and *ApoE*<sup>118</sup> increased plaque-associated neuritic dystrophy, highlighting the beneficial effects of this subset of microglia in the AD brain. Thus, more effective treatments for AD may involve designing targets for specific subsets of microglia – modulating the function of microglia in plaque-distal areas that may be involved in A $\beta$  seeding, but preserving subsets of neuroprotective microglia that are plaque-proximal.

Collectively, numerous studies implicate microglial reactivity in AD pathogenesis, but point to dichotomous roles of microglia throughout the disease course. In earlier stages of AD, many reports suggest that microglial phagocytosis and clearance of A $\beta$  is crucial to curtail disease progression; however, recent evidence suggests that microglia may contribute to the appearance of plaques in the AD brain. Once plaques appear in AD, microglia exert neuroprotective functions by encapsulating plaques with their processes

and cell bodies, limiting the interaction of toxic A $\beta$  species with nearby neurons. In contrast to this, microglia in advanced stages of AD fail to clear A $\beta$  from the brain, unless induced with sufficient stimulation, indicating that these cells are not key regulators of A $\beta$ /plaque levels *in vivo* in the presence of extensive A $\beta$  pathology. Thus, further experimentation is needed to determine the contributions of microglia at different stages in the disease and identify the ways in which GWAS-identified myeloid genes influence the onset and progression of AD.

#### **D. Microglial elimination via administration of CSF1R inhibitors**

##### *Microglial depletion approaches*

While various methods of microglial ablation are available, the technical requirements necessary to achieve sustained microglial elimination limit the utility of most depletion paradigms. For example, the CX3CR1<sup>cre<sup>ER</sup></sup> x DTR<sup>ff</sup> mouse model relies on administration of diphtheria toxin, which not only induces a cytokine storm, but also limits microglial elimination to 5 days<sup>120</sup>. The CD11b-HSVTK model requires intracerebroventricular infusion of ganciclovir in order to deplete appreciable numbers of microglia, which in turn induces BBB damage and myelotoxicity, resulting in increased mortality following 4 weeks of ganciclovir treatment<sup>104</sup>. Clodronate liposome administration is also reported to deplete microglia, however, this effect is short-lived and requires intrahippocampal infusion, as clodronate liposomes are incapable of crossing the BBB<sup>121</sup>. Thus, this highlights the need for more precise and targeted approaches to deplete microglia.

### *Colony-stimulating factor 1 receptor (CSF1R)*

CSF1R is expressed on all myeloid-derived cells and binding by one of the two CSF1R ligands (Colony-stimulating factor 1 (CSF-1) or interleukin 34 (IL-34)) leads to auto-phosphorylation of the tyrosine kinase receptor. Following ligand binding, downstream signal transduction pathways are activated allowing for the regulation of myeloid cell differentiation, proliferation, migration, and survival<sup>122-125</sup>. Even though low expression of *Csf1r* has been reported in some neurons in the hippocampus<sup>126</sup>, CSF1R expression is predominantly restricted to microglia in the CNS. Genetic evidence for the consequences of CSF1R activation *in vivo* indicates that CSF1R primarily plays a homeostatic role in regulating the viability and proliferation of microglia<sup>127,128</sup>. In mice, knockout of both CSF1R alleles is embryonically lethal and the brains of these mice lack microglia, indicating that signaling through this receptor is necessary for microglial and animal survival during developmental processes<sup>123,124</sup>. Moreover, genetic deletion of either of its ligands, CSF1<sup>129</sup> or IL-34<sup>125</sup>, reduces microglial numbers without animal mortality, suggesting that compensatory actions by the remaining ligand of the CSF1R allows these mice to survive, as opposed to total knockout of the CSF1R. In humans, dominant loss-of-function mutations in CSF1R cause adult-onset leukoencephalopathy with axonal spheroids and pigmented glia (ALSP)<sup>130,131</sup>. The clinical manifestation of ALSP includes progressive white matter loss, memory decline, and motor impairments. Due to the specificity of CSF1R expression in microglia in the CNS, this demonstrates that perturbations in microglial function via altered CSF1R signaling alone can induce neurodegenerative phenotypes. Thus, techniques that manipulate CSF1R signaling may present a novel route to investigate and modulate microglial biology/numbers.

*Microglia in the adult brain are dependent on CSF1R signaling for their survival*

Given the role of CSF1R in regulating microglial numbers, pharmacological inhibitors of this receptor were developed as an approach to investigate microglial dynamics. PLX3397 and PLX5622 are two CSF1R inhibitors initially developed as cancer therapeutics (Fig. 2), with PLX3397 in phase III clinical trials for Pigmented Villonodular Synovitis (PVNS). PLX5622 was designed using a structure-guided drug design strategy based on the existing CSF1R/KIT/FLT3 inhibitor PLX3397<sup>35,132</sup>, combined with *in vivo* screening for optimal pharmacokinetics (PK) and brain penetrance. Two key structural differences between PLX5622 and PLX3397 contribute to the improved selectivity to CSF1R based on crystallographic analysis. *In vivo*, PLX5622 demonstrated desirable PK properties in mice, rats, dogs, and monkeys, with a brain penetrance of ~20% (compared to ~5% for PLX3397)<sup>133</sup>.

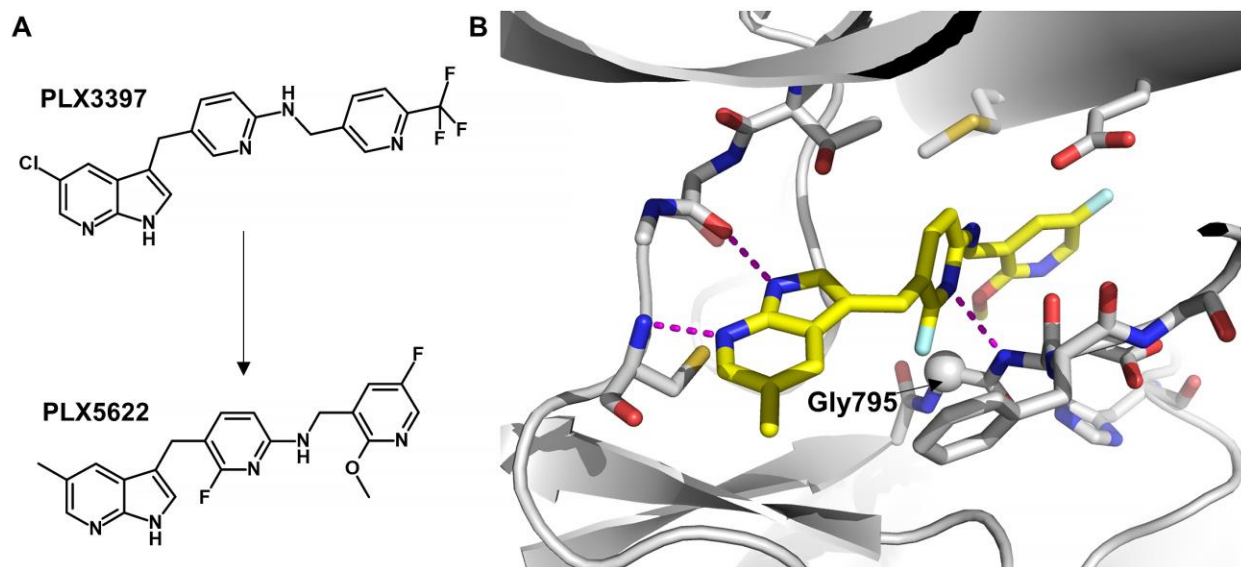


**Figure 2 Chemical structures of CSF1R inhibitors PLX3397 and PLX5622. A,** Chemical structure of selective CSF1R inhibitor PLX5622. PLX5622 is structurally similar to CSF1R/KIT/FLT3 inhibitor PLX3397 with modifications concentrated on the two pyridine moieties. **B,** X-ray crystal structure of the CSF1R-PLX5622 complex. The CSF1R selectivity is largely determined by the interaction between PLX5622 and Gly795 (represented as a sphere), which is a bulkier residue (cysteine) in KIT and FLT3. The substitutions on the tail pyridine ring also contribute to the selectivity. This group displaces the juxtamembrane (JM) region (absent in the structure) from the allosteric site. In contrast, PLX3397 binds CSF1R in the presence of the JM region.

Previously, our lab demonstrated that microglia rely on CSF1R signaling for their survival in the healthy murine adult brain<sup>133</sup>. We found that oral administration of PLX3397 eliminates >90% of microglia within 7 days, and up to 99% by 21 days (Fig.

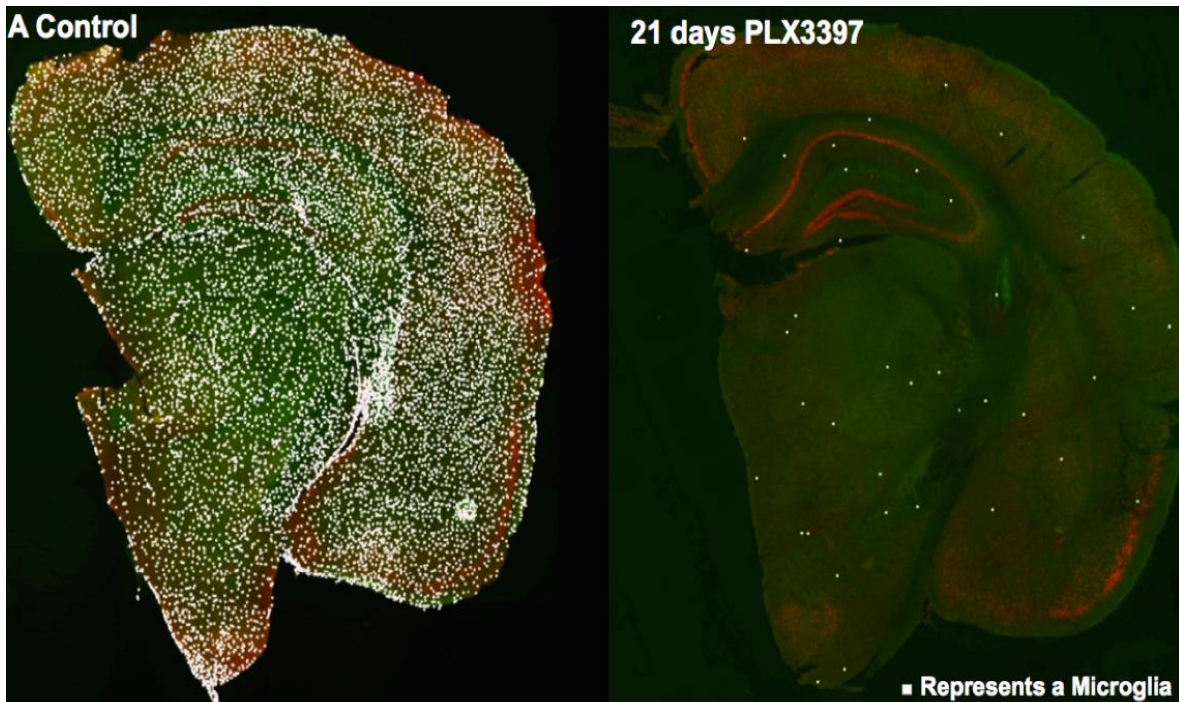


**Figure 3 CSF1R Inhibition Eliminates Microglia from the Healthy, Adult Mouse Brain** 2-month-old wild-type mice (C57BL6/J; n=4-5/group) were treated with control diet or PLX3397 (290 mg/kg) for 21 days. **A**, Representative coronal sections of the brain from a control-treated mouse (left) and PLX3397-treated mouse (right). Microglial were immunolabeled with IBA1 and tissue was subsequently analyzed with Imaris Software to generate images with a white dot overlaying each IBA1 cell body.

3)<sup>133</sup>. As microglia are heavily implicated in shaping the synaptic landscape of the brain, we assessed behavior and cognition and found no abnormalities, indicating that microglia are not necessary for these domains in adulthood<sup>133</sup>. Biochemical and immunohistochemical approaches have shown no effects on other cell types in the brain (i.e., neurons, astrocytes, and oligodendrocytes) with CSF1R inhibition<sup>133</sup>, nor any significant effects on peripheral myeloid cells, highlighting the specificity of microglial elimination via pharmacological inhibition of the CSF1R. Another attractive feature of our approach is that microglial elimination is completely reversible. We demonstrate that

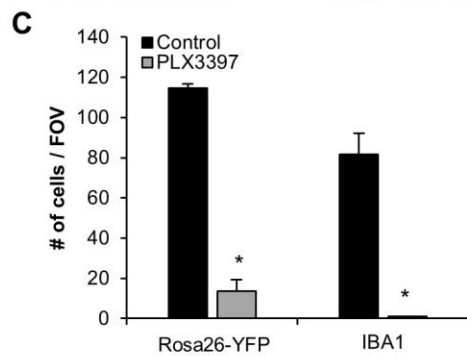
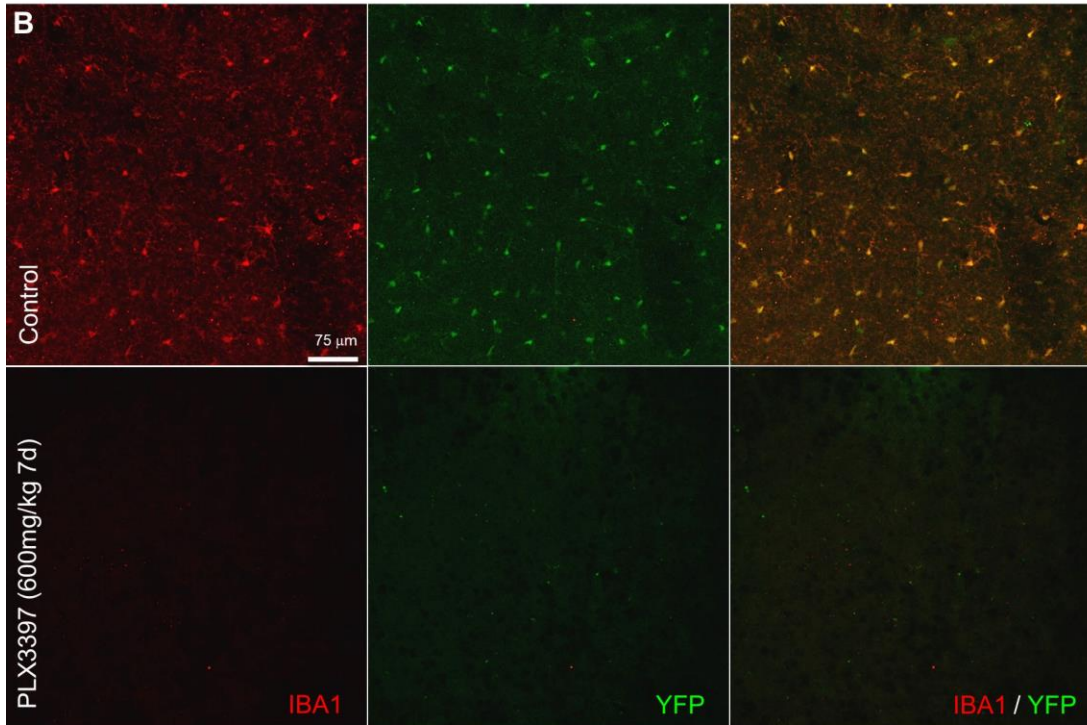
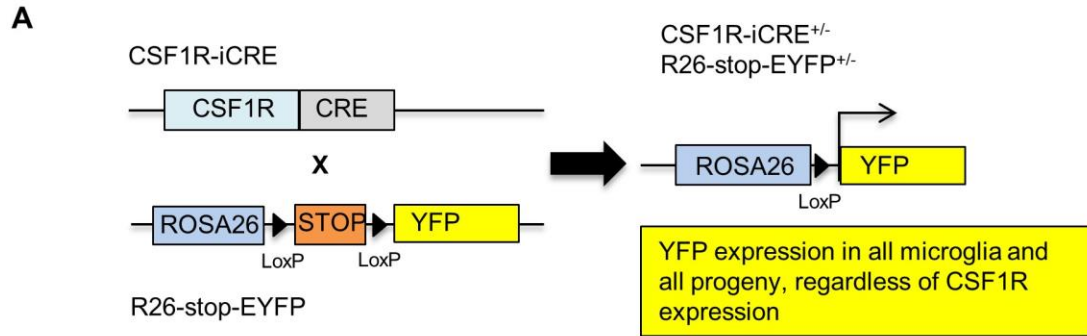


**Figure 4 Treatment with the CSF1R inhibitor PLX3397 eliminates microglia in Rosa26-YFP mice.** Two-month-old mice were treated with PLX3397 (600 mg/kg) for 7 days to eliminate microglia. **A**, Schematic of the breeding strategy to yield offspring with YFP expressing microglia. **B**, Immunolabelling for microglia (IBA1 in red) and expression of YFP in CSF1R<sup>+</sup>-derived cells (YFP in green). **C**, Quantification of the number of YFP<sup>+</sup> and IBA1<sup>+</sup> cells is reduced in the cortex by 88% (  $P < 0.0001$ ) and 99% (  $P < 0.0001$ ), respectively, with PLX3397 treatment. Statistical significance is denoted by \*  $P < 0.05$ . Error bars indicate SEM (  $n = 4$ /group).

withdrawal of inhibitor stimulates rapid repopulation of the microglial compartment with new cells that are capable of fully reconstituting the brain with new microglia within 14

days<sup>133</sup>. Importantly, multiple groups have utilized and verified PLX3397, as well as the CSF1R-specific inhibitor PLX5622, as an effective tool for studying and eliminating microglia<sup>134-138</sup>, without inducing adverse effects on cognitive function in healthy, adult mice<sup>35,139</sup>. To address the possibility that CSF1R inhibitor treatment induces the loss of the microglial signature without cell elimination, we obtained CSF1R-iCRE [FVB-Tg(Csf1r-icre)1Jwp/J] and *Rosa26<sup>YFP</sup>*(B6.129X1-Gt(ROSA)26Sor<sup>tm1(EYFP)Cos</sup>/J) reporter mice from The Jackson Laboratory. Crossing these mice yielded CSF1R-iCRE/*Rosa26YFP* progeny that express yellow fluorescent protein (YFP) in all cells that either transiently or constitutively express CSF1R, which in the brain predominantly labels microglia (see schematic in Fig. 4A). Two-month-old mice were treated for 7 days with PLX3397 (600 mg/kg in chow) to eliminate microglia (Fig. 4B). We found that ~90% of YFP cells were depleted with 7 days of treatment (Fig. 4C), indicating that CSF1R inhibitor treatment results in the elimination of microglia, rather than a downregulation of microglia-associated genes. Thus, our lab has demonstrated with reproducibility that CSF1R inhibitor administration is an effective technique to ablate the microglial compartment.

Prior to the start of my dissertation, our lab had utilized CSF1R inhibitors to eliminate microglia in healthy<sup>133</sup> and diseased murine brains, using a model of inducible hippocampal neuronal lesion<sup>35,36</sup> and the 3xTg-AD mouse model<sup>35,133,139</sup>. Given the increasing interest in microglia in AD pathogenesis, for my dissertation I sought to determine the precise roles these cells play over the course of disease progression using CSF1R inhibitor-induced microglial ablation. My findings are described in the following chapters of this dissertation.

# CHAPTER ONE

## ESTABLISHING THE ROLES OF CHRONICALLY ACTIVATED MICROGLIA IN AGED ALZHEIMER'S DISEASE MICE

### INTRODUCTION

Alzheimer's disease (AD) is a progressive, neurodegenerative disease classically characterized by the presence of amyloid plaques and neurofibrillary tangles. However, histological studies demonstrate that neuroinflammation is also a key feature of the Alzheimer's disease brain<sup>140-144</sup>, as well as being prominently observed in amyloid precursor protein (APP) overexpressing transgenic mouse models<sup>145</sup>. These studies show that activated microglia surround extracellular plaques<sup>146-148</sup>, likely in an attempt to clear the toxic deposits, and stain positively for inflammatory markers, including major histocompatibility complex (MHC) class II, cyclooxygenase (COX)-2, tumor necrosis factor (TNF)- $\alpha$ , interleukin (IL)-1 $\beta$ , and IL-16<sup>149</sup>. Inevitably, the sustained activation of microglia results in a chronic neuroinflammatory response and the increased production of pro-inflammatory cytokines, such as TNF- $\alpha$  and IL-1 $\beta$ <sup>150-152</sup>. Previous investigations indicate that this chronic neuroinflammation response is synapto- and neurotoxic<sup>153-155</sup> and exacerbates cognitive decline<sup>156</sup>. Indeed, mouse models of AD display striking dendritic spine loss that is spatially associated with these microglia-surrounded plaques<sup>157-159</sup>. In humans, studies have identified synaptic loss as a correlate of, and a major contributor to, cognitive decline<sup>160,161</sup>. Of relevance, recent genome-wide association studies (GWAS) have uncovered several risk-associated genes in the development of sporadic AD<sup>162</sup>. Most of these risk genes are either expressed by

microglia or associated with their reactivity, including *CD2AP*<sup>163</sup>, *CD33*<sup>164</sup>, *BIN1*<sup>165</sup>, *CR1*<sup>166</sup>, *PICALM*<sup>167</sup>, *ABCA7*<sup>168</sup>, *TREM2*<sup>169</sup>, and *CLU*<sup>170</sup>. Thus, genetic changes in microglia-associated genes correspond strongly with an increased risk of developing AD. For these reasons, we hypothesized that microglia play a critical role in the development and progression of AD by limiting A $\beta$ /plaque loads but contribute to synaptic and neuronal loss.

We have previously shown that microglia in the adult brain are fully dependent on CSF1R signaling for their survival<sup>133</sup>. Administration of CSF1R inhibitors that cross the blood brain barrier (BBB) lead to brain-wide elimination of ~80% of all microglia within 7 days of treatment. Moreover, these microglia remain eliminated for the duration of treatment, even for weeks or months. Since microglia are the only cell type to express CSF1R in the adult brain parenchyma, the effects of this treatment are largely restricted to this cellular compartment. Of note, peripheral myeloid populations are also known to express CSF1R, but those explored thus far are not dramatically eliminated by the doses and compounds used in this study<sup>133,134,171-173</sup>, although their functions/response to disease may be altered due to inhibition.

In this study, we have set out to show that microglia in the AD brain are also dependent on CSF1R signaling and to explore the effects of chronic microglial elimination on AD pathologies and memory in 5xfAD mice. The 5xfAD mice represent an aggressive model of amyloid pathologies, with A $\beta$  plaques first depositing from 2 months of age<sup>174</sup>. Notably, 5xfAD mice exhibit marked synaptic and neuronal loss as pathology develops, with neuronal loss seen in the subiculum from 10 months of age<sup>175-178</sup>, allowing for investigations into how the pathology drives damage to neurons and neuronal

structures. Through the elimination of microglia in advanced pathology 5xfAD mice, we show recovery of contextual memory, a reversal of dendritic spine loss and prevention of neuronal loss, yet no changes on A $\beta$  levels or plaque loads, highlighting the roles that microglia may play in the AD brain.

## **MATERIALS AND METHODS**

**Compounds:** PLX3397 was provided by Plexxikon Inc. and formulated in AIN-76A standard chow by Research Diets Inc. at 290 mg/kg or 600 mg/kg, as previously described<sup>133</sup>. PLX5622 was provided by Plexxikon Inc. and formulated in AIN-76A standard chow by Research Diets Inc. at 1200 mg/kg.

**Animal treatments:** All rodent experiments were performed in accordance with animal protocols approved by the Institutional Animal Care and Use Committee at the University of California, Irvine. The 5xfAD mouse model has been previously described in detail<sup>174</sup>. Using a 2  $\times$  2 factorial design, forty male and female 10-month-old wild-type (C57BL/6 background) or 5xfAD mice were treated with either PLX3397 for 28 days to eliminate microglia or control chow, creating four treatment groups ( $n = 10/\text{group}$ ): Control (six males and four females), PLX3397 (six males and four females), 5xfAD (four males and six females), and 5xfAD + PLX3397 (four males and six females). At this age, 5xfAD mice display extensive pathology, synaptic loss, and neuronal loss<sup>174,175</sup>. After 28 days of treatment, behavioural testing commenced while animals remained on their respective diets. A second cohort of 14-month-old 5xfAD mice ( $n = 4/\text{group}$ ; 5xfAD = four males, and 5xfAD + PLX5622 = three males and one female)

was treated with either PLX5622 for 28 days to deplete microglia or control chow (5xfAD versus 5xfAD + PLX5622). A third cohort of 1.5-month-old 5xfAD mice ( $n = 4/\text{group}$ ; two males and two females) was treated with PLX3397 or control for 28 days (5xfAD versus 5xfAD + PLX3397). Following behavioural testing in the 10-month-old cohort, and following inhibitor treatment in the 14-month-old and 1.5-month-old cohorts, mice were euthanized via CO<sub>2</sub> inhalation and transcardially perfused with phosphate-buffered saline. For both studies, brains were removed and hemispheres separated along the midline. Brain halves were either flash frozen for subsequent biochemical analysis, drop-fixed in 4% paraformaldehyde (Thermo Fisher Scientific) for subsequent immunohistochemical analysis, or placed in Golgi impregnation solution for subsequent dendritic spine analysis. Fixed half brains were sliced at 40  $\mu\text{m}$  using a Leica SM2000 R freezing microtome. The flash-frozen hemispheres were ground with a mortar and pestle to yield a fine powder. One-half of the powder was homogenized in Tissue Protein Extraction Reagent, T-PER (Life Technologies) with protease (Roche) and phosphatase inhibitors (Sigma-Aldrich). The second half was processed with an RNA Plus Universal Mini Kit (Qiagen) for RNA analysis.

**Behavioural testing:** Behaviour was analysed 28 days after the administration of PLX3397 treatment to eliminate microglia. Methods for testing mice on contextual fear conditioning were based on previous literature<sup>133,179</sup>. To assess contextual memory, freezing behaviour, defined as the total lack of body movement except for respiration, was scored live and video-recorded. Behaviour was scored using 1-0 sampling every 10 s, with a 1 denoting positive freezing behaviour and 0 indicating the absence of freezing

behaviour. For the training trial, mice were placed in a fear-conditioning chamber (Gemini, San Diego Instruments; 24.1-cm length × 20.3-cm width × 20.3-cm height) and allowed to explore for 2 min before receiving one foot shock (3 s, 0.2 mA). Animals were returned to their home cage 30 s after the shock. Testing was conducted 24 h later, in which the animals were placed in the chamber and allowed to explore for 5 min.

**Confocal microscopy:** Immunofluorescent labelling was performed following a standard indirect technique as previously described<sup>180</sup>. Primary antibodies and dilutions used are as follows: anti-ionized calcium-binding adapter molecule 1 (IBA1; 1:1000; Wako), anti-amyloid- $\beta$ <sub>1-16</sub> (6E10; 1:1000; Covance), anti-s100 $\beta$  (1:200; Abcam), anti-aldehyde dehydrogenase family 1 member L1 (Aldh1L1; 1:50; UC Davis), and anti-glia fibrillary protein (GFAP; 1:1000; Abcam). Thioflavin-S (Sigma-Aldrich) staining was carried out as previously described<sup>181</sup>. Total microglia and plaque counts were obtained by imaging comparable sections of tissue from each animal at the 10× objective, followed by automated analyses using Bitplane Imaris 7.5 spots or surfaces modules, respectively. To determine the number of plaque-associated microglia, equal perimeters were drawn around each plaque using ImageJ software (NIH), and cells were manually counted.

**Immunoblotting:** Immunoblotting was performed as previously described<sup>133</sup>. Antibodies and dilutions used in this study include: 6E10 (as described above), CT20 (1:1000; Calbiochem) for C99 and C83, and  $\beta$ -actin (1:10,000; Sigma-Aldrich).

Quantitative densitometric analyses were performed on digitized images of immunoblots with ImageJ software.

**Amyloid- $\beta$  enzyme-linked immunosorbent assay:** Isolated protein samples were transferred to a blocked MSD Human/Rodent (4G8) amyloid- $\beta$  triplex ELISA plate (amyloid- $\beta_{1-38}$ , amyloid- $\beta_{1-40}$ , amyloid- $\beta_{1-42}$ ) and incubated for 2 h at room temperature with an orbital shaker. The plate was then washed and measurements obtained using a SECTOR Imager 2400, according to the manufacturer's instructions (Meso Scale Discovery).

**NanoString RNA analysis:** One hundred and eighty inflammation-, Alzheimer's disease-, plasticity-, and ageing-related genes were selected for analysis and probes were designed and synthesized by NanoString nCounter™ technologies (NanoString) against mouse genes. Total mRNA was extracted using an RNA Plus Universal Mini Kit (Qiagen) and was hybridized and multiplexed with NanoString probes, according to the manufacturer's instructions. Counts for target genes were normalized to house-keeping genes (*Eef1g*, *G6pdx*, *Hprt*, *Polr1b*, *Polr2a*, *Ppia*, *Rpl19*, *Sdha*, and *Tbp*) to account for variability in the RNA content. Background signal was calculated as a mean value of the negative hybridization control probes. Normalized counts were log-transformed for downstream statistical analysis.

**Golgi staining and spine quantification:** Half brains were sliced coronally with a vibratome at 100  $\mu$ m, mounted on gelatin-coated slides, and subsequently stained using

a SuperGolgi Kit, per the manufacturer's instructions (Bienno Tech). Five non-primary apical dendrites in the CA1 per animal ( $n = 3/\text{group}$ ) were traced using a 100× oil-immersion objective and Neurolucida software for dendritic spine analysis (MBF Bioscience). Spines were classified based on previous literature using head-to-neck ratios and quantified according to the following categories: total, mushroom, stubby, and thin spines<sup>182</sup>.

**Cresyl violet staining and neuron quantification:** Cresyl violet staining was performed on fixed tissue and neurons in the subiculum were counted in a double-blind unbiased stereological fashion, as previously described<sup>183</sup>. All unbiased stereological assessments were performed using Stereo Investigator (MBF Bioscience) and Neurolucida softwares. The stereological quantification of neurons in the subiculum was performed on every sixth section (40  $\mu\text{m}$  coronal sections between  $-2.48$  mm and  $-3.28$  mm posterior to bregma) of one brain hemisphere ( $n = 4/\text{group}$ ). A counting frame of 50  $\times$  50  $\mu\text{m}$  in a sampling grid of 100  $\times$  100  $\mu\text{m}$  was used, with a guard zone height of 3  $\mu\text{m}$  for the top and bottom. The subiculum was defined using a 5× objective and the Cresyl violet stained cells were counted using a 100× oil-immersion objective. Neuronal nuclei were randomly sampled from the defined subiculum using the optical dissector probes.

**Statistics:** Behavioural, biochemical, and immunohistological data were analysed using either unpaired Student's *t*-test (Control versus wild-type or 5xfAD versus 5xfAD + PLX3397/PLX5622) in Microsoft Excel or as a two-way ANOVA (Diet: Control versus PLX3397 and Genotype: wild-type versus 5xfAD) using the MIXED procedure of the

Statistical Analysis Systems software (SAS Institute Inc.), a general linear model that accounts for both fixed and random variables, as previously described<sup>184</sup>. *Post hoc* paired contrasts were used to examine biologically relevant interactions from the two-way ANOVA regardless of statistical significance of the interaction. Symbols denote significant differences between groups ( $P < 0.05$ ): \*Control versus PLX3397; † Control versus 5xfAD; # PLX3397 versus 5xfAD + PLX3397; ¶ 5xfAD versus 5xfAD + PLX3397. Data are presented as raw means  $\pm$  standard error of the mean (SEM). For all analyses, statistical significance was accepted at  $P < 0.05$  (\*) and trends at  $P < 0.10$  (#).

## RESULTS

### **CSF1R inhibition improves contextual memory deficits in 5xfAD mice following microglial elimination**

10-month-old 5xfAD mice were selected for this study as they show extensive amyloid pathology at this age, along with robust neuroinflammation and also synaptic loss, mimicking the human condition. Crucially, these mice begin to exhibit neuronal loss from 10 months of age. Following 28 days of PLX3397 or control chow treatment, 5xfAD and WT mice were tested in contextual fear conditioning to assess hippocampal memory (see experimental schematic; Fig. 1.1A,  $n=12$ /group). Analysis of behavioral performance revealed that 5xfAD mice spent significantly less time freezing compared to controls, but this effect trended toward recovery in 5xfAD mice administered PLX3397 to eliminate microglia ( $p=0.0813$ ; Fig. 1.1B). Following behavioral testing, the brains of these mice were analyzed for Thioflavin-S (Thio-S) staining and IBA1 immunolabeling to visualize dense core plaques and microglia, respectively (Fig. 1.1C

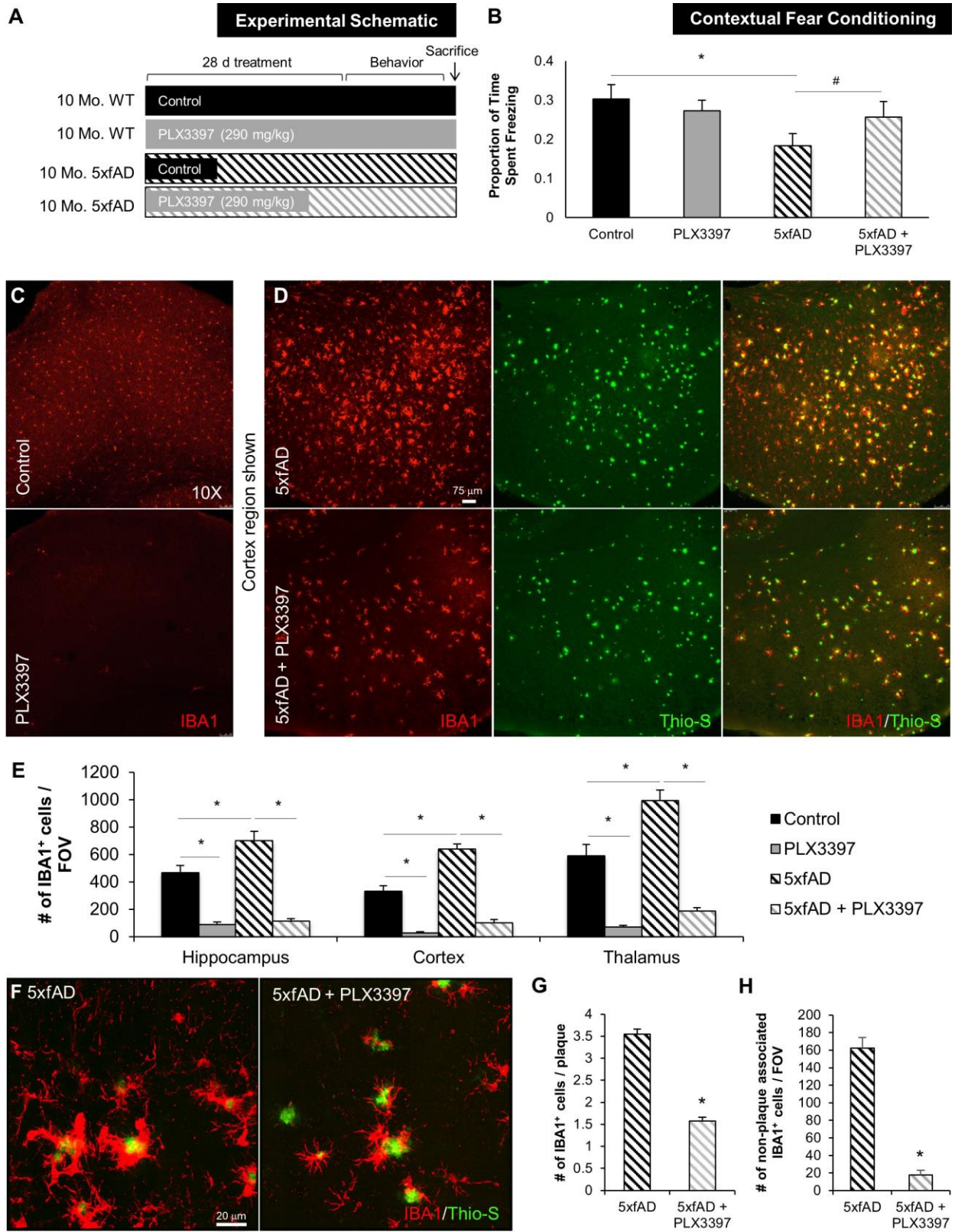


**Figure 1.1 Chronically activated microglia in 5xfAD mice are dependent on CSF1R signaling for their survival:** 10-month-old WT or 5xfAD mice were treated with control chow or PLX3397 for 28 days to eliminate microglia. **A**, Experimental design. **B**, In contextual fear conditioning, 5xfAD mice spent significantly less time freezing compared to control (via two-way ANOVA,  $p=0.0196$ ) and 5xfAD + PLX3397 treated mice trended to an increased freezing time (via two-way ANOVA,  $p=0.0813$ ). **C, D**, Immunolabeling for microglia (IBA1 in red) and staining for dense-core plaques (Thio-S in green). **E**, Microglia number is increased by ~40% in 5xfAD mice compared to control (via two-way ANOVA,  $p<0.0001$ ). PLX3397 treatment eliminates ~80% of microglia in both WT and 5xfAD mice (via two-way ANOVA,  $p<0.001$ ). **F**, Representative 63X IBA1 Thio-S immunofluorescent staining of the cortex. **G**, Quantification of plaque-associated microglia reveals the number of these cells was reduced by ~50% with PLX3397 treatment (two-tailed unpaired t-test,  $p<0.0001$ ). **H**, The number of non-plaque associated microglia is reduced by ~90% with PLX3397 treatment in 5xfAD mice (two-tailed unpaired t-test,  $p<0.0001$ ). Statistical significance is denoted by \* $P<0.05$  and statistical trends by # $P<0.10$ . Error

and D). 5xfAD mice had significantly elevated total numbers of IBA1<sup>+</sup> cells, but these were reduced by ~80% in the hippocampus, cortex, and thalamus of PLX3397-treated animals (Fig. 1.1E), revealing the majority of these cells to be dependent on CSF1R signaling for their survival, particularly in the intra-plaque spaces. High power Z-stack images showed a high association of myeloid cells with dense core plaques in these mice (Fig. 1.1F). Importantly, PLX3397 treatment significantly reduced these plaque-associated myeloid cells by ~50% (Fig. 1.1G). Quantification of the number of non-plaque associated IBA1<sup>+</sup> cells revealed a ~90% reduction in the treated 5xfAD mice (Fig. 1.1H), highlighting the preferential elimination of non-plaque associated IBA1<sup>+</sup> cells.

Moreover, immunolabeling tissue for the microglial-specific markers 4D4 (data unpublished) and P2RY12<sup>165</sup> evidenced the plaque-associated myeloid cells in 5xfAD mice as microglia (Fig. 1.2A- C). We found a stark reduction in P2RY12 expression in PLX5622-treated mice compared to WT (Fig. 1.2C), confirming that CSF1R inhibitor treatment eliminates microglia in the healthy brain. Importantly, myeloid cells in PLX3397-treated 5xfAD mice also expressed the microglial-specific markers (Fig. 1.2B

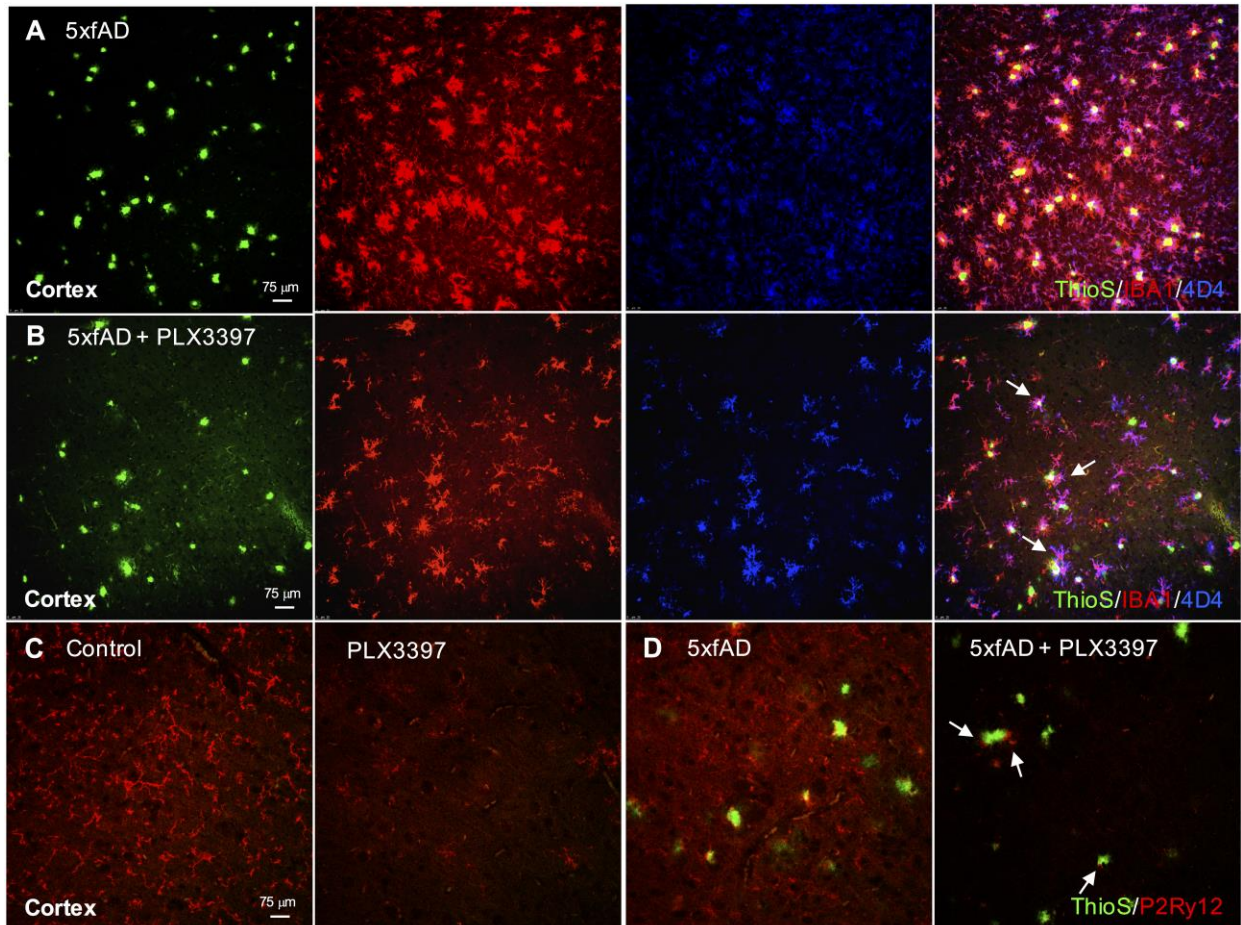


**Figure 1.2 Surviving IBA1+ cells are of microglial identity.** **A, B**, Representative cortical sections from 5xfAD groups stained for dense-core plaques (Thio-S in green) and immunolabeled for microglial cells (IBA1 in red, 4D4 in blue). **C, D**, Cortical images of dense-core plaque staining (Thio-S in green) and immunolabeling for microglia (P2RY12 in red), showing microglia surrounding Thio-S<sup>+</sup> deposits (n=6-7/group).

and D, as shown by white arrows), suggesting that a population of microglia are resistant to CSF1R inhibitor treatment. Combined, these findings indicate that microglia in 5xfAD mice may be involved in mediating contextual memory deficits, which can be partially attenuated by eliminating the microglial compartment.

### **Microglia do not modulate A $\beta$ pathology**

To determine if microglia mediate amyloid pathology, we examined the effects of eliminating microglia on A $\beta$  levels in the brain. Staining for dense-core plaques via Thio-S showed that microglial depletion did not significantly affect plaque numbers or average plaque size in any brain region analyzed (Fig. 1.3A-D). Plaques were categorized by size (i.e., <150 $\mu\text{m}^2$ , 150-1000  $\mu\text{m}^2$ , or >1000  $\mu\text{m}^2$ ) in the thalamus, due to high plaque load observed in this region (refer to Fig. 1.3A-D), but no differences were found between control- and PLX3397-treated mice (Fig. 1.3E). We further analyzed both soluble and insoluble levels of A $\beta_{1-38}$ , A $\beta_{1-40}$ , and A $\beta_{1-42}$  by triplex ELISA. In WT mice, there was no effect of microglial elimination on levels of endogenous A $\beta$  species (Fig. 1.3F), while A $\beta_{1-38}$  was below detection limits. We also found no significant differences in A $\beta$  levels in either soluble or insoluble fractions in 5xfAD mice (Fig. 1.3G and H). Finally, we immunolabeled tissue with 6E10 antibody, to assess the effect of PLX3397 treatment on diffuse plaque load and quantified the size of plaques (Fig. 1.3I). In the cortex, we found no differences in diffuse plaque load or size with PLX3397 treatment (Fig. 1.3J and K). Collectively, these data indicate that microglia do not play a substantial role in A $\beta$  production/clearance or plaque deposition/remodeling in pathological 5xfAD mice.

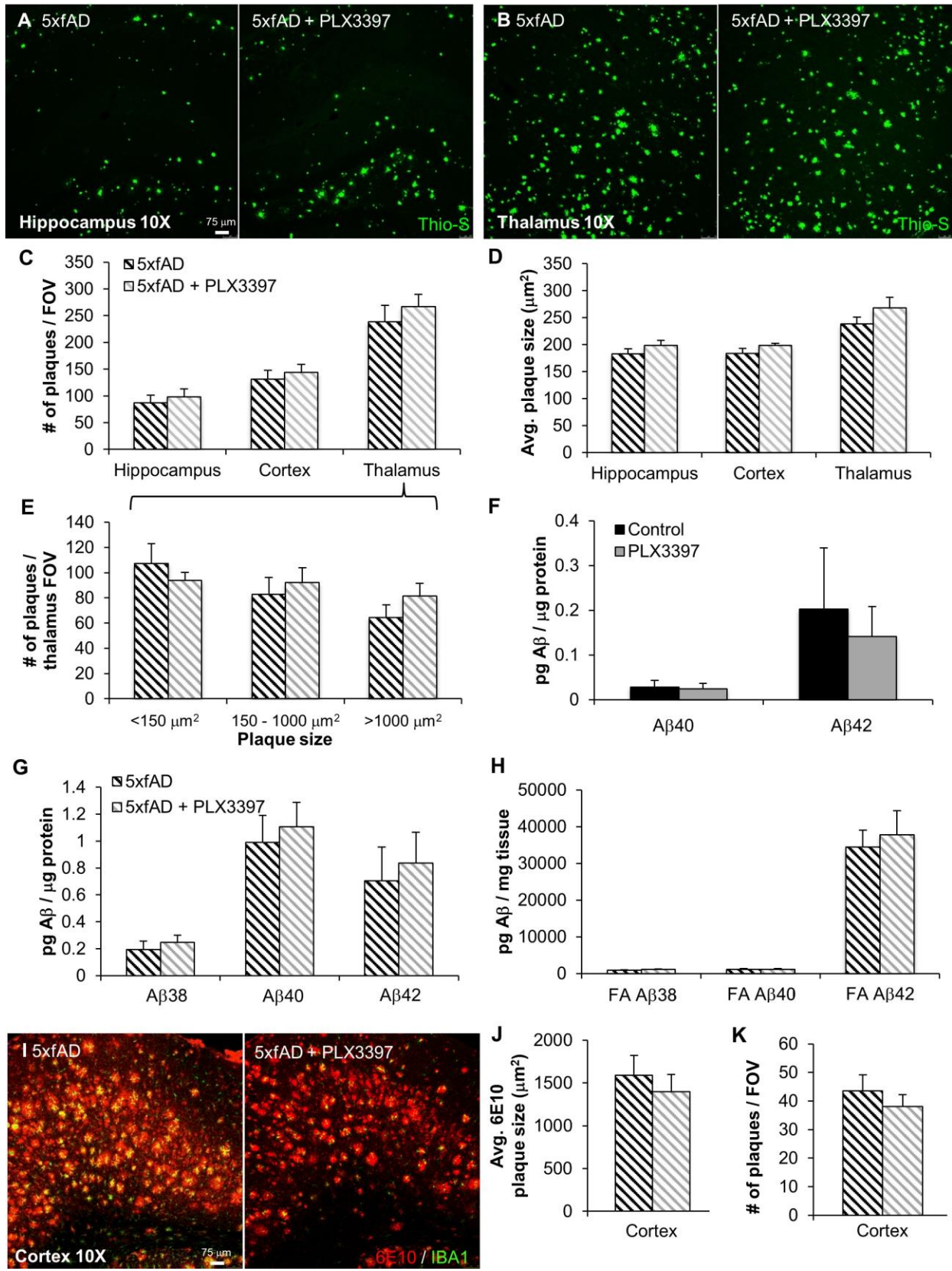


**Figure 1.3** Elimination of microglia does not modulate A $\beta$  levels or plaque load. **A, B**, Representative hippocampal and thalamic 10X images of dense core plaques (Thio-S) in 5xfAD and 5xfAD mice treated with PLX3397. **C, D**, Quantification of number of Thio-S<sup>+</sup> plaques and average area of the plaques in the hippocampus, cortex, and thalamus. **E**, Microglial elimination has no effect on plaques of any size. **F**, Levels of A $\beta_{1-40}$  and A $\beta_{1-42}$  were unchanged with microglial elimination in WT mice. Levels of A $\beta_{1-38}$  were below detection threshold. **G, H**, Levels of A $\beta$  species in detergent-soluble and formic acid-soluble (FA) fractions are not changed with microglial elimination. **I**, Representative 10X 6E10 and IBA1 immunofluorescent images of the thalamus. **J, K**, Quantification of 6E10<sup>+</sup> plaque size and numbers reveals no effect of microglial elimination. Error bars indicate SEM; (n=7/group).

## Elimination of microglia in young 5xfAD mice reveals no changes in A $\beta$ pathology

Given the surprising result that elimination of microglia did not affect A $\beta$  load or levels in pathological 5xfAD mice, we sought to determine if microglia were protective at younger

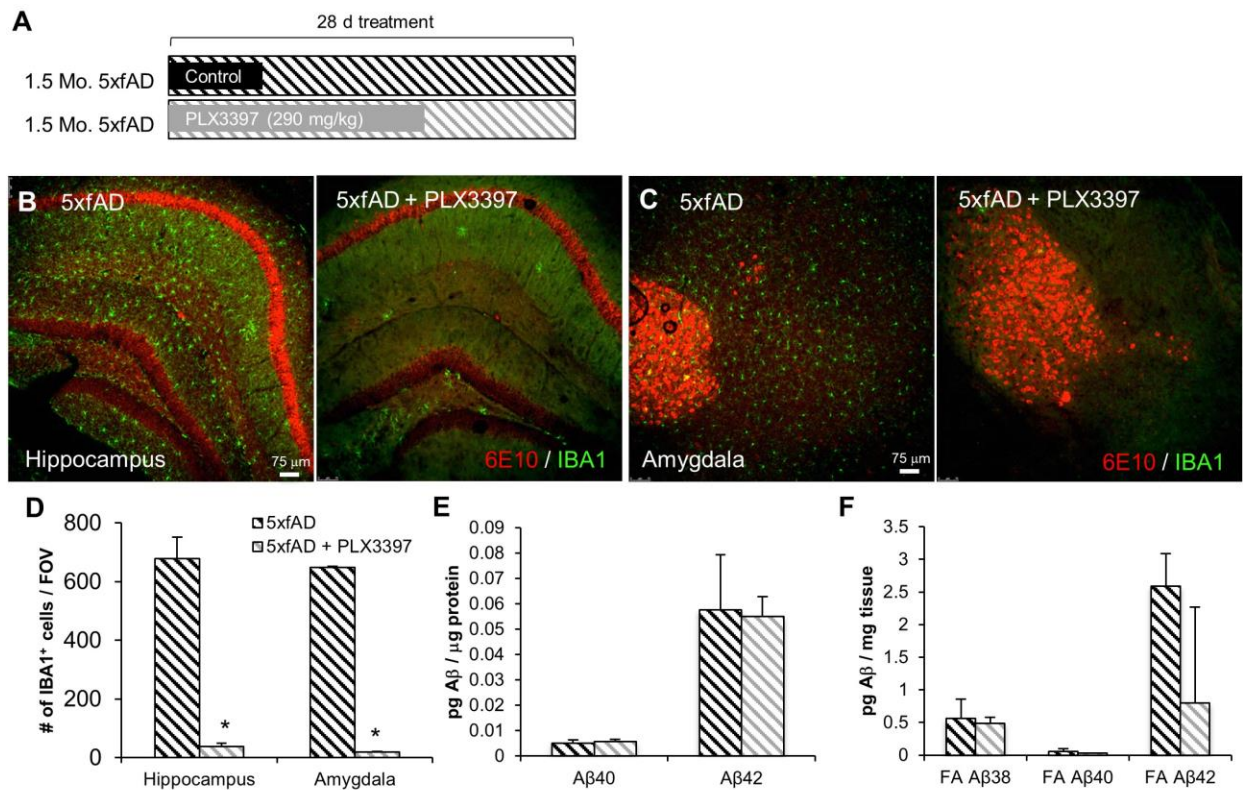


**Figure 1.4 Microglial elimination in young 5xfAD mice does not affect A $\beta$  pathology:** 1.5-month-old 5xfAD mice were treated with PLX3397 or control chow for 28 days. **A**, Experimental design. **B, C**, Representative 10X immunofluorescent IBA1 and 6E10 images of the hippocampus and amygdala. **D**, Quantification of microglial cells shows a significant reduction in the 5xfAD + PLX3397 group compared to the 5xfAD group in the hippocampus and amygdala (two-tailed unpaired t-test, p < 0.0001). **E, F**, Levels of A $\beta$  species in detergent-soluble fractions are unchanged with the elimination of microglia. Levels of A $\beta_{1-38}$  in the detergent-soluble fraction were below detection threshold. Statistical significance is denoted by \*P < 0.05. Error bars indicate SEM; (n=4/group).

ages or in the absence of pathology. As 5xfAD mice develop plaques from ~2 months of age, we treated 1.5-month-old mice with PLX3397 for 28 days (Fig. 1.4A). Immunolabeling for IBA1 and 6E10 (Fig. 1.4B and C) revealed extensive intraneuronal 6E10-reactivity in CA1 and amygdala neurons in both groups, but no extracellular plaques were observed. Microglial counts in these regions showed a ~95% decrease with PLX3397 treatment (Fig. 1.4D). To further analyze A $\beta$ , we used triplex ELISA to assess protein levels of A $\beta$ <sub>1-38</sub>, A $\beta$ <sub>1-40</sub>, and A $\beta$ <sub>1-42</sub>. We found no effect of microglial elimination on the amount of soluble (Fig. 1.4E) or insoluble (Fig. 1.4F) A $\beta$  protein. Together, these data indicate that microglia do not protect against A $\beta$  accumulation in the 5xfAD mice at a pre-plaque age.

### **Elimination of microglia in aged 5xfAD mice with the specific CSF1R inhibitor PLX5622**

PLX5622 is a brain-penetrant inhibitor of CSF1R that quickly eliminates microglia, but does not inhibit c-kit<sup>134,139</sup>. In order to confirm the effects of PLX3397 and to rule out other off-target effects, we treated a second cohort of 14-month-old 5xfAD mice for 28 days with 1200 mg/kg PLX5622 in chow. We again stained tissue for dense core plaques using Thio-S and immunolabeled microglia with IBA1 (Fig. 1.5A). Microglia were dramatically depleted with treatment, with most of the remaining cells being associated with dense core plaques, as with PLX3397 treatment (Figure 1.5B and E). Quantification revealed on average ~1 cell per plaque remaining (Fig. 1.5C), however, many plaques had 0 IBA1<sup>+</sup> cells associated with them (Fig. 1.5D). Further analyses

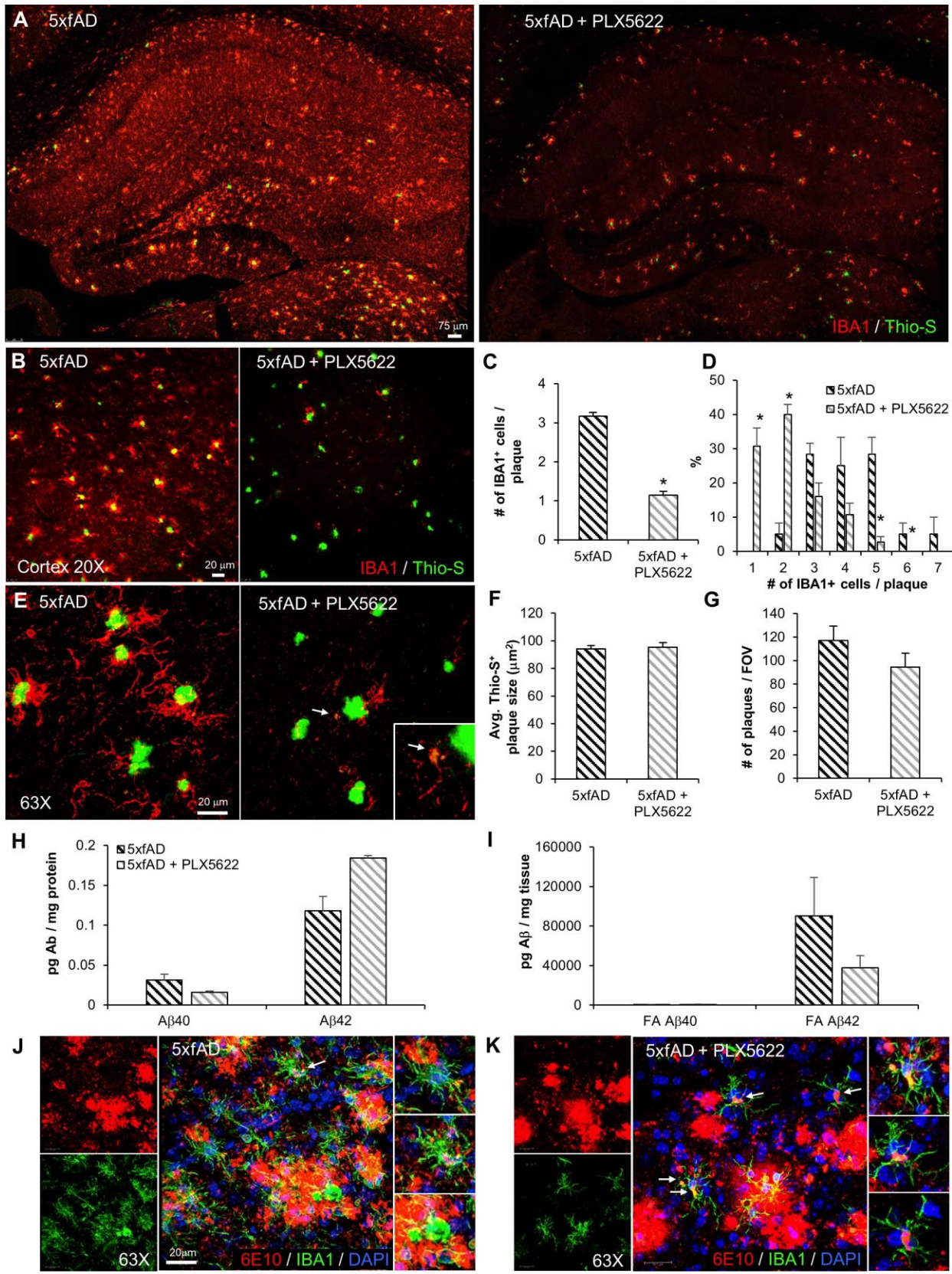


**Figure 1.5 Elimination of microglia with PLX5622:** 14-month-old 5xfAD mice were treated with PLX5622 or control chow for 28 days. **A, B, and E,** representative images showing dense-core plaques (Thio-S in green) and microglia (IBA1 in red) in the hippocampus and cortex. **C, D,** Quantification reveals ~65% decrease in plaque-associated microglia with PLX5622 treatment (two-tailed unpaired t-test;  $p < 0.0001$ ) and a significant increase in specifically 0 to 1 IBA1<sup>+</sup> cells associated with plaques in the PLX5622 group (two-tailed unpaired t-test;  $p < 0.0001$ ). **F, G,** Quantification of Thio-S<sup>+</sup> plaque areas and number of 6E10<sup>+</sup> plaques shows no effect of microglial elimination. **H, I,** Levels of soluble and insoluble A $\beta$  species in 5xfAD mice show no significant changes with microglial elimination. **J, K,** 63X image of microglia (IBA1 in green), plaques (6E10 in red), and cell nuclei (DAPI in blue). Statistical significance is denoted by \* $P < 0.05$ . Error bars indicate SEM ( $n = 4/\text{group}$ ).

revealed that all remaining IBA1<sup>+</sup> cells had cell bodies containing A $\beta$  (Fig. 1.5K; shown by white arrows) – in contrast, most IBA1<sup>+</sup> cells around plaques in untreated 5xfAD brains did not contain any A $\beta$  (Fig. 1.5J). Indeed, some of these IBA1<sup>+</sup> cells in the treated mice were Thio-S positive (Fig. 1.5E panel). However, as with the PLX3397-treated mice, we observed no change in the plaque area or total number (Fig. 1.5F and G), nor any significant changes in A $\beta$  protein levels (Fig. 1.5H and I), with this cohort of microglia-eliminated 5xfAD mice.

### **AD-related gene transcription is altered in 5xfAD mice**

RNA was extracted from flash-frozen brain tissue from 10-month-old mice treated with PLX3397 to analyze transcript levels of 180 inflammation-, Alzheimer's disease-, age-related genes, as part of a custom panel. Interestingly, transcript levels of *ApoE*, *Cstc*, and *Cstd*, which are implicated in lipid metabolism and protein degradation, respectively, were significantly increased in 5xfAD mice and attenuated with microglial elimination (Fig. 1.6A). No changes in APP, BACE1, or ADAM10 mRNA were found with either genotype or treatment. Similarly, AD-related signaling is largely unaffected by microglial elimination. In accordance with mRNA data, western blot analysis of steady-state levels of APP showed no differences with treatment (Fig. 1.6B and C).

Likewise, levels of the C-terminal fragments C99 and C83 showed no differences among groups (Fig. 1.6B and C).

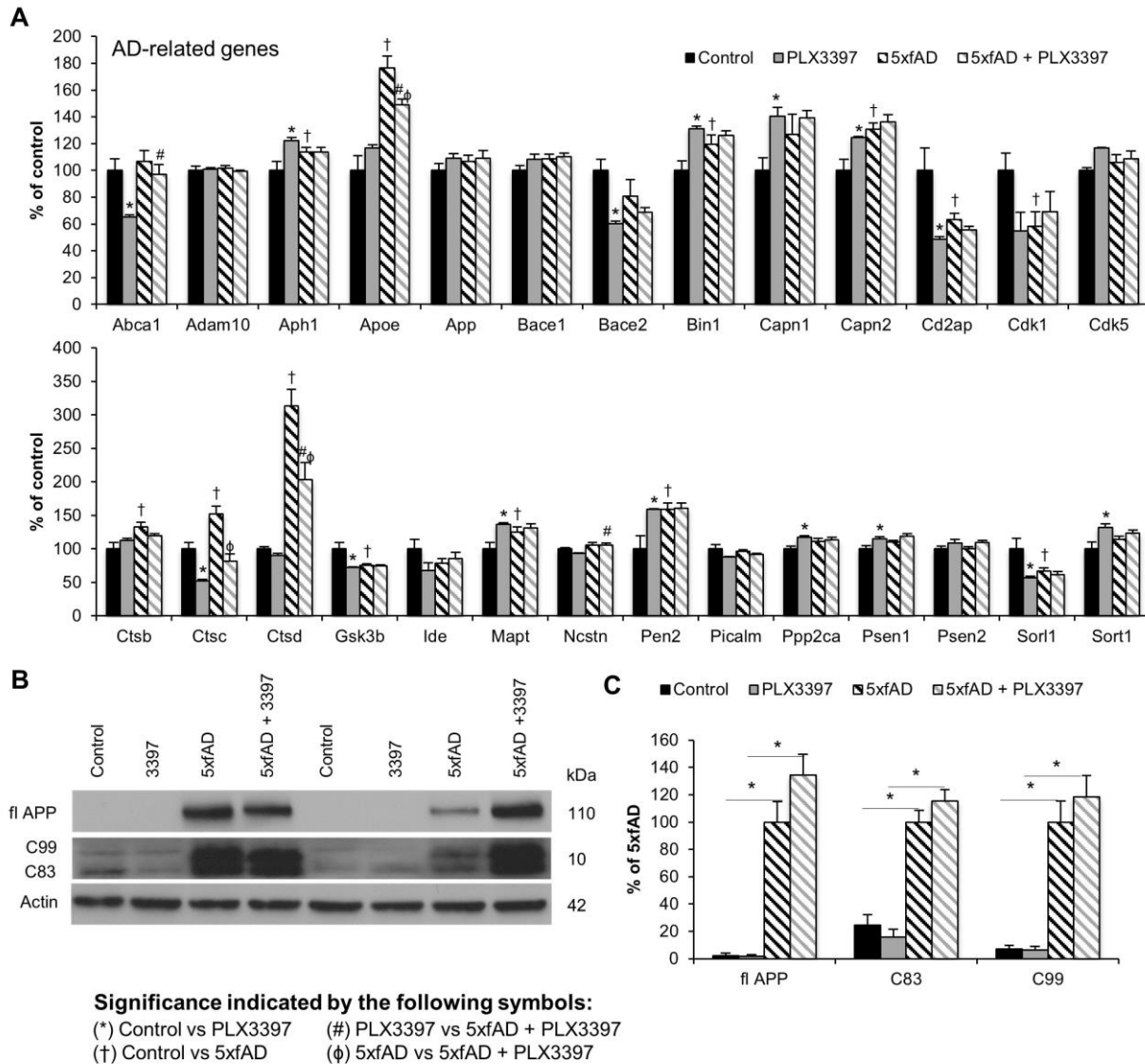


**Figure 1.6 Modest changes in Alzheimer's disease-related genes with microglial elimination:** transcript levels for Alzheimer's disease-related genes were analyzed using NanoString nCounter platform and immunoblots were performed to assess components of APP processing. **A**, Alzheimer's disease-related gene transcript levels in all four experimental groups. Symbols denote significant differences between groups ( $p < 0.05$ ): \*Control vs. PLX3397; †Control vs. 5xfAD; #PLX3397 vs. 5xfAD + PLX3397; ‡5xfAD vs. 5xfAD + PLX3397. **B**, **C**, Immunoblotting for full length APP, C99, and C83 showed significantly increased levels of each protein in 5xfAD mice compared to Control (via two way ANOVA;  $p < 0.0001$ ) and in 5xfAD + PLX3397 mice compared to PLX3397 (via two way ANOVA;  $p < 0.0001$ ), but showed no effect of microglial elimination in 5xfAD mice. Statistical significance is denoted by \* $P < 0.05$ . Error bars indicate SEM; ( $n = 4/\text{group}$ ).

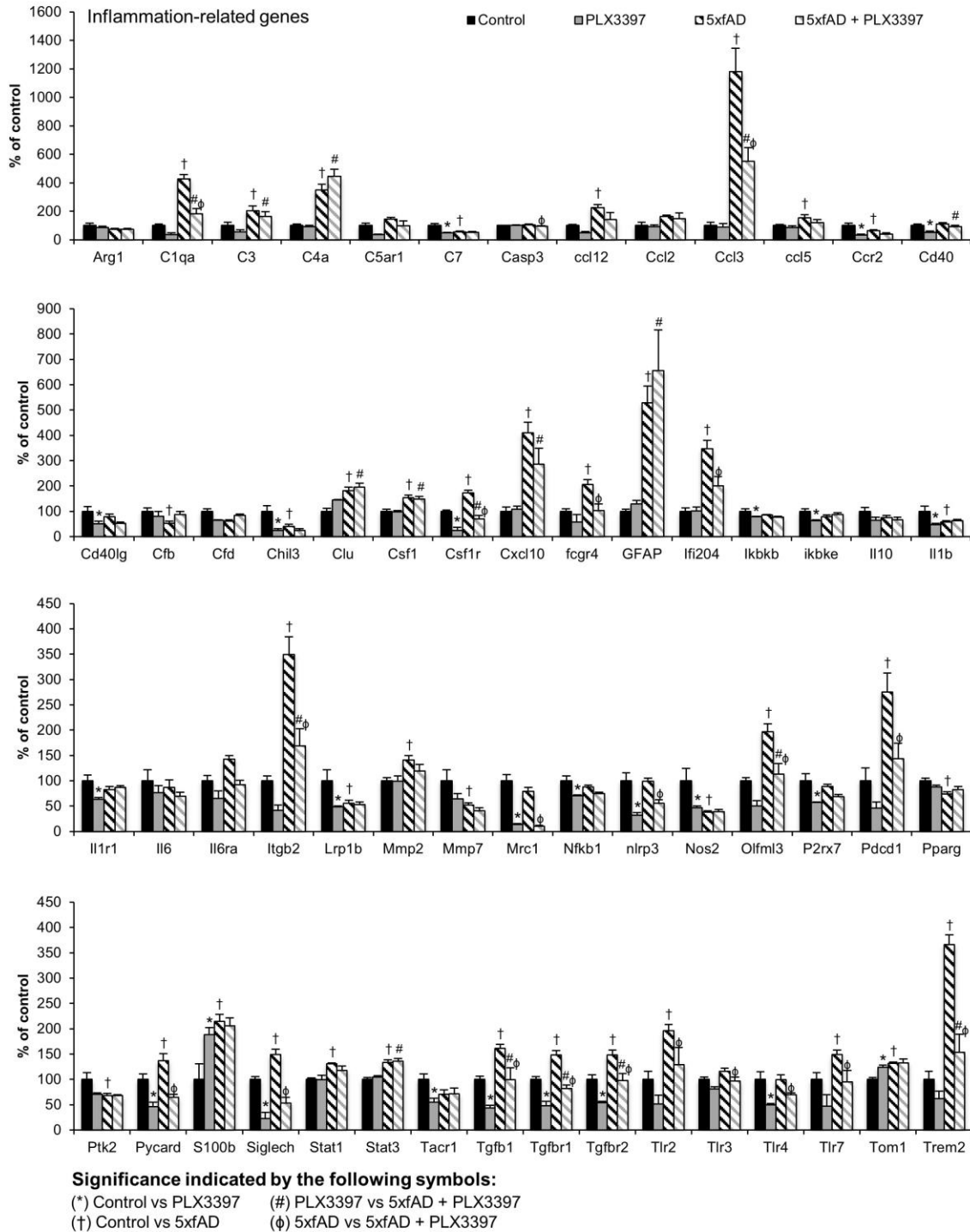


**Figure 1.7 Microglial elimination reduces neuroinflammatory signaling:** RNA transcripts for inflammation-related genes were analyzed using NanoString nCounter platform. Symbols denote significant differences between groups ( $p < 0.05$ ): Symbols denote significant differences between groups ( $p < 0.05$ ): \*Control vs. PLX3397; †Control vs. 5xfAD; #PLX3397 vs. 5xfAD + PLX3397; φ5xfAD vs. 5xfAD + PLX3397. Error bars indicate SEM; (n=4/group).

### **Microglial elimination reduces inflammation-related gene transcripts**

Since microglia are the primary immune cells of the brain, we wanted to determine how inflammatory signaling as a whole was impacted by microglial elimination in 5xfAD mice. RNA levels of many inflammation-related genes were significantly increased in 5xfAD mice compared to WT including complement (C1qa, C4a, and C3), chemokines (Ccl12, Ccl3, and Ccl5), and astrocytic genes (GFAP and S100). Crucially, the majority of increases are attenuated with microglial elimination in the 5xfAD mice (Fig. 1.7).

### **Astrocyte numbers are largely unaffected with microglial elimination**

As reactive gliosis is an important feature of Alzheimer's disease, we wanted to discern if microglial elimination impacts astrocyte numbers or responses. We immunolabeled tissue for reactive astrocytes using GFAP (green) and S100 $\beta$  (blue) with 6E10 (red) for plaques in the cortex and hippocampus (Fig. 1.8A, B, and D). GFAP expression is restricted to the hippocampal area in WT mice but is expressed in astrocytes around plaques in the cortex of 5xfAD mice, signifying reactive astrocytes. Accordingly, the number of GFAP<sup>+</sup> astrocytes was also increased in the hippocampal area, whilst S100 $\beta$ <sup>+</sup> astrocytes were also increased in both brain regions examined (Fig. 1.8C). Notably, the number of GFAP<sup>+</sup> cells was reduced in the cortex of 5xfAD mice treated with PLX3397, while treatment did not affect GFAP<sup>+</sup> cells in the hippocampus, or S100 $\beta$ <sup>+</sup> cells in either brain region. We also probed for Aldh1L1<sup>+</sup> astrocytes – another marker of astrocyte reactivity. No Aldh1L1<sup>+</sup> cells were detected outside blood vessels in WT mice but were apparent in 5xfAD animals where they were also GFAP<sup>+</sup> (Fig. 1.8E-G). Quantification of Aldh1L1<sup>+</sup> astrocytes in hippocampus and cortex of 5xfAD mice

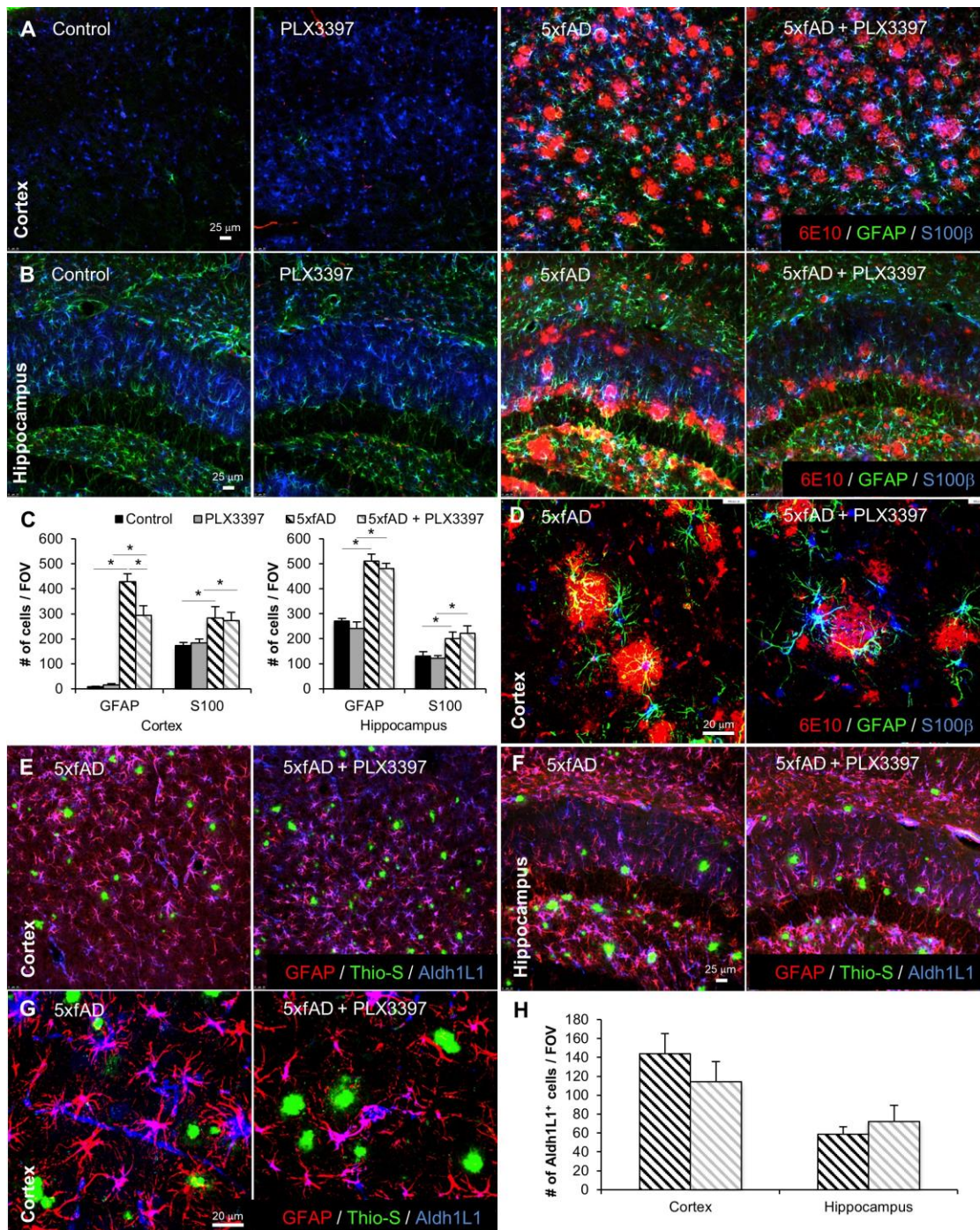


**Figure 1.8 Astrocyte numbers are not affected by microglial elimination.** **A, B**, 20X images of immunolabeling of astrocytes with GFAP (green) and S100β (blue) and plaques with 6E10 (red) in the cortex and hippocampus. **C**, Quantification revealed significant increases in GFAP<sup>+</sup> and S100β<sup>+</sup> cells in the 5xfAD mice compared to Control (via two-way ANOVA,  $p < 0.001$ ) and in 5xfAD + PLX3397 mice compared to PLX3397-treated mice (via two-way ANOVA,  $p < 0.001$ ). **D**, Representative 63X images of astrocytes and plaques in the cortex. **E, F**, 20X images of immunolabeling of astrocytes with GFAP (red) and Aldh1L1 (blue) with Thio-S staining plaques (green) in the cortex and hippocampus. **G**, Representative 63X images of astrocytes and plaques in the cortex. **H**, Quantification of Aldh1L1<sup>+</sup> cells showed no changes in expression with microglial elimination. Statistical significance is denoted

showed no changes in expression with microglial elimination (Fig. 1.8H).

### **Microglial elimination restores dendritic spine number in 5xfAD mice**

As activated microglia are thought to mediate synaptic stripping<sup>23,31</sup>, we sought to determine whether microglial elimination could affect dendritic spine number in 5xfAD mice. To that end, we stained tissue using the Golgi method (Fig. 1.9A) and counted and classified dendritic spines on non-primary apical dendrites in the CA1 region of the hippocampus (Fig. 1.9B and C). Total spine density was significantly decreased in 5xfAD mice compared to WT and a recovery of this effect was observed following microglial elimination (Fig. 1.9D). Specifically, mushroom spines were significantly decreased in the 5xfAD mice compared to controls, but the elimination of microglia significantly increased mushroom spines in 5xfAD mice. Elimination also shows a trend toward recovery of thin spines in these mice (Fig. 1.9D). Together, these data confirm previous findings of significant spine loss in the 5xfAD mouse model, and indicate that microglia modulate this process, as the elimination of these cells allows for the regeneration of previously lost dendritic spines.

### **Elimination of microglia prevents neuronal loss in 5xfAD mice**

An important and distinct feature of the 5xfAD mouse model is that these mice display overt neuronal loss in the subiculum at later stages<sup>176</sup>. As we had eliminated microglia over this crucial period, we stained brain tissue with cresyl violet to visualize cell nuclei and stereologically quantified the number of neurons in the subiculum (Fig. 1.9E). Quantification of neuronal populations revealed a significant decrease in neuronal number in the 5xfAD mice in the microglia-intact animals, whereas microglial elimination

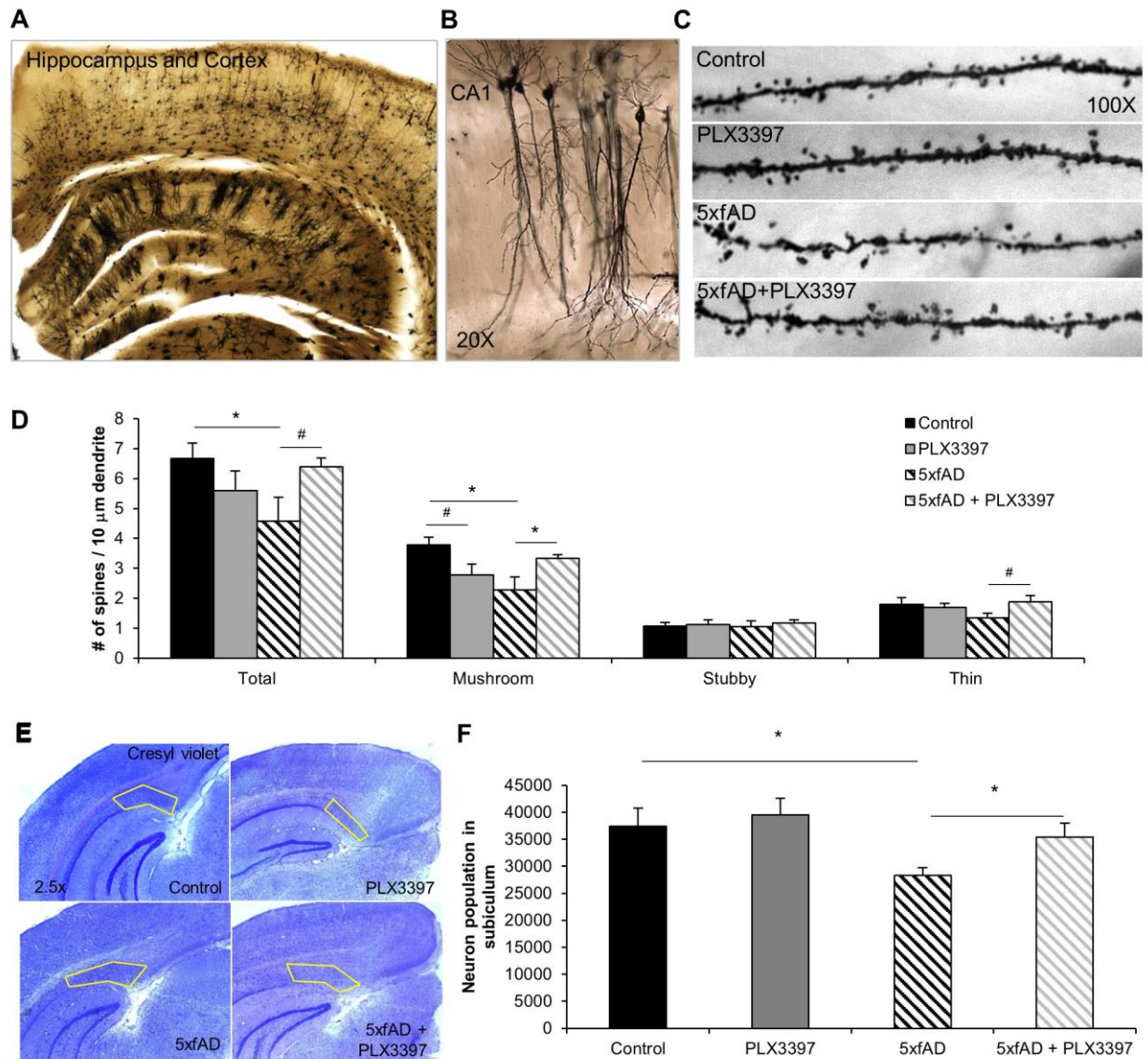


**Figure 1.9 Microglia modulate dendritic spine number in the CA1 and prevent neuronal loss in the subiculum of 5xfAD mice.** **A**, Representative 2.5X image of Golgi staining in hippocampus and cortex. **B**, Representative 20X image of CA1 neurons and dendritic branches. **C**, Representative 100X images of CA1 dendritic branches showing spines. **D**, The number of total (two-way ANOVA;  $p=0.0337$ ) and mushroom (via two-way ANOVA;  $p=0.0091$ ) dendritic spines is significantly decreased in 5xfAD mice, compared to control. 5xfAD + PLX3397 mice show significantly increased mushroom spine density (via two-way ANOVA;  $p=0.0416$ ) and a trend for recovery of total spine loss (via two-way ANOVA;  $p=0.0561$ ), as well as a trend for increased thin spine density compared to 5xfAD (via two-way ANOVA;  $p=0.066$ ). **E**, Representative 2.5X images of cresyl violet staining with the subiculum outlined in yellow. **F**, Stereological quantification of the number of neurons in the 5xfAD group showed a significant decrease in cell number compared to control (two-way ANOVA;  $p=0.0181$ ). The neuronal loss in the 5xfAD group is prevented with microglial elimination in the 5xfAD + PLX3397 group (two-way ANOVA;  $p=0.0458$ ). Statistical significance is denoted by \* $P<0.05$  and statistical trends by # $P<0.10$ . Error bars indicate SEM; ( $n=3-4$ /group).

in 5xfAD mice prevented this neuronal loss (Fig. 1.9F). These data corroborate previous reports of neuronal loss in the 5xfAD model in the subiculum at this age and indicate that microglia are actively contributing to neuronal loss in these mice.

## DISCUSSION

The importance of microglia in Alzheimer's disease has been highlighted by GWAS, which have identified a number of single nucleotide polymorphisms (SNPs) associated with risk for the development of Alzheimer's disease that are associated with microglia function, including *TREM2*<sup>169</sup>, *CD33*<sup>185</sup>, *BIN1*<sup>186,187</sup>, and *CR1*<sup>188</sup>. Thus, understanding the various roles that microglia play in the healthy and Alzheimer's disease brain are crucial in order to determine how these polymorphisms affect microglial function.

We have previously shown that microglial elimination can be achieved in the healthy adult mouse brain by treatment with small-molecule inhibitors of the CSF1R<sup>133,139</sup>, with many groups confirming our findings<sup>134-137</sup>. We also found that chronically activated microglia following extensive neuronal injury can be eliminated with the same approach. Our studies also revealed that microglial elimination following neuronal insult improved functional outcomes, whereas elimination of microglia during the lesion exacerbated neuronal loss, revealing differential roles of microglia in injury response<sup>35</sup>. In this study, we sought to define the roles of microglia in mediating Alzheimer's disease pathogenesis through the administration of CSF1R inhibitors at doses sufficient to eliminate microglia, rather than at lower doses that modulate microglial function without eliminating them. We first set out to determine if microglia in the brains of aged 5xfAD mice are still dependent on CSF1R signaling for their survival. Importantly, we show that

28 days of continuous treatment with either PLX3397 or PLX5622 leads to an ~80-90% reduction in microglia, respectively, throughout the CNS in adult 5xfAD mice.

The elimination of microglia for 28 days from 5xfAD mice allows us to explore the role that these cells play in A $\beta$  and plaque homeostasis/pathogenesis. Traditionally, it has been thought that microglia respond to the presence of A $\beta$  plaques by helping clear them from the brain via phagocytosis of A $\beta$ -fibrils<sup>93</sup>. Reactive microglia have been shown to encircle plaques and A $\beta$  can be detected within their cytoplasm<sup>95,96,98</sup>. Furthermore, a recent study showed that microglia tightly surround plaques and prevent further growth<sup>117</sup>. However, results from a study of inducible microglial ablation found that eliminating microglia from the brains of APP overexpressing mice for 4 weeks does not affect plaque burden<sup>104</sup>. Our findings are in complete agreement with this, as we observed no changes in A $\beta$  levels, either soluble or insoluble following microglial elimination. Moreover, plaque load and average plaque size were also unaffected with CSF1R inhibitor treatment. Thus, microglia do not appear to affect brain A $\beta$  levels and are not a source of significant A $\beta$  clearance from the CNS, even in young, pre-pathological mice. Notably, we found a subset of CSF1R-inhibitor resistant IBA1<sup>+</sup> cells following treatment and further analysis revealed that many of these cells associated with dense core plaques and contained A $\beta$  within their cell bodies. The presence of these CSF1R-inhibitor resistant cells demonstrates heterogeneity of IBA1<sup>+</sup> cells around plaques – even cells surrounding the same plaque may have different origins and functions. For example, recent studies that have crossed TREM2 knockout mice to APP mice, including the 5xfAD model, have demonstrated a stark reduction in plaque-associated IBA1<sup>+</sup> cells with TREM2 deletion. One study suggested that the reduction in

these cells was due to a lack of infiltrating monocytes from the periphery<sup>44</sup> – as monocytes are not eliminated with the doses of CSF1R inhibitors used in this study<sup>134,173</sup> – this could also explain the subset of CSF1R-inhibitor resistant cells around plaques. Alternatively, TREM2 can act as a survival signal in place of CSF1R signaling<sup>43</sup>, and it could be that a subset of IBA1<sup>+</sup> cells around plaques upregulate TREM2, allowing them to survive in the presence of CSF1R inhibitors.

As a parallel to our own findings, in a mouse model of glioblastoma multiforme with CSF1R inhibitor treatment, researchers found reduced numbers of tumor-associated IBA1<sup>+</sup> cells, but not a complete eradication of these cells<sup>189</sup>, providing further support of the existence of heterogeneous populations of IBA1<sup>+</sup> cells in the brain. Regardless of the origin of the surviving IBA1<sup>+</sup> cells, more than 30% of plaques in treated mice had no IBA1<sup>+</sup> cells associated with them, and as we observed no effect on plaque number or size, these findings suggest that remaining IBA1<sup>+</sup> cells are not significantly contributing to the regulation or maintenance of A $\beta$  pathologies. Further evidence that microglia in the diseased brain are not protective against plaque development and growth has also come from studies with inducible APP transgenic mice, in which switching off the APP transgene after plaque formation does not lead to the breakdown of plaques by the brain<sup>115</sup>. Additionally, recent studies have shown that microglia around plaques are in a non-productive state due to overproduction of IL-10<sup>105</sup>, and that deletion of IL-10 restimulates microglia to phagocytose and clear plaques<sup>190</sup>. Similarly, it has been shown that Prostaglandin E2 (PGE2) is overproduced in these conditions, and deletion of PGE2 stimulates the clearance of plaques<sup>106</sup>. Likewise, studies using Alzheimer's disease mice on a NOS2 null background (to mimic the human system) show that

microglia are suppressed around plaques and inhibitors of arginase can also restimulate these microglia to protect against Alzheimer's disease pathology<sup>107</sup>. Following the findings that microglia in the presence of Alzheimer's disease pathology appear to be suppressed, stimulation of microglia is known to induce plaque breakdown, with agents such as IL-1 $\beta$ <sup>109</sup>, CSF1<sup>191</sup>, and lipopolysaccharide (LPS)<sup>108</sup>, as well as repeated scanning ultrasound treatments<sup>192</sup>. Collectively, these results are in congruence with our data and suggest that microglia in the Alzheimer's disease brain are not able to effectively clear A $\beta$  from the CNS or protect against plaque formation or growth. Thus, given their chronic reactivity, it is imperative to determine what effects microglia are exerting in the Alzheimer's disease brain.

We found that elimination of microglia reduces brain-wide inflammatory signaling in 5xfAD mice, as indicated by RNA analysis of several inflammation-related genes. We observed reductions in microglia reactivity-associated transcripts, including *C1q*, *Tlr2*, *Tlr3*, *Tlr4*, *Tlr7*, *Ccl3*, *Nlrp3*, and *Pdcd1*, as well as reductions in anti-inflammatory/phagocytic markers, such as *Tgfb1*, *Tgfb1r1*, *Tgfb1r2*, *Mrc1*, and *Itgb2*. Additionally, our results show that elimination of microglia is beneficial for a hippocampal-dependent cognitive task. These findings are in line with many others that show modulating microglial function in Alzheimer's disease models can restore/improve memory<sup>193-196</sup>. Furthermore, others have shown that inflammatory factors are necessary for A $\beta$ -induced LTP deficits<sup>197</sup>. Altogether, this suggests that microglia contribute to the memory impairments seen in Alzheimer's disease transgenic mice. Microglia produce a plethora of modulatory substances, but also interact with the local brain environment, and it is likely a combination of these activities that contributes to impairments. For

example, *in vivo*, microglia have been shown to cause neuronal loss in Alzheimer's disease mice via signaling through CX3CR1, a chemokine receptor expressed by microglia involved in neuron-microglia communication<sup>198</sup>. Synaptic and neuronal loss is well documented in the 5xfAD model and is likely one mechanism contributing to deficits in contextual memory<sup>175-177</sup>. In our study, we find the total number of dendritic spines to be significantly decreased in 5xfAD mice compared to controls, and this is accounted for primarily by decreases in mushroom spines. Critically, the elimination of microglia reversed reductions in mushroom spines in 5xfAD mice, suggesting that the absence of microglia allows for the regeneration of lost spines seen in the Alzheimer's disease brain. Additionally, we found a significant reduction of neurons in the subiculum of 5xfAD mice, which was prevented with the elimination of microglia, indicating an important and detrimental function of microglia in mediating neuronal loss in aged 5xfAD mice.

Overall, our results show that microglia in the diseased brain are dependent on CSF1R signaling for their survival. Importantly, we find that chronic microglial elimination is not detrimental to animals, but rather, improves functional outcomes and disease-related synaptic aberrations, while preventing neuronal loss.

## CHAPTER TWO

### ASCERTAINING MICROGLIAL FUNCTIONS IN ALZHEIMER'S DISEASE ONSET AND PROGRESSION

#### INTRODUCTION

Alzheimer's disease (AD) is a progressive, age-related neurodegenerative disorder thought to be triggered by the appearance and build-up of amyloid- $\beta$  (A $\beta$ ) plaques in the cortex<sup>199,200</sup>. These plaques subsequently spread throughout the forebrain and lead to a cascade of events, culminating in synaptic and neuronal loss that underlie the disease-associated memory impairments. Genome-wide association studies have identified numerous genes that confer increased risk for developing the disease; however, the mechanisms underlying plaque formation remain unclear. Discerning commonalities in the function of these disease-associated genes may elucidate potential biological mechanisms involved in the production of plaques<sup>201</sup>. Several of the top identified risk-conveying genes are highly enriched in myeloid cells (*CR1*, *CD33*, *ABCA7*, *TREM2*, *MS4A*, *EPHA1*, *SPI1*<sup>169,185,202</sup>), highlighting the link between myeloid biology and the risk for developing AD. Within the CNS, microglia perform homeostatic maintenance, immune-related, and phagocytic functions. Their reported capacity for A $\beta$  phagocytosis and clearance<sup>203</sup> led to the suggestion that age-related changes in microglial function reduce clearance of neuronally-derived A $\beta$  from the brain<sup>204</sup>, thus allowing plaque formation, as modeled in *ex-vivo* systems<sup>94,205</sup>. Indeed, we and other groups report that following the initial period of plaque formation, microglia surround the plaques and subsequently mount a harmful and non-resolving inflammatory response. Despite this

response, however, A $\beta$  clearance and plaque modulation/dynamics is unaffected<sup>115,132,206</sup>, yet the removal of the microglia at advanced stages of pathology protects against synaptic and neuronal loss<sup>132</sup>. Here, we set out to explore the contribution(s) of microglia to plaque formation in the initial stages of the disease, which requires prolonged depletion of microglia throughout the plaque-forming period. To that end, we designed, synthesized, and optimized a potent, specific, orally bioavailable, and brain-penetrant CSF1R inhibitor, PLX5622, to deplete microglia for >6 months in 5xfAD mice. With the elimination of microglia, we uncovered critical roles of these cells in plaque formation, compaction, and growth, mitigating neuritic dystrophy, and modulating hippocampal neuronal gene expression in response to A $\beta$  pathology. These results implicate microglia as critical and causative in the development and progression of multiple facets of AD.

## **MATERIALS AND METHODS**

**Compounds:** PLX3397 (pexidartinib) was synthesized following the published procedure<sup>207</sup>. For long term dosing, the compounds were formulated in AIN-76A standard chow by Research Diets Inc. at 1200 ppm (PLX5622), 300 ppm (PLX5622), 600 ppm (PLX3397), and 75 ppm (PLX3397).

**Animal Treatments:** All rodent experiments were performed in accordance with animal protocols approved by the Institutional Animal Care and Use Committee at the University of California, Irvine. The 3xTg-AD<sup>208</sup> and 5xfAD<sup>174</sup> mouse models have been previously described in detail. At the end of treatments, mice were euthanized via CO<sub>2</sub>

inhalation and transcardially perfused with 1X phosphate buffered saline (PBS). For all studies, brains were removed, and hemispheres separated along the midline. Brain halves were either flash frozen for subsequent biochemical analysis or drop-fixed in 4% paraformaldehyde (PFA (Thermo Fisher Scientific, Waltham, MA)) for immunohistochemical analysis. Fixed half brains were sliced at 40  $\mu$ m using a Leica SM2000R freezing microtome. The flash-frozen hemispheres were microdissected into cortical, hippocampal, and thalamic/striatal regions and then ground with a mortar and pestle to yield a fine powder. One-half of the powder from cortical and thalamic regions was homogenized in 500 or 250  $\mu$ l Tissue Protein Extraction Reagent (TPER (Life Technologies, Grand Island, NY)), respectively, with protease (Roche, Indianapolis, IN) and phosphatase inhibitors (Sigma-Aldrich, St. Louis, MO) and centrifuged at 100,000 g for 1 hour at 4°C to generate TPER-soluble fractions. For formic acid-fractions, pellets from TPER-soluble fractions were homogenized in 500 or 250  $\mu$ l 70% Formic Acid and centrifuged at 100,000 g for 1 hour at 4°C. Protein concentration in each fraction was determined via Bradford<sup>209</sup> and Lowry assays (Bio-Rad, per manufacturer's instructions). For RNA analyses, the second half of powder was processed with an RNA Plus Universal Mini Kit (Qiagen, Valencia, CA) according to the manufacturer's instructions.

**Human Tissue:** Human postmortem tissue from non-demented, non-demented high pathology, and Alzheimer's disease subjects was obtained from the Alzheimer's Disease Research Center, UC Irvine with consent from the UC Irvine Ethics Committee. Neuropathological examination included Braak and Braak staging for plaques and

tangles and diagnosis of neuropathological AD using National Institute on Aging-Reagan criteria.

**Behavioral Testing:** ANY-Maze software was employed to video-record and track animal behavior. The following behavioral paradigms were carried out as previously described<sup>132,133,174</sup>:

Elevated plus maze (EPM): Mice were placed in the center of an elevated plus maze (arms 6.2 x 66cm, with side walls 15 cm high on two closed arms, elevated 46 cm above the ground) for 5 min to assess anxiety.

Morris water maze (MWM): Mice were placed in a plastic circular pool filled with opaque tap water (water mixed with water-soluble white paint). A white plastic platform was submerged 0.5 cm below the surface of the water. Distinct two-dimensional visual cues were positioned around the perimeter of the pool. The pool was visually divided into four quadrants, and the hidden platform was placed in one of these quadrants (#2), where it remained throughout the acquisition trials. Visual cues were taped to the walls to allow mice to create a spatial map during acquisition of the task. At the beginning of each acquisition trial, mice were placed on the platform for 10 s and then subsequently placed in the pool (quadrants were pseudorandomized) to swim freely for 60 s or until the platform was located. After all mice completed four trials, they were returned to their home cages. Twenty-four hours after the last day of acquisition testing, the platform was removed and the mice were subjected to a 60 s probe trial to assess spatial memory for the platform location.

**Flow Cytometry:** Blood was drawn via cardiac puncture and incubated with ammonium-chloride-potassium lysing buffer for red blood cell lysis. Blood leukocytes were subsequently blocked with anti-mouse CD16/32 (BioLegend) and stained with fluorophore-conjugated antibodies A700 anti-mouse CD45, PE anti-mouse CD11b, APC-Cy7 anti-mouse CD11c, PE-Cy7 anti-mouse CD4, APC anti-mouse CD8 and FITC anti-mouse CD19 (BioLegend) as well as propidium iodide (PI; Invitrogen) for live/dead discrimination. Data were acquired on a BD FACSAria II and analyzed using the FlowJo software to assess peripheral cell counts. Cells were gated on CD45<sup>+</sup>PI<sup>-</sup> live singlets.

**Confocal Microscopy:** Immunofluorescent labeling was performed on mouse and human brain sections following a standard indirect technique as previously described<sup>180</sup>. Mice were perfused with PBS prior to tissue fixation, followed by tissue sectioning to produce 40  $\mu\text{m}$  thick floating sections. Human sections were obtained from 4% PFA drop-fixed regions of the middle frontal gyrus of the cortex and processed into 25  $\mu\text{m}$  thick floating sections. Primary antibodies and dilutions used are as follows: anti-ionized calcium-binding adapter molecule 1 (IBA1; 1:1000; Wako, Osaka, Japan), anti-A $\beta$ <sub>1-16</sub> (6E10; 1:1000; BioLegend, San Diego, CA), anti-A11 oligomers (A11; 1:100; Thermo-Fisher Scientific), anti-amyloid fibrils OC (OC; 1:100; gifted from Charles Glabe, Irvine, CA), anti-A $\beta$ <sub>1-42</sub> (1:200, Abcam), anti-CD68 (1:500; Bio-Rad, Hercules, CA), anti-CD11b (1:50, Bio-Rad), anti-CD31 (1:200; BD Pharmingen, San Diego, CA), anti- $\beta$ -amyloid [pyroglutamate-3] (p3GluA $\beta$ ; 1:500; Novus Biologicals, Littleton, CO), anti-lysosomal associated membrane protein 1 (LAMP1; 1:200; Santa Cruz Biotechnology, Dallas, TX), anti-amyloid precursor protein (APP), c-terminal (1:500; Sigma-Aldrich, St. Louis,

Missouri), anti-S100 $\beta$  (1:200; Abcam, Cambridge, MA), anti-Apolipoprotein E (ApoE; 1:100; Abcam), and anti-gial fibrillary protein (GFAP; 1:1000; Abcam). Thioflavin-S (Thio-S; Sigma-Aldrich) staining was carried out as previously described<sup>181</sup>. Amylo-Glo (Biosensis, Thebarton, South Australia, AU) staining was performed according to the manufacturer's instructions. Total microglia and plaque counts/volumes were obtained by imaging comparable sections of tissue from each animal at the 20X objective, at multiple z-planes, followed by automated analyses using Bitplane Imaris 7.5 spots or surfaces modules, respectively. Plaque circularity was evaluated using ImageJ software. Hemisphere stitches were imaged using StereoInvestigator Software on a Zeiss Imager.M2 Stereology Scope. Three-dimensional reconstruction of microglia and plaques was generated using the surfaces module of Bitplane Imaris 7.5.

**Immunoblotting:** Immunoblotting was performed as previously described<sup>132,133</sup>. Antibodies and dilutions used include anti-6E10 (as described above), anti-APP C-Terminal (1:1000; Calbiochem, San Diego, CA) for C99 and C83, anti-ADAM10 (1:1000; Abcam), anti- $\beta$ -secretase 1 (BACE1; 1:1000; Abcam), anti-Presenilin-1 (PS1; 1:1000; Abcam), anti-Presenilin enhancer 2 (PEN2; 1:500; Abcam), anti-A11 (1:1000, Thermo-Fisher Scientific), and anti- $\beta$ -actin (1:10,000; Sigma-Aldrich). Quantitative densitometric analyses were performed on digitized images of immunoblots with ImageJ software.

**A $\beta$  ELISA:** Isolated protein samples were transferred to a blocked MSD Human (6E10) A $\beta$  triplex ELISA plate (A $\beta$ <sub>1-38</sub>, A $\beta$ <sub>1-40</sub>, A $\beta$ <sub>1-42</sub>) and incubated for two hours at room temperature with an orbital shaker. The plate was then washed and measurements

obtained using a SECTOR Imager 2400, per the manufacturer's instructions (Meso Scale Discovery, Gaithersburg, MD).

**RNA Sequencing:** Whole transcriptome RNA sequencing (RNA-Seq) libraries were produced from Wild-type (WT), PLX5622, 5xfAD, and 5xfAD + PLX5622 mice treated from 1.5 – 7 months of age, brains that were microdissected into Cortex, Hippocampus, and Thalamus (n=4/group for each of the 3 brain regions = 48 total samples). Briefly, 100-600ng of RNA were depleted of ribosomal RNA, fragmented, reverse transcribed and ligated to indexed sequencing adapters using the KAPA RNA HyperPrep Kit with RiboErase. Amplified libraries were combined into 4 pools of 12 libraries and sequenced on 4 lanes of a HiSeq4000 producing 50bp single-end reads. This work used the Vincent J. Coates Genomics Sequencing Laboratory at UC Berkeley, supported by NIH S10 OD018174 Instrumentation Grant.

Reads were mapped to the reference mouse genome (mm10) using STAR<sup>210</sup> aligner and quantified with the featureCounts function of the *Rsubread*<sup>211</sup> package in R<sup>212</sup>. After filtering out low-count genes, count distributions were scaled using the calcNormFactors function of the *edgeR*<sup>213</sup> package. Transgene/human alignments were not filtered out from mouse reads. Principal component analysis was performed using the plotMDS function of the *limma*<sup>214</sup> package in R. Normalized counts were prepared and fitted to linear models using the voom and lmf functions of *limma* respectively. Gene set testing was performed using the camera function of the *limma* package.

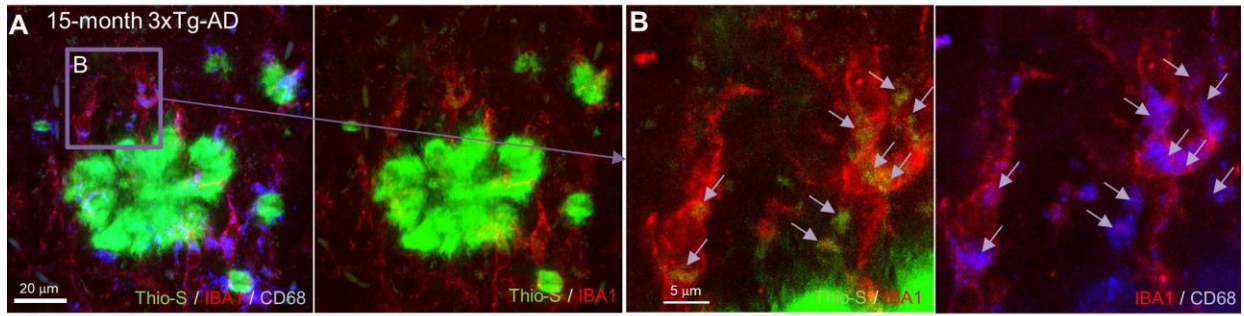
**Statistics:** Every reported  $n$  is the number of biologically independent replicates. No statistical methods were used to predetermine sample sizes; however, our sample sizes are similar to those reported in recently published similar studies<sup>132,215</sup>. Behavioral, biochemical, and immunohistological data were analyzed using either two-tailed independent-samples t-test (Control vs. Wild-type (WT) or 5xfAD vs. 5xfAD + PLX3397/PLX5622) in Microsoft Excel or as a one- (Diet: Control vs. PLX3397/PLX5622 vs. Repopulation) or two-way ANOVA (Diet: Control vs. PLX3397/PLX5622 and Genotype: WT vs. 5xfAD) using GraphPad Prism Version 6 (La Jolla, CA). Tukey's post hoc tests were employed to examine biologically relevant interactions from the two-way ANOVA regardless of statistical significance of the interaction. For RNA analyses, moderated t-statistics and corresponding p-values (raw) were calculated for each of the relevant comparisons for each gene (5xfAD vs. WT in cortex, hippocampus, or thalamus, 5xfAD + PLX5622 vs. 5xfAD in cortex, hippocampus, or thalamus, and WT + PLX5622 vs. WT in cortex, hippocampus, or thalamus), as well as the comparisons between brain regions (cortex vs. hippocampus, cortex vs. thalamus, and hippocampus vs. thalamus for both WT and 5xfAD mice) using the eBayes function in *limma*. Raw p-values were adjusted across all comparisons to account for multiple testing using the decideTests function (Benjamini-Hochberg method). Genes with an adjusted p-value below 0.05 were considered differentially expressed. Data distribution was assumed to be normal, but this was not formally tested. Symbols denote significant differences between groups: \* $p < 0.05$ , \*\* $p < 0.01$ , and \*\*\* $p < 0.001$ . Statistical trends are accepted at  $p < 0.10$  (#). Data are presented as raw means and standard error of the mean (SEM).

## RESULTS

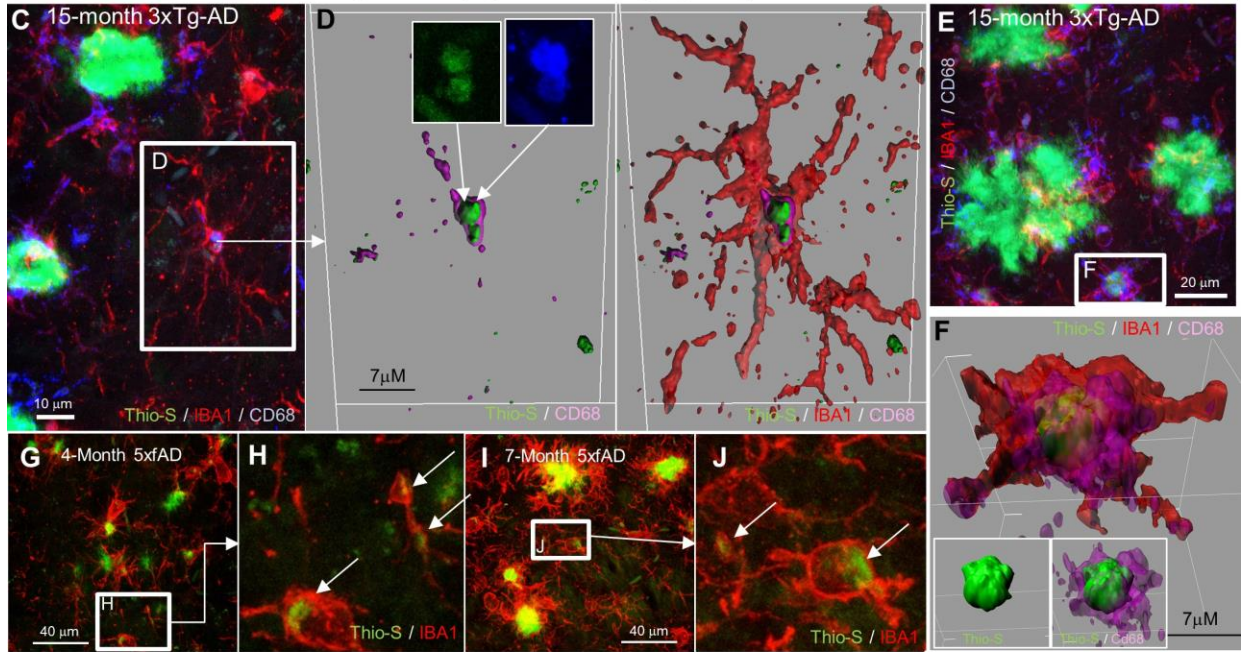
### **Non-plaque associated microglia contain A $\beta$ aggregates in mouse models of AD and humans**

The aggregation of A $\beta$  is an initial step in the formation of plaques, requiring an acidic pH<sup>216</sup> and micromolar concentrations of A $\beta$  monomers<sup>217</sup>. The extracellular space does not meet these requisite conditions, suggesting that A $\beta$  aggregation originates elsewhere. In contrast to the extracellular space, microglial lysosomes provide a suitable environment to facilitate A $\beta$  aggregation, potentially contributing to the onset of plaque pathology<sup>218</sup>. To investigate the potential for microglia-mediated plaque formation, we examined A $\beta$  aggregates within microglia in transgenic mouse models of AD. In 15-month-old 3xTg-AD mice, a time point at which plaques are beginning to form, we stained tissue for Thio-S (aggregated A $\beta$ ), microglia, and lysosomes. While plaque-associated microglia show accumulation of aggregates within their lysosomes (Fig. 2.1A, B; as well established<sup>219</sup>), we also observed non-plaque-associated microglia, including ramified microglia, accumulating aggregates within lysosomal compartments (Fig. 2.1C, D), and microglia containing intracellular aggregates the size of small plaques (Fig. 2.1E, F). The absence of nearby plaques suggests that existing aggregated A $\beta$  was not the source of these intracellular deposits. Similarly, non-plaque-associated microglia in 4- and 7-month old 5xfAD brains also showed accumulation of Thio-S<sup>+</sup> material (Fig. 2.1G-J), as well as aged human postmortem brains, including non-demented, high pathology non-demented, and Alzheimer's disease subjects (Fig.

Plaque-associated microglia contain aggregated A $\beta$  in their lysosomes in AD mouse models



Microglia distal to plaques also contain aggregated A $\beta$  in AD mouse models



Microglia distal to plaques also contain aggregated A $\beta$  in Human tissue

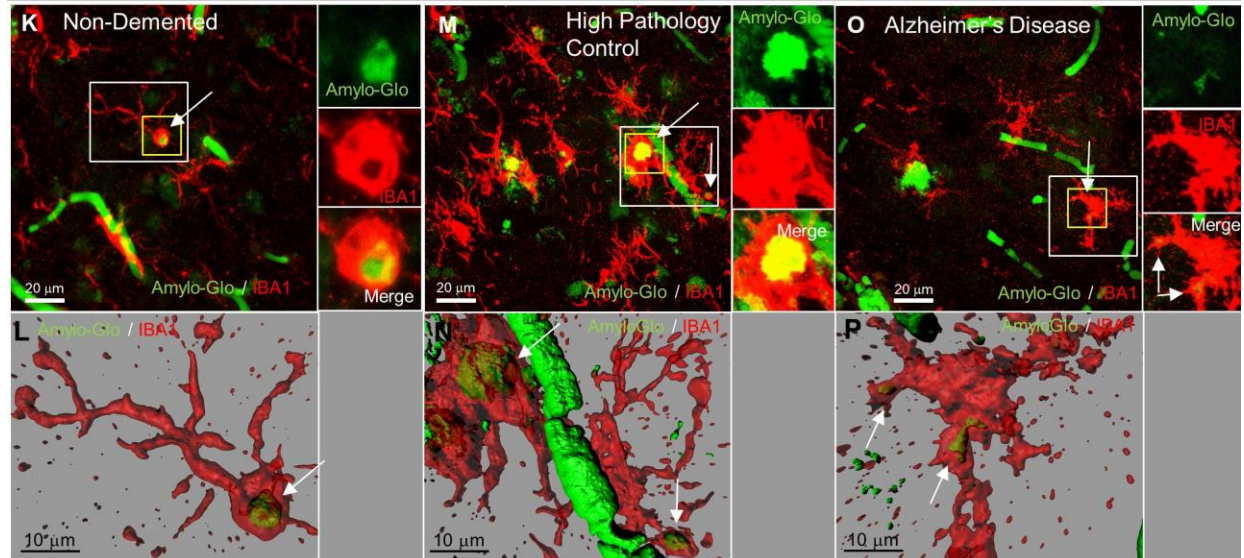


**Figure 2.1: Plaque-distal microglia contain aggregated A $\beta$ .** **A-C, E**, 15-month-old 3xTg-AD mice were stained for dense core deposits with Thio-S (in green), and immunolabeled for microglia (IBA1 in red) and macrophage lysosomes (CD68 in blue; **A, C**, and **E**) with zoomed image (**B**) of Thio-S<sup>+</sup> material within microglia and within lysosomes, separately. **D-F**, Three-dimensional reconstruction of microglia (IBA1 in red), the microglial lysosome (CD68 in purple), and fibrillar A $\beta$  (Thio-S in green), demonstrating the localization of A $\beta$  to the microglial lysosome in non-plaque associated microglia. **G-J**, 5xfAD animals stained for dense-core deposits (Thio-S in green) and immunolabeled for microglia (IBA1 in red; **G** and **I**), with zoomed images (**H** and **J**) demonstrating Thio-S<sup>+</sup> aggregates in microglial cell bodies in 4- and 7-month-old 5xfAD mice. **K, M, O**, Representative images from human cortical sections of non-demented, high pathology non-demented, and AD subjects, respectively, stained for A $\beta$  plaques (Amylo-Glo in green) and microglia (IBA1 in red). **L, N, P**, Three-dimensional reconstruction of microglia (IBA1 in red) and aggregated A $\beta$  (Amylo-Glo in green), showing plaque-distal microglia containing A $\beta$ .

2.1K-P). Thus, microglia in plaque-forming regions in mouse and human brains can accumulate aggregated A $\beta$  intracellularly, and we hypothesize that this could be an initial and crucial step toward plaque formation.

### **Extended elimination of microglia does not induce cognitive or peripheral circulating cell abnormalities**

Having designed and optimized PLX5622 for microglia depletion, we sought to explore the contributions of these cells in the initial stages of AD pathology. To that end, 5xfAD animals, which exhibit plaque pathology from 3 months of age, underwent treatment at 1.5 months of age with PLX5622-formulated chow (1200 ppm) or control diet continuously for either 10 or 24 weeks. Four treatment groups were included: Wild-type, PLX5622, 5xfAD, and 5xfAD + PLX5622 (n=12/group; sex-balanced; Fig. 2.2A). Initial characterization focused on the 24-week treated animals. Terminal PK values revealed no differences between PLX5622-treated groups in either plasma or brain (Fig. 2.2B) and no significant differences were seen in circulating leukocyte subsets (Fig. 2.2D) with treatment.

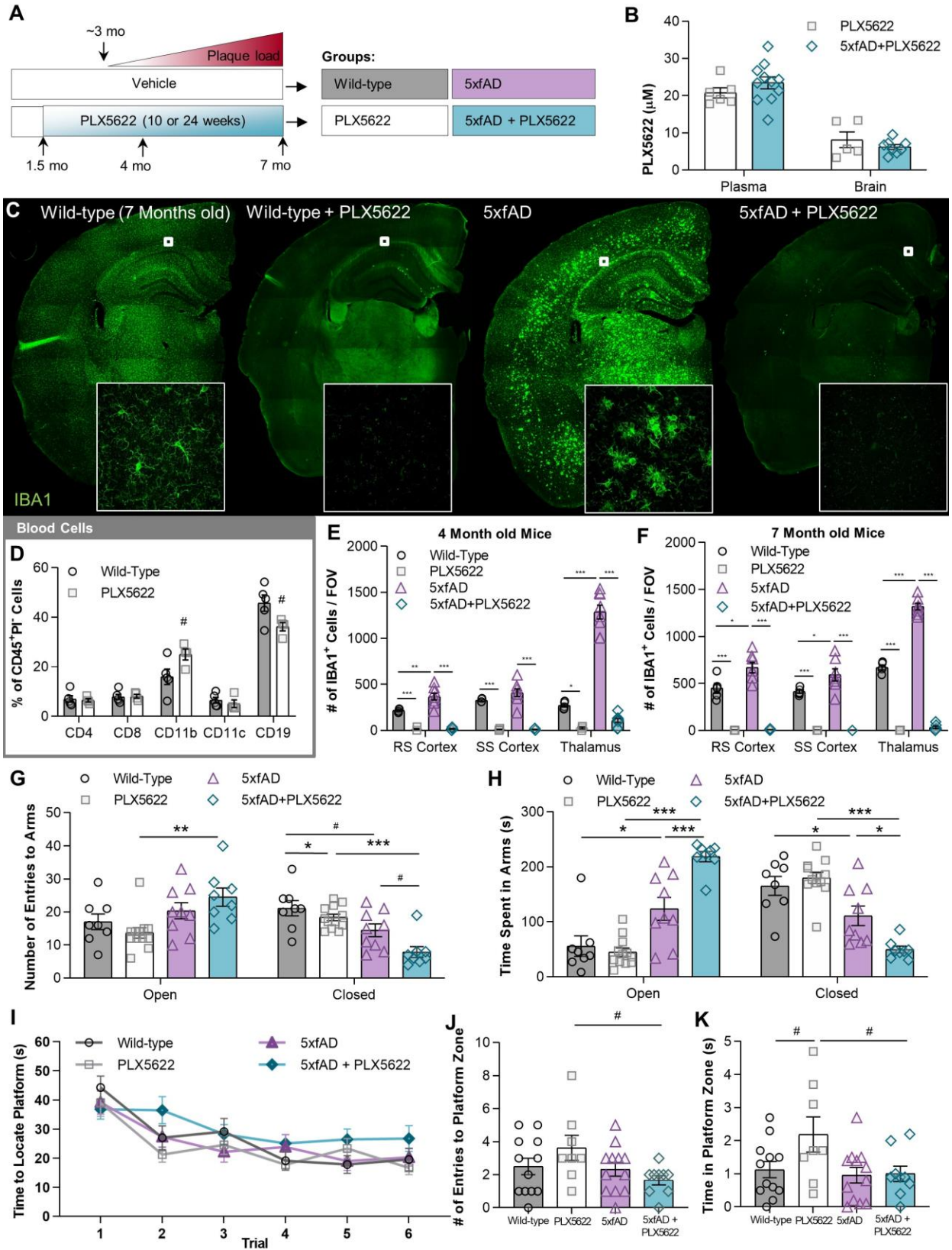


**Figure 2.2: Long-term elimination of microglia with PLX5622 treatment does not induce peripheral leukocyte or behavioral abnormalities.** 1.5-month-old wild-type (WT) or 5xfAD mice were treated with control chow or PLX5622 for 10 or 24 weeks to eliminate microglia. **A**, Experimental design. **B**, Terminal PK of PLX5622 and 5xfAD + PLX5622 groups showed no differences in drug concentration in the plasma or brain. Two-tailed independent t-test. n = 5-6 for PLX5622, n = 8-11 for 5xfAD + PLX5622. **C**, Representative hemisphere stitches of immunolabeling for microglia (IBA1 in green) 7-month-old cohort. **D**, Analysis of different subsets of leukocytes showed no significant alterations with PLX5622 treatment compared to WT (p=0.059 for CD11b and p=0.052 for CD19, all others NS). NS, not significant. Two-tailed independent t-test; n = 4-5 for Wild-type, n = 3-4 for PLX5622. **E**, Quantification of microglial number in 4-month old animals revealed an elevation in 5xfAD mice compared to WT (p=0.001, NS, p<0.001) and reductions in microglial number in PLX5622 (p<0.001, p<0.001, p=0.044) and 5xfAD + PLX5622 groups (p<0.001, p<0.001, p<0.001). All analyses listed in respective order for retrosplenial (RS) cortex, somatosensory (SS) cortex, and thalamus. NS, not significant. Two-way ANOVA with Tukey's post hoc test; n = 5 for Wild-type, n = 4 for PLX5622, n = 8 for 5xfAD, n = 9 for 5xfAD + PLX5622. **F**, In 7-month-old animals, microglial number is increased in 5xfAD mice compared to WT (p=0.015, p=0.024, p<0.001). Lifelong CSF1R inhibitor treatment eliminates 99% and 97% of microglia in PLX5622 (p<0.001 for all regions) and 5xfAD + PLX5622 mice (p<0.001 for all regions), respectively. All analyses listed in respective order for retrosplenial (RS) cortex, somatosensory (SS) cortex, and thalamus. Two-way ANOVA with Tukey's post hoc test; n = 4-5 for Wild-type, n = 6 for PLX5622, n = 5-8 for 5xfAD, n = 6 for 5xfAD + PLX5622. **G**, 5xfAD + PLX5622 mice entered the open arm more (p=0.007) and the closed arm less (p<0.001) than PLX5622 mice. Additionally, 5xfAD animals entered the closed arm less than WT (p=0.050), which was further enhanced with PLX5622 treatment in 5xfAD mice (p=0.056). **H**, The 5xfAD group spent more time in the open arm (p=0.016) and less time in the closed arm (p=0.046) compared to WT. This phenotype was exacerbated in the 5xfAD + PLX5622 group, as these mice spent more time in the open arm (p<0.001) and less time in the closed arm (p=0.020) than the 5xfAD group. Additionally, the 5xfAD + PLX5622 group spent more time in the open arms (p<0.001) and less time in the closed arms (p<0.001) than the PLX5622 group. **I**, Morris water maze (MWM) acquisition revealed no differences between groups for time to locate platform over training trials. **J**, In MWM probe test, platform entries trended to an increase in PLX5622 mice compared to 5xfAD+PLX5622 animals (p=0.071). **K**, For time spent in platform zone in MWM probe test, time in platform zone trended to an increase in the PLX5622 group relative to wild-type (p=0.094) and 5xfAD+PLX5622 mice (p=0.073). For all behavioral analyses: Two-way ANOVA with Tukey's post hoc test; n = 8-12 for Wild-type, n = 8-12 for PLX5622, n = 9-12 for 5xfAD, n = 8-9 for 5xfAD + PLX5622. Statistical significance is denoted by \*p<0.05, \*\*p<0.01, and \*\*\*p<0.001. Statistical trends are denoted by #p<0.10. Error bars indicate SEM.

In the brain, 5xfAD mice displayed increased numbers of microglia/myeloid cells at both 4 and 7 months of age compared to wild-type mice, with masses of enlarged, plaque-associated cells seen throughout the brain (Fig. 2.2C). Oral PLX5622 treatment led to almost complete microglial elimination (97-100% reduction; Fig. 2.2C and quantified in E and F), even with 24 weeks of treatment, showing that PLX5622 allows for extended elimination of microglia. Given the unprecedented absence of microglia for ~6 months, or essentially the entire adult lives of the animals, we conducted a battery of behavioral and cognitive performance tests. The extended absence of microglia in wild-type mice

did not induce any measurable negative effects in tests of anxiety (Fig. 2.2G, H). Compared to wild-type animals, 5xfAD mice showed altered behaviors in the elevated plus maze, which were further exacerbated with microglial elimination (Fig. 2.2G, H). To assess hippocampal-dependent memory, mice underwent testing using Morris water maze (MWM). In acquisition trials, 5xfAD mice did not show impairments (Fig. 2.2I). Interestingly, in the probe portion of the MWM, PLX5622-treated wild-type mice tended to spend more time in the platform zone compared to wild-type mice (Fig. 2.2K), indicating that the long-term absence of microglia is not detrimental to murine cognitive function and may be beneficial, consistent with our prior findings<sup>35,133</sup>.

### **The absence of microglia diminishes plaque formation and shifts A $\beta$ accumulation to the vasculature**

Having demonstrated robust microglial elimination prior to and throughout the period of plaque formation in 5xfAD mice, we next determined the consequences of microglial ablation on pathology. In wild-type mice, CSF1R inhibitor treatment for 10 weeks eliminated >99% of microglia in the cortex (Fig. 2.3A, C, and F), but a fraction of cells remained in the thalamus (Fig. 2.3I). Treatment of 5xfAD mice with PLX5622 again reduced >99% of microglia in the cortex (Fig. 2.3D, G), but as with wild-type mice, a fraction of cells remained in the thalamus (Fig. 2.3J). In the absence of microglia, we observed a stark lack of dense-core plaques within cortical regions (quantified in Fig. 2.3L; retrosplenial (RS) and somatosensory (SS) cortices examined). Notably, a band of plaques were found in the RS cortex, but these were all associated with a few microglia that had survived treatment (Fig. 2.3D, D1). Plaques were also formed within the

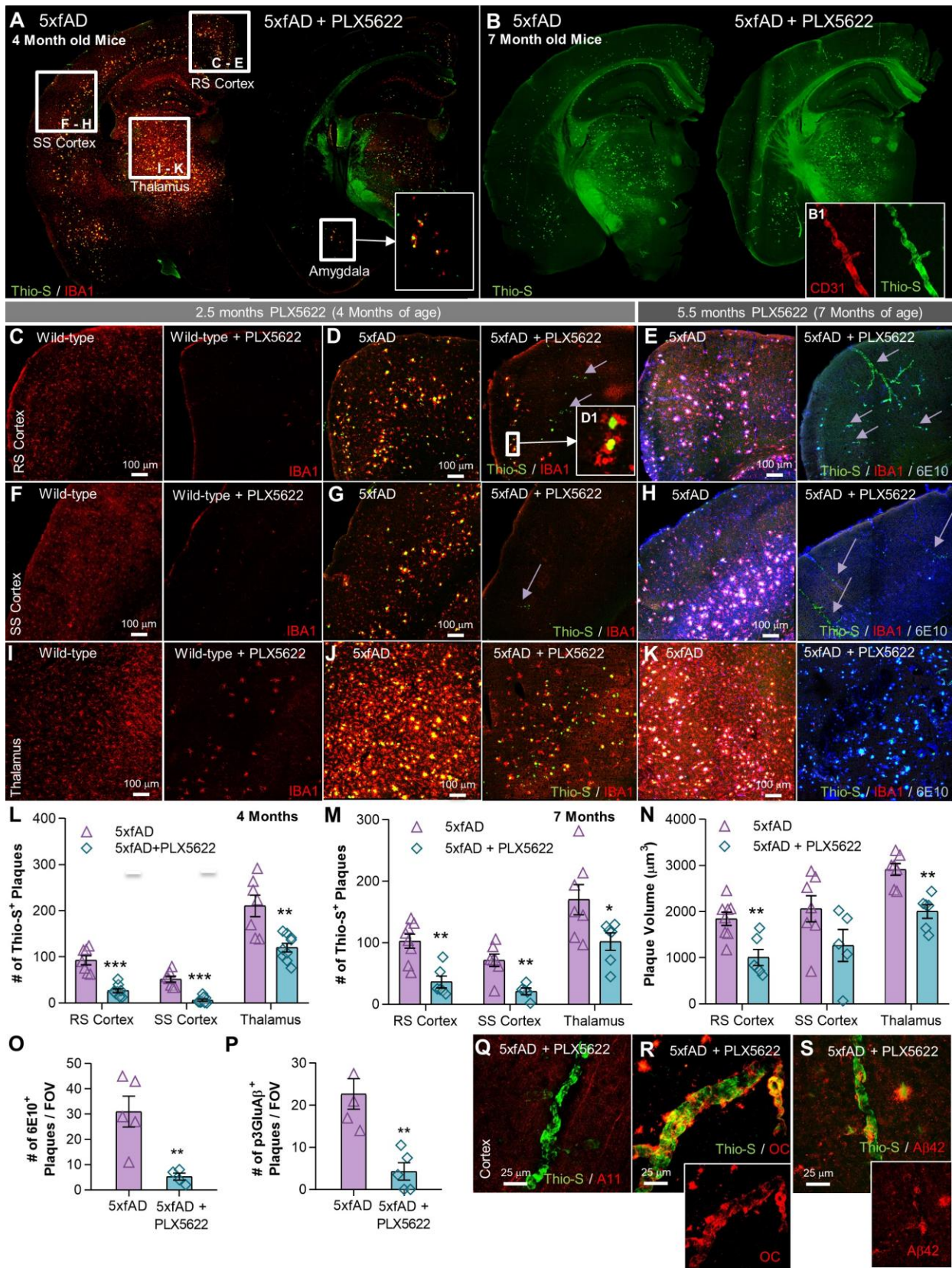


**Figure 2.3: Long-term elimination of microglia in 5xfAD mice reduces plaque number and volume and is accompanied by cerebral amyloid angiopathy (CAA) onset.** All analyses listed in respective order for retrosplenial (RS) cortex, somatosensory (SS) cortex, and thalamus. **A**, Representative hemisphere stitches of dense-core deposits stained with Thioflavin-S (Thio-S) in green and microglia (IBA1 in red) **B**, Representative images of brain hemispheres stained for dense-core plaques (Thio-S in green) with immunolabeling for blood vessels (CD31 in red) alongside Thio-S (**B1**), illustrating the appearance of cerebral amyloid angiopathy (CAA) throughout the cortex of 5xfAD mice devoid of microglia. **C-D, F-G, I-J**, Confocal images of sections from 10 week treated animals stained for dense-core plaques (Thio-S in green) and immunolabeled for microglia (IBA1 in blue). **E, H, K**, Images from 24 week treated animals stained for dense-core plaques (Thio-S in green) and immunolabeled for microglia (IBA1 in red) and diffuse plaques (6E10 in blue). **L**, 5xfAD mice treated with PLX5622 for 10 weeks exhibited reductions in Thio-S<sup>+</sup> plaque number relative to untreated 5xfAD mice ( $p < 0.001$ ,  $p < 0.001$ ,  $p = 0.001$ ). Two-tailed independent t-test;  $n = 7$  for 5xfAD,  $n = 8$  for 5xfAD + PLX5622. **M**, Quantification of Thio-S<sup>+</sup> plaque number in 7-month-old mice revealed a 40-70% decrease in 5xfAD + PLX5622 mice ( $p = 0.001$ ,  $p = 0.004$ ,  $p = 0.041$ ) compared to untreated 5xfAD mice. Two-tailed independent t-test;  $n = 7-8$  for 5xfAD,  $n = 5-6$  for 5xfAD + PLX5622. **N**, Plaque volume in 7-month-old mice was reduced by 45%-75% in the RS cortex and thalamus ( $p = 0.003$ , NS,  $p = 0.007$ ) of 5xfAD mice treated with the CSF1R inhibitor and was unchanged in the SS cortex. NS, not significant. Two-tailed independent t-test;  $n = 7-8$  for 5xfAD,  $n = 5-6$  for 5xfAD + PLX5622. **O-P**, Immunolabeling 7-month-old 5xfAD animals for 6E10 and pyroglutamate-3-modified A $\beta$  revealed reductions ( $p = 0.002$  and  $p = 0.008$ , respectively) in cortical expression of these amyloid markers with PLX5622 treatment. Two-tailed independent t-test;  $n = 4-5$  for 5xfAD,  $n = 4-5$  for 5xfAD + PLX5622. **Q-S**, 7-month-old PLX5622-treated 5xfAD animals stained for dense core deposits (Thio-S in green) and immunolabeled for oligomeric A $\beta$  (A11), protofibrillar A $\beta$  (OC) and A $\beta$ <sub>1-42</sub>, respectively.

thalamus but were again predominantly associated with the remaining microglia that had survived the treatment (Fig. 2.3J). Close examination of the Thioflavin-S (Thio-S) stained slices revealed deposits beginning to form within cortical blood vessels (Fig. 2.3D, G – yellow arrows). These results suggest that microglia are critical regulators of plaque formation and that few surviving microglial cells are sufficient to facilitate some degree of plaque formation (i.e., as seen in the thalamus).

Consistent with the 10-week treated 5xfAD mice, examination of pathology in the 24 week treated mice revealed diminished Thio-S<sup>+</sup> dense-core plaque numbers in the cortices of the 5xfAD mice devoid of microglia (Fig. 2.3E, H; quantified in M). In the 10-week treated cohort, we noted the appearance of plaques in areas that exhibited small populations of surviving microglia (RS cortex and thalamus; Fig. 2.3D and J). With an additional 14 weeks of treatment (i.e., 24 weeks treated animals), microglia were

completely eliminated from the brain (Fig. 2.3E, H, and K), but Thio-S plaques persisted in these areas (i.e., the thalamus and RS cortex). Average plaque volumes were ~30-40% smaller, across all brain regions (Fig. 2.3N), suggesting that microglia contribute to plaque growth in the 5xfAD brain. Thus, even with increased treatment duration to 7 months of age, plaque formation is prevented in the absence of microglia. Notably, abundant Thio-S staining was discovered within large cortical blood vessels in the 5xfAD mice devoid of microglia (i.e., Fig. 2.3E, H), indicative of cerebral amyloid angiopathy (CAA). Whole brain stitches of Thio-S staining show clear vascular pathology rather than cortical plaques in microglia-depleted 5xfAD mice (Fig. 2.3B). Colocalization of Thio-S with the endothelial cell marker CD31 confirms the accumulation of A $\beta$  within blood vessels (Fig. 2.3B1). The appearance of CAA occurred only in 5xfAD mice in the absence of microglia, as CAA was not observed in untreated 5xfAD mice or in treated wild-type mice. In addition to Thio-S, CAA and plaques stained for fibrils, via the conformation specific antibody OC<sup>220</sup> (Fig. 2.3R) and A $\beta$ 42 (Fig. 2.3S), but were negative for oligomers via A11 antibody<sup>221</sup> (Fig. 2.3Q). Staining for pyroglutamate-3 A $\beta$  (data not shown), which forms the plaque cores<sup>222</sup>, revealed a sharp reduction in immunoreactivity in PLX5622-treated 5xfAD mice relative to untreated 5xfAD animals in the cortex (Fig. 2.3P), along with reductions in 6E10<sup>+</sup> diffuse plaques (Fig. 2.3O). Of note, pyroglutamate-3 immunoreactivity was found in areas of treated 5xfAD mice that exhibited plaque pathology (i.e., thalamus; not shown).

The absence of microglia did not significantly alter the levels of A $\beta$ 38, A $\beta$ 40, or A $\beta$ 42, in detergent-soluble or -insoluble cortical and thalamic homogenates in either the 4- or 7-month cohorts (Fig. 2.4A-H), in line with multiple studies showing that CSF1R inhibition

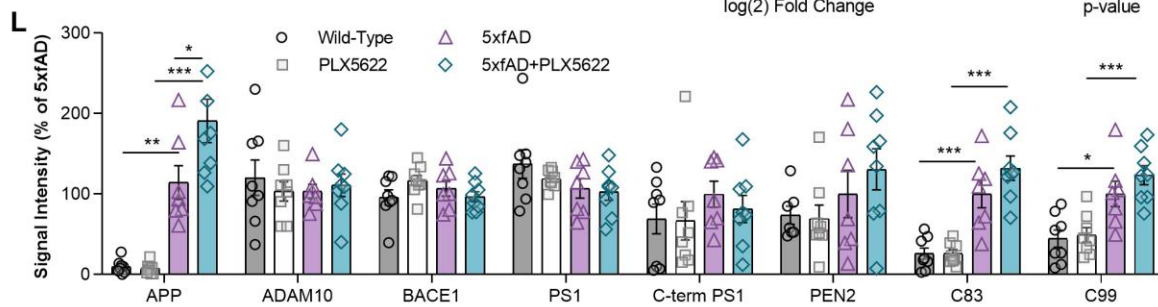
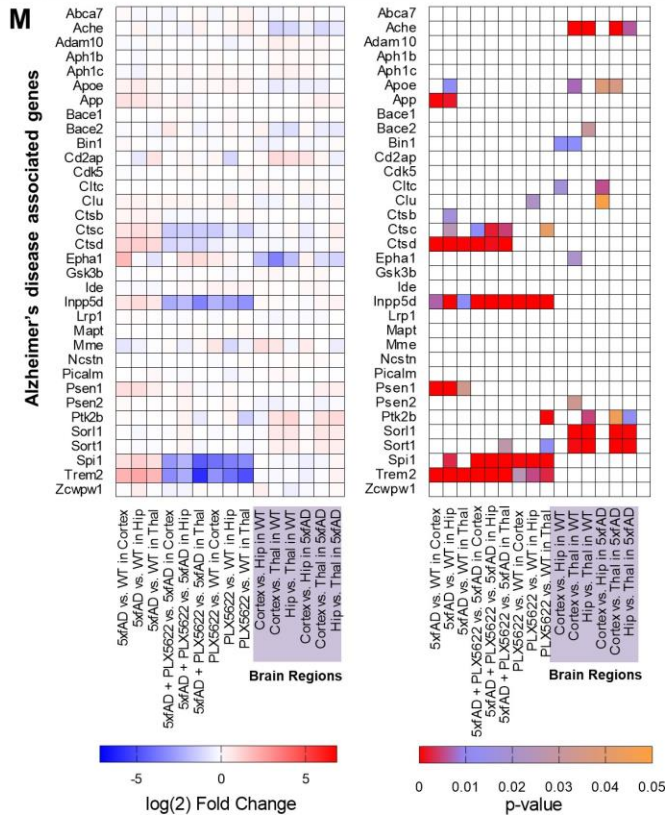
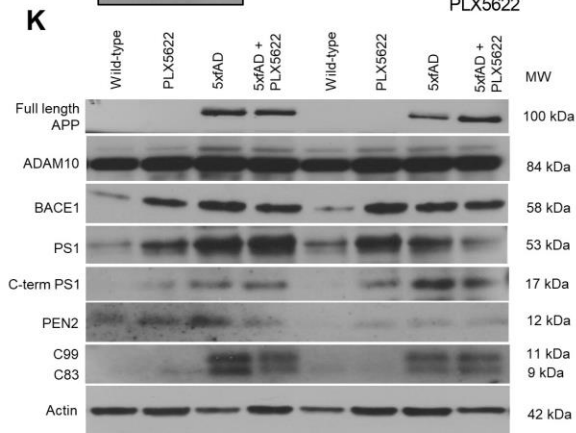
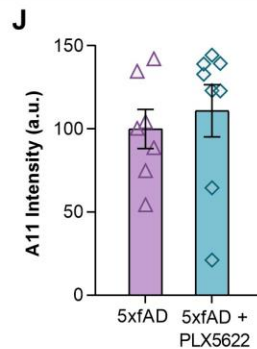
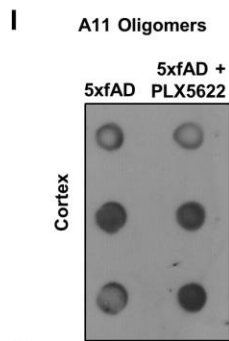
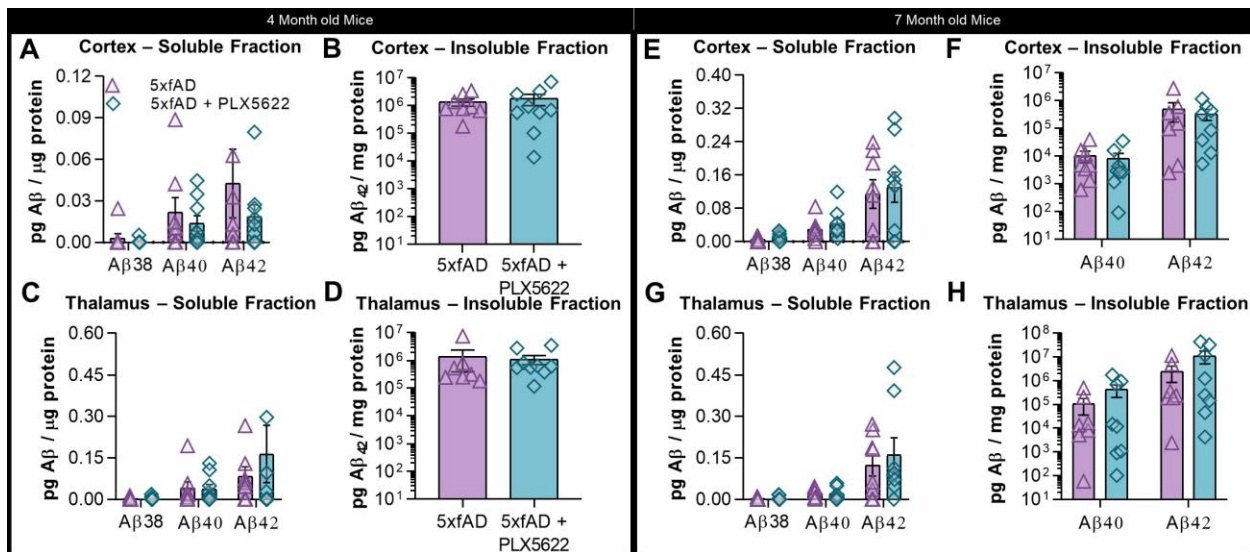


**Figure 2.4: No detectable alterations in A $\beta$  levels or APP processing with microglia elimination in 5xfAD mice.** **A-H**, A $\beta$  levels from cortical (**A-B**, **E-F**) or thalamic brain homogenates (**C-D**, **G-H**) from 5xfAD mice treated with vehicle or PLX5622 (1200 ppm in chow) from 1.5 months of age to either 4 (**A-D**), or 7 (**E-H**) months of age, for both the detergent-soluble and insoluble fractions. In the 4-month-old mice, insoluble A $\beta_{1-38}$  and A $\beta_{1-40}$  were below detection threshold. In the 7-month-old mice, insoluble A $\beta$  levels were plotted on log(10) scale and insoluble A $\beta_{1-38}$  was below detection threshold. Two-tailed independent t-test. For 4-month-old cohort: n = 3-6 for 5xfAD, n = 4-6 for 5xfAD + PLX5622. For 7-month-old cohort: n = 5-6 for 5xfAD, n = 5-6 for 5xfAD + PLX5622. **I-J**, Cortical homogenates of 7-month-old mice immunoprobed and quantified, respectively, for A11. Two-tailed independent t-test; n = 7 for 5xfAD, n = 8 for 5xfAD + PLX5622. **K-L**, Immunoblotting and quantification, respectively, for components of the amyloid-precursor protein (APP) processing pathway in cortical homogenates from 7-month-old animals. Full length APP and APP Carboxy-terminal fragments C99 and C83 are increased in 5xfAD animals relative to Wild-type (p=0.009, p=0.031, p=0.033, respectively), but no significant alterations in protein levels were observed with microglia elimination in 5xfAD animals. Two-way ANOVA with Tukey's post hoc test; n = 4 for Wild-type, n = 4 for PLX5622, n = 4 for 5xfAD, n = 4 for 5xfAD + PLX5622. **M**, Left panel - heatmap of log(2) fold change of genes associated with Alzheimer's disease, including APP/A $\beta$  production and metabolism shown for each of the 9 comparisons and the 6 comparisons between brain regions. Right panel – heatmap of the corresponding p-values for each of the comparisons. Log(2) fold change and p-values indicated by respective scale bar. n = 4 for all groups. Error bars indicate SEM.

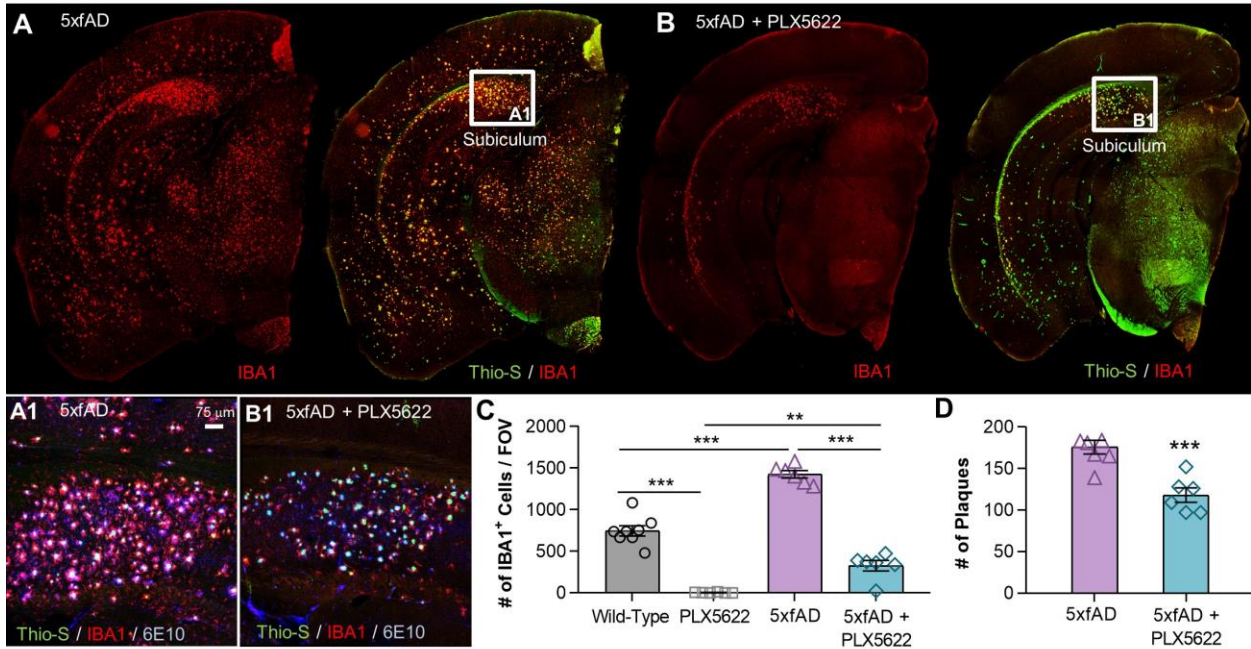
does not affect A $\beta$  production/clearance<sup>132,139,215</sup>. Thus, the absence of microglia modulates the location of A $\beta$  accumulation (i.e., parenchyma vs. vasculature) but does not alter the net amounts present. Investigations into oligomeric species of A $\beta$  (via A11 immunoblotting) found no significant changes in protein levels with microglia elimination in 5xfAD mice (Fig. 2.4I, J). To confirm that APP processing was unchanged with microglia elimination in 5xfAD mice at the protein level, we immunoblotted cortical tissue for various components of the APP processing pathway including APP and its cleavage products, as well as proteins associated with  $\alpha$ - (ADAM10),  $\beta$ - (BACE1), and  $\gamma$ - (PEN2 and PS1) secretase activity. We found significant elevations in full-length (fl) APP and Carboxy-terminal fragments of APP (C99 and C83) in 5xfAD mice relative to wild-type (Fig. 2.4K, L), but observed no differences in protein levels with PLX5622 treatment in 5xfAD animals. Additionally, gene expression analyses of AD-related genes were performed (Fig. 2.4M; methods described in greater detail for Figs. 2.8 and 2.9) and we found no overt changes with microglia depletion. Collectively, these data indicate that

microglia elimination via PLX5622 treatment does not induce alterations in APP processing or other AD-related genes that could account for the reduction in plaque pathology.

### **Microglial plaque compaction ameliorates the extent of neuritic dystrophy in 5xfAD mice**

Upon examining caudal brain regions, we found some IBA1<sup>+</sup> cells present within the subiculum and associated white matter tracts in the otherwise microglia-devoid 5xfAD animals (mice treated through 1.5-7 months of age; Fig. 2.5A, B). While PLX5622 treatment extensively reduced myeloid cell numbers in the subiculum (77% reduction; Fig. 2.5C), there was a tight spatial association between the surviving cells and Thio-S plaques (Fig. 2.5A1, B1), similar to that seen in the thalamus of the 10-week-treated 5xfAD mice (Fig. 2.3J). In fact, plaques were predominantly observed in the immediate vicinity of surviving IBA1<sup>+</sup> cells – within the subiculum and associated white matter tract – while the cortex contained only vascular Thio-S<sup>+</sup> deposits, in stark contrast to untreated 5xfAD mice (Fig. 2.5A vs. B). Quantification of Thio-S<sup>+</sup> subicular plaques revealed a 33% decrease in plaque number (Fig. 2.5D) with PLX5622 treatment in 5xfAD mice. Importantly, these results highlight a clear relationship between microglia/myeloid cells, even when substantially reduced in number, and the appearance of plaques. This relationship/association provides further evidence for a role of microglia/myeloid cells in facilitating the formation of plaques, and again emphasizes that few cells are required for this process to occur.

A surviving population of microglia in the subiculum directly associate with plaque formation



Reduced plaque compaction and increased dystrophic neurites in the absence of microglia

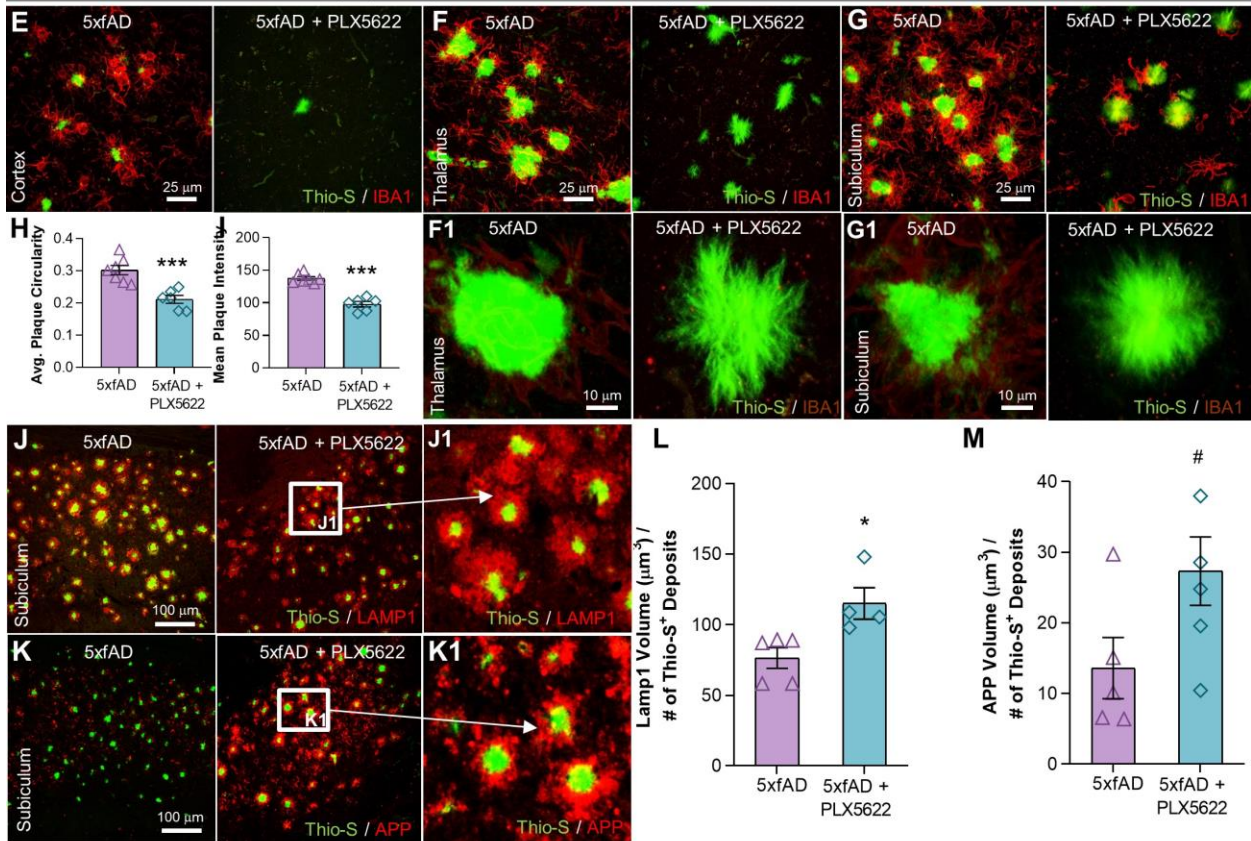


**Figure 2.5: Microglia facilitate plaque formation and compaction.** **A, B,** Representative hemisphere stitches of 5xfAD and 5xfAD + PLX5622 mice stained for dense-core plaques (Thio-S in green) and immunolabeled for microglia (IBA1 in red). Confocal images of subicula (**A1** and **B1**) stained with Thio-S for dense core plaques (green) and immunolabeled with IBA1 for microglia (red) and 6E10 for diffuse plaques (blue). **C,** Quantification of IBA1<sup>+</sup> cells in the subiculum revealed an increase in 5xfAD mice compared to wild-type ( $p < 0.001$ ). PLX5622 treatment reduces IBA1<sup>+</sup> cell number in wild-type and 5xfAD groups by 99% ( $p < 0.001$ ) and 77% ( $p < 0.001$ ), respectively. Two-way ANOVA with Tukey's post hoc test;  $n = 7$  for Wild-type,  $n = 6$  for PLX5622,  $n = 6$  for 5xfAD,  $n = 6$  for 5xfAD + PLX5622. **D,** Plaque number within the subiculum is reduced by 33% in 5xfAD + PLX5622 mice compared to 5xfAD animals ( $p < 0.001$ ). Two-tailed independent t-test;  $n = 6$  for 5xfAD,  $n = 6$  for 5xfAD + PLX5622. **E-G,** Confocal images of dense-core plaques (Thio-S in green) and microglia (IBA1 in red) in the cortex, thalamus, and subiculum, respectively, of both 5xfAD groups showing an alteration in plaque morphology with CSF1R inhibitor treatment. Zoomed images of dense-core plaques (Thio-S in green) in the thalamus (**F1**) and subiculum (**G1**) of 5xfAD and 5xfAD + PLX5622 mice. **H-I,** Plaque circularity and Thio-S fluorescence intensity is decreased by ~30% with PLX5622 treatment in 5xfAD mice compared to untreated 5xfAD animals ( $p < 0.001$  for both), respectively. Two-tailed independent t-test;  $n = 6-7$  for 5xfAD,  $n = 6$  for 5xfAD + PLX5622. **J-K,** Images of subicula stained for dense-core deposits with Thio-S and immunolabeled for dystrophic neurites with LAMP1 (in red) or APP (in red), respectively. Zoomed images of plaque-associated dystrophic neurites (**J1** and **K1**) in PLX5622-treated 5xfAD animals. **L-M,** Quantification of LAMP1 and APP immunoreactive dystrophic neurites, showing a ~50% ( $p = 0.020$ ) and ~100% ( $p = 0.068$ ) increase with microglial elimination in 5xfAD animals, respectively. Two-tailed independent t-test;  $n = 5$  for 5xfAD,  $n = 4-5$  for 5xfAD + PLX5622. Statistical significance is denoted by \* $p < 0.05$ , \*\* $p < 0.01$ , and \*\*\* $p < 0.001$ . Statistical trends are denoted by # $p < 0.10$ . Error bars indicate SEM.

Structural examination of the plaques that had formed in PLX5622-treated 5xfAD mice (treated through 1.5-7 months of age), presumably due to the presence of surviving microglia at the time of their formation, revealed morphological differences compared to plaques formed and maintained in the presence of microglia (Fig. 2.5E-G, and magnified in F1 and G1). These plaques displayed an irregular shape with structured filaments radiating out from a central fissure/point and lacked the homogenous staining intensity of plaques in microglia-intact 5xfAD mice. As such, both plaque circularity (Fig. 2.5H) and mean Thio-S intensities (Fig. 2.5I) were significantly reduced in the 5xfAD mice devoid of microglia. These features were common to all areas explored, including in the subiculum, where some IBA1<sup>+</sup> cells were still present, suggesting that a threshold density of microglial cells is required for full plaque compaction/restructuring. Dystrophic neurites are found in a halo around fibrillar plaques and are characterized by the

accumulation of LAMP1 and APP<sup>223,224</sup>. To evaluate the role of microglia in regulating the growth of dystrophic neurites, we stained for LAMP1 and APP (Fig. 2.5J-K) and found that the absence of microglia enhanced the dystrophic neurite halo area (Fig. 2.5L, M). These results fully confirm prior studies showing that microglia form a physical barrier around plaques and compact A $\beta$  into dense deposits, protecting against local neurite damage<sup>91,116-118,225,226</sup>.

### **Microglia incorporate free A $\beta$ into plaques, facilitating growth, in 5xfAD animals**

The plaques that we observe in CSF1R inhibitor treated 5xfAD mice likely result from surviving microglia at the time of plaque onset (i.e., Fig. 2.2C, E), which die with further CSF1R inhibitor treatment, after the plaque is formed (i.e., Fig. 2.3D-K). Notably, we find these plaque volumes are smaller (Fig. 2.3N), suggesting that seeded plaques subsequently failed to expand/grow in the absence of microglia. To explore if microglia play a role in the growth of dense core plaques, we infused fluorescently-labeled A $\beta$ <sub>1-42</sub> into the cortex of 5xfAD animals, evaluating the ability of free A $\beta$  to incorporate into existing plaques in the presence or absence of microglia. Three-month-old 5xfAD animals, an age of rapid plaque growth and spreading, were treated with control or PLX3397 (600ppm in chow) for 2 weeks to eliminate microglia. At this time, mice received a single cortical injection of fluorescently-labeled A $\beta$ <sub>1-42</sub> and were euthanized one week later (see schematic, Fig. 2.6A). Quantification of Thio-S<sup>+</sup> plaque volumes revealed a significant reduction following the elimination of microglia (Fig. 2.6F), confirming that microglia are promoting the expansion/growth of plaques. In untreated 5xfAD animals, we found that the infused A $\beta$ <sub>1-42</sub> was restricted to the Thio-S<sup>+</sup> plaque

core (Fig. 2.6B, D), demonstrating that free A $\beta$  becomes fully incorporated into the fibrillar core in the presence of microglia. In the absence of microglia, fluorescent A $\beta_{1-42}$  does not fully incorporate into the dense core, instead forming a distinct halo around the

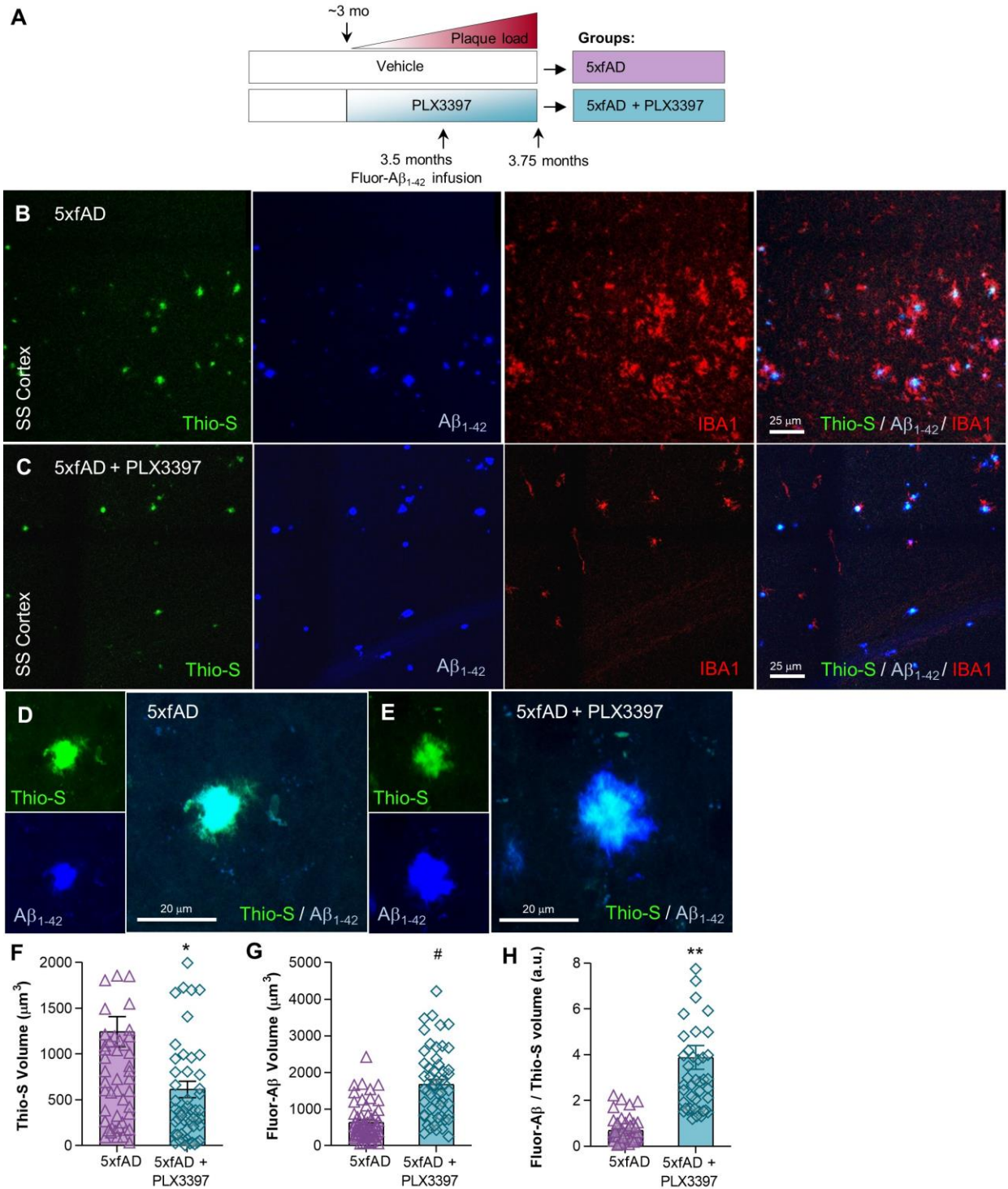


**Figure 2.6: Microglia deposit available A $\beta$  into the plaque core.** **A**, Experimental design. **B,C**, Representative images of the somatosensory (SS) cortex injected with fluorescently-labeled A $\beta_{1-42}$  (blue) and stained for dense-core deposits (Thio-S in green) and microglia (IBA1 in red). **D,E**, Zoomed images of fluorescently-labeled A $\beta_{1-42}$  (blue) bound to dense-core plaques (Thio-S in green). **F**, Quantification of Thio-S plaque volumes in 5xfAD and 5xfAD mice treated with PLX3397, showing a ~50% reduction in the size of dense-core deposits with microglia elimination ( $p=0.0105$ ). **G**, A $\beta_{1-42}$  volume increased ~170% in the absence of microglia ( $p=0.0581$ ), resulting in the appearance of a halo surrounding dense-core plaques. **H**, The ratio of A $\beta_{1-42}$  volume to Thio-S volume in microglia-intact and -devoid 5xfAD animals shows a ~300% increase with PLX3397 treatment ( $p=0.0030$ ). Statistical significance is denoted by \* $p<0.05$ , \*\* $p<0.01$ , and \*\*\* $p<0.001$ . Statistical trends are denoted by # $p<0.10$ . Error bars indicate SEM; ( $n=4-5$ /group; 58 plaques for 5xfAD; 53 plaques for 5xfAD + PLX3397).

Thio-S<sup>+</sup> plaque core (Fig. 2.6D, E). Accordingly, quantification revealed a stark increase in fluorescently-labeled A $\beta_{1-42}$  associated with Thio-S<sup>+</sup> plaques in the absence of microglia (Fig. 2.6G, H). Thus, arresting plaque growth with microglia elimination (seen via changes in Thio-S<sup>+</sup> plaque volume and fluorescently-labeled A $\beta_{1-42}$  incorporation) indicates that these cells incorporate free A $\beta_{1-42}$  into the fibrillar plaque core, facilitating plaque growth.

### **Replication of diminished plaque formation with an alternative CSF1R inhibitor**

Given the striking effects of PLX5622 treatment/microglial depletion on reducing plaque formation, we wanted to confirm the results with alternative CSF1R inhibitor paradigms. We established that PLX3397 formulated at 600 ppm in chow could achieve robust brain-wide microglial elimination (>99%)<sup>227</sup>, and thus, treated 1.5-month-old 5xfAD mice with this formulation until 5 months of age (Fig. 2.7A). Again, examination of the brains of these treated mice showed minimal plaque pathology and the appearance of CAA (Fig. 2.7C, D). We further examined the role of peripheral CSF1R inhibition on AD pathology by treating 1.5-month-old 5xfAD mice for 5 months with PLX3397 (75 ppm) chow (Fig. 2.7A) – a formulation that provides robust peripheral CSF1R inhibition

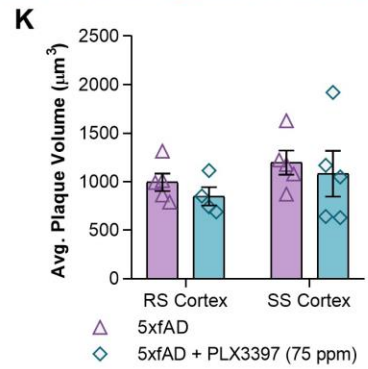
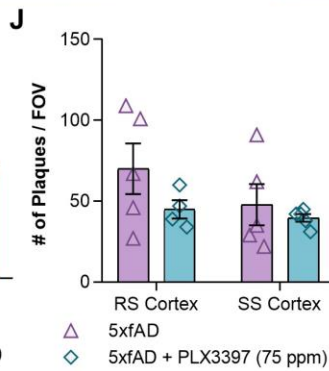
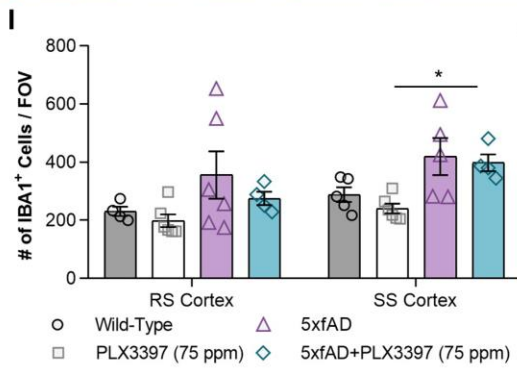
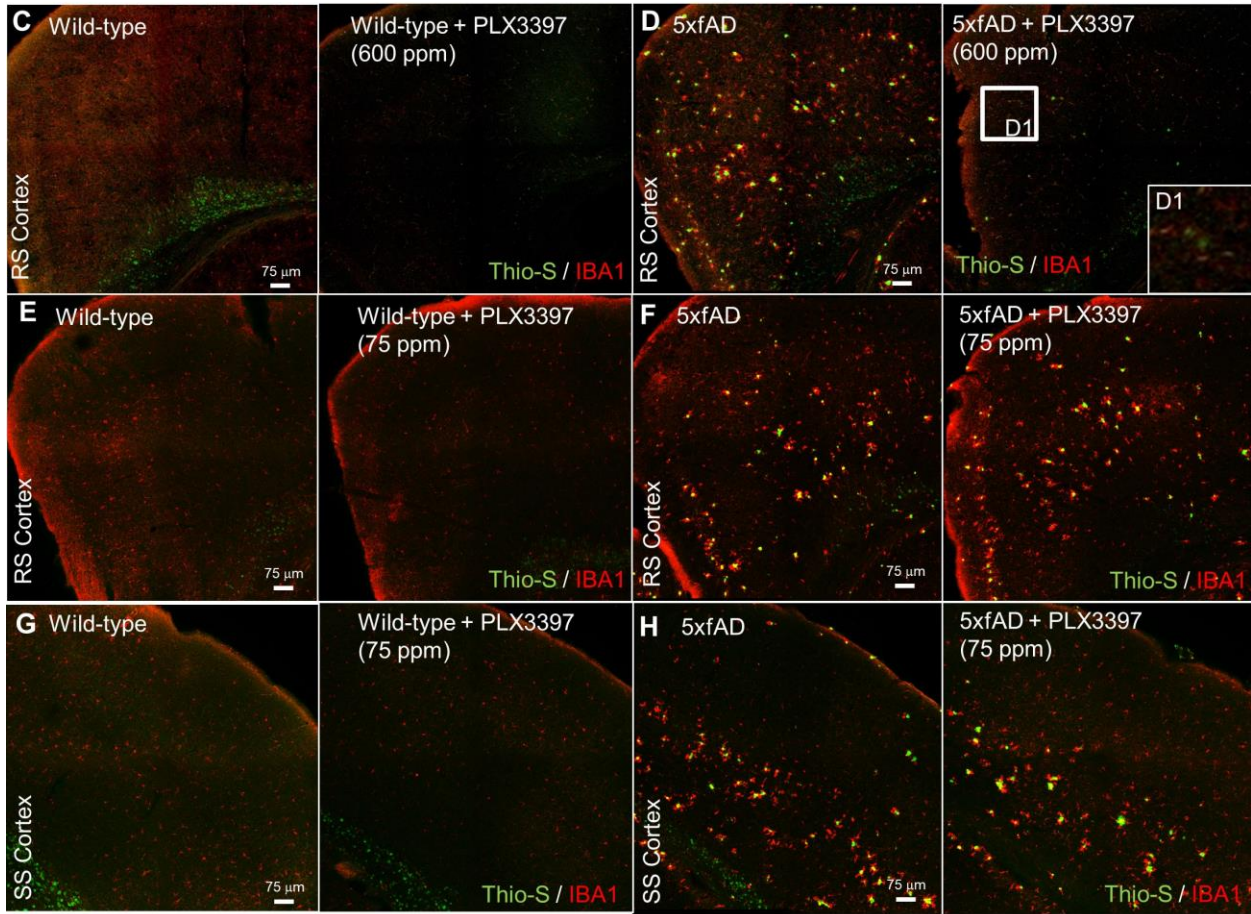
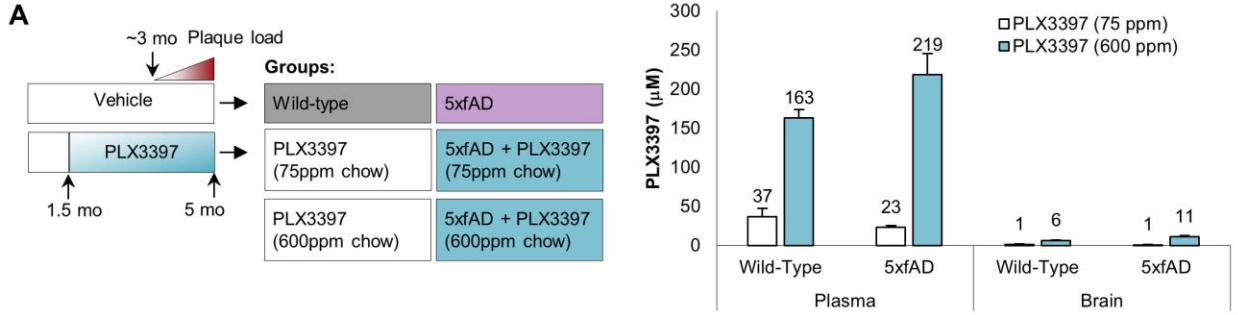


**Figure 2.7: Administration of an analogous CSF1R inhibitor, PLX3397 (75 ppm and 600 ppm), to 5xfAD mice. A,** Experimental design. **B,** Terminal PK of wild-type and 5xfAD groups treated with PLX3397. **C-D,** Confocal images of tissue stained for dense-core plaques (Thio-S in green) and immunolabeled for microglia (IBA1 in red) in 600 ppm PLX3397-treated and control mice. **E-H,** Sections of the retrosplenial (RS) and somatosensory (SS) cortex, respectively, stained for dense-core plaques (Thio-S in green) and immunolabeled for microglia (IBA1 in red) in mice treated with control or 75 ppm PLX3397. **I,** Quantification of IBA1<sup>+</sup> cell number in the RS and SS cortex. Two-way ANOVA with Tukey's post hoc test; n = 4 for Wild-type, n = 6 for PLX3397, n = 6 for 5xfAD, n = 4 for 5xfAD + PLX3397. **J-K,** Quantification of cortical plaque number and volume, respectively, revealing no change in these measures with 75 ppm PLX3397 treatment in 5xfAD mice. Two-tailed independent t-test; n = 4-5 for 5xfAD, n = 4-5 for 5xfAD + PLX3397. Statistical significance is denoted by \*p<0.05. Statistical trends are denoted by #p<0.10. Error bars indicate SEM.

without microglial elimination<sup>133</sup>. This lower dose achieved brain levels of ~ 1  $\mu$ M, compared to ~ 10  $\mu$ M with the higher dose (Fig. 2.7B), and accordingly, microglia numbers were unchanged relative to untreated animals (Fig. 2.7E-I). With 75 ppm PLX3397, no reductions in plaque load or appearance of CAA were detected in treated 5xfAD animals compared to controls (Fig. 2.7E-K). Thus, peripheral CSF1R inhibition or simply the presence of CSF1R inhibitor within the CNS do not attribute to the reductions in plaque pathology and more complete microglial elimination is necessary to perturb plaque formation processes.

### **Gene expression analyses of Wild-type and 5xfAD mice in the presence and absence of microglia, across brain regions:**

Given the prolonged absence of microglia throughout the adult life of wild-type and 5xfAD mice, the stark reduction in plaque formation in the absence of microglia, and the differences in pathology deposition and microglial number in various brain regions (i.e., no plaques but CAA in cortex, plaques but no microglia in thalamus and hippocampus/subiculum), we explored alterations in regional gene expression (mice treated through 1.5-7 months of age). To that end, brains were microdissected into cortical, hippocampal, and thalamic+striatal regions. RNA was extracted, and

subsequently analyzed by RNA-seq (n=4/group; Fig 2.8). A searchable database of all RPKM values can be found at [https://rnaseq.mind.uci.edu/green/ad\\_plx/gene\\_search.php](https://rnaseq.mind.uci.edu/green/ad_plx/gene_search.php).

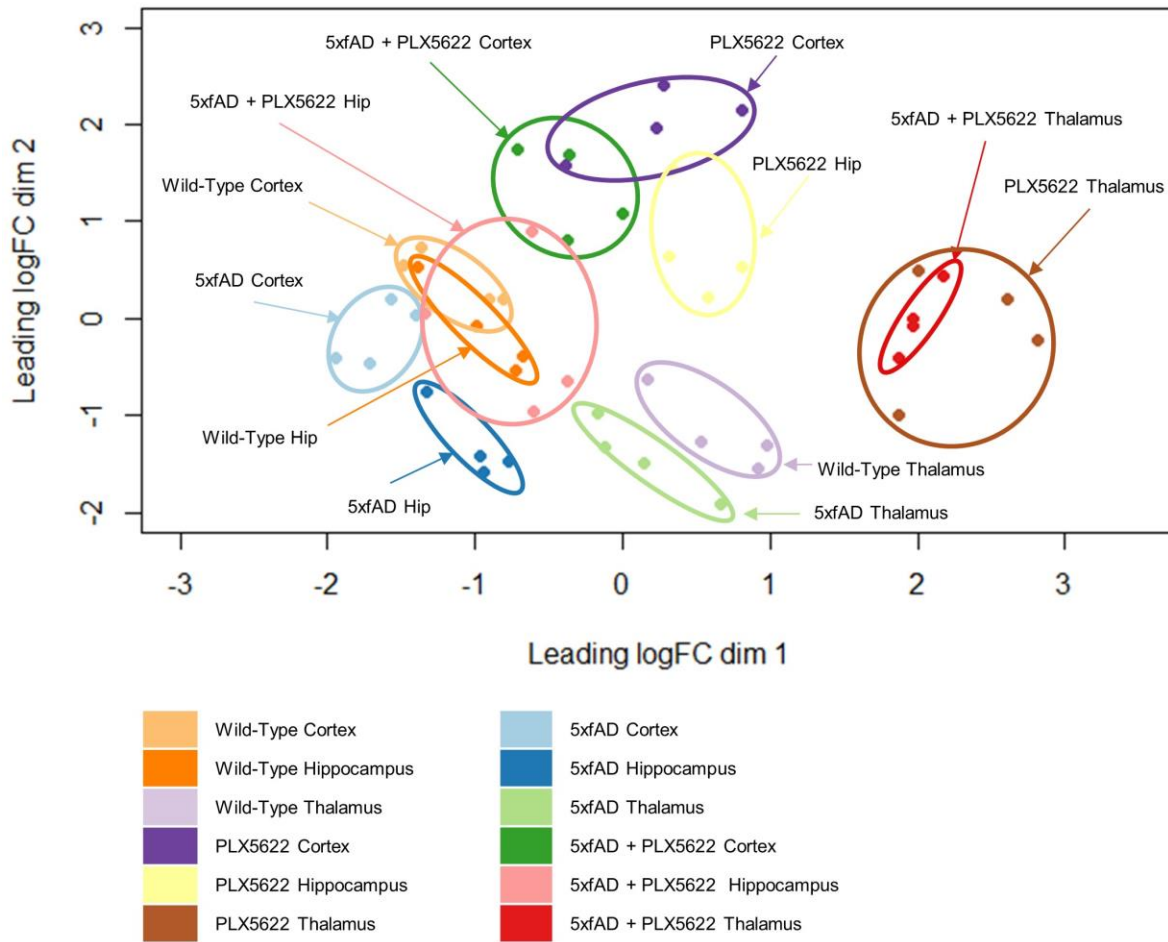
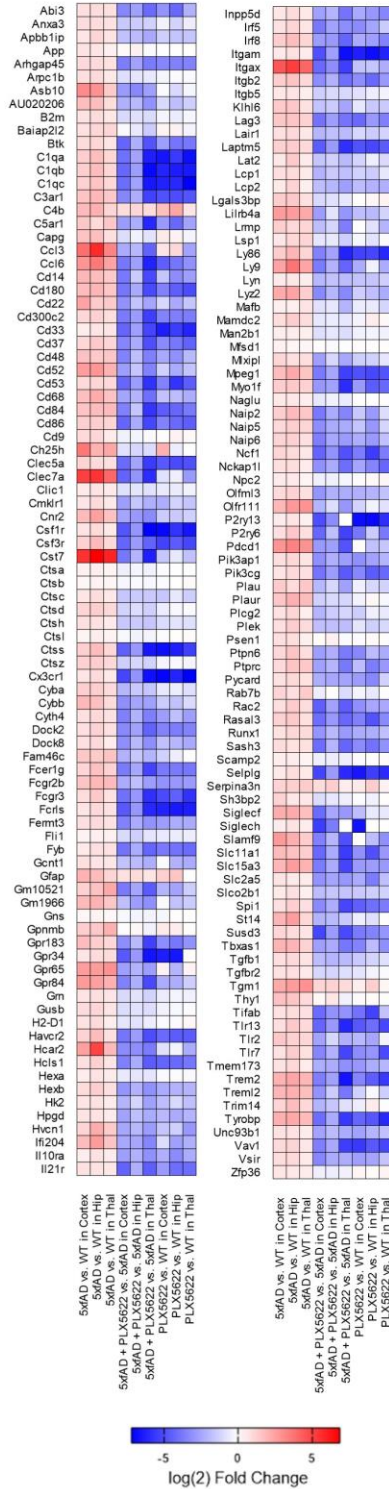


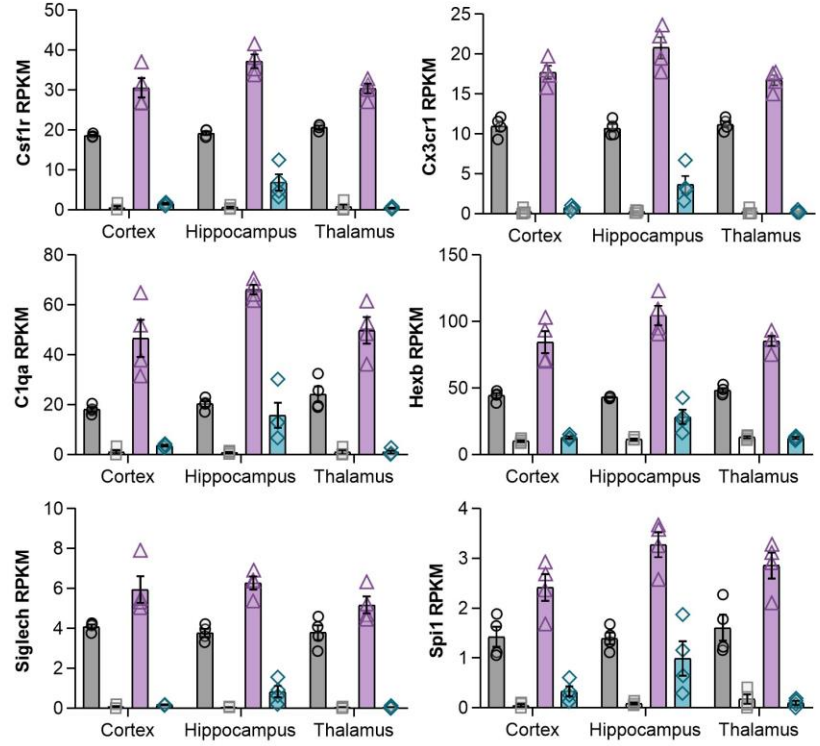
**Figure 2.8 Principal component analysis of RNA-seq data.** Principal component analysis of log counts per million mapped reads for each of the 12 groups (Wild-type Cortex, Hippocampus, and thalamus; PLX5622 Cortex, Hippocampus, and thalamus; 5xfAD Cortex, Hippocampus, and thalamus; and 5xfAD + PLX5622 Cortex, Hippocampus, and thalamus), after filtering genes that were not expressed and normalizing gene expression distributions. Groups denoted by color and arrows. n = 4 for all groups.

*Extensive microgliosis across all brain regions in 5xfAD mice:* To assess the global effects of pathology on gene expression, we compiled a list of genes significantly changed (using raw p-values) in all 3 brain regions in 5xfAD vs. wild-type mice (Fig.

**A Genes changes in all 3 brain regions (Wild-type vs. 5xfAD mice)**



**B Microglial homeostatic genes**



**C Disease-associated microglial genes**

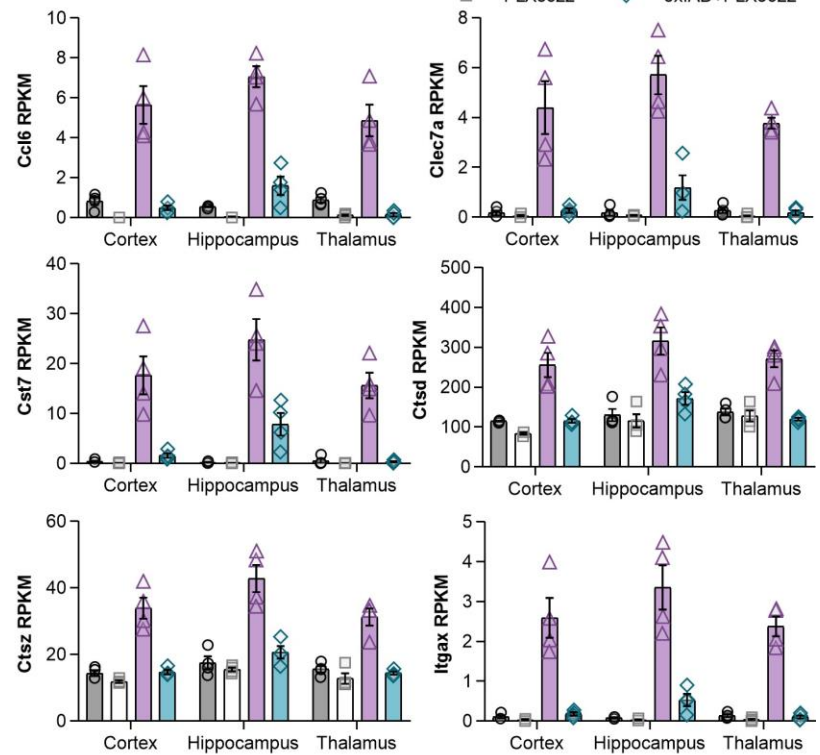


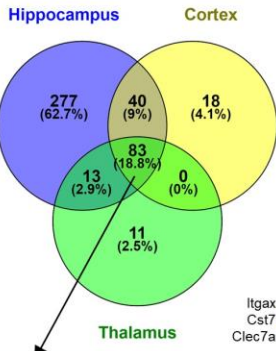
**Figure 2.9: Remaining plaque-forming microglia in the microdissected hippocampus exhibit a DAM expression profile.** **A**, All gene expression changes where  $p < 0.05$  for Wild-type (WT) vs. 5xfAD in all three brain regions shown as Log(2) fold change for each gene, for the 9 relevant comparisons (5xfAD vs. WT in cortex, hippocampus, or thalamus, 5xfAD + PLX5622 vs. 5xfAD in cortex, hippocampus, or thalamus, and WT + PLX5622 vs. WT in cortex, hippocampus, or thalamus). **B**, RPKM values shown for a subset of the homeostatic microglial genes from (A), including *Csf1r*, *Cx3cr1*, *C1qa*, *Hexb*, *Siglech*, and *Spi1*. **C**, RPKM values shown for a subset of the disease-associated microglial genes from (A), including *Ccl6*, *Clec7a*, *Cst7*, *Ctsd*, *Ctsz*, and *Itgax*. RPKM values for all genes/brain regions can be found at [https://rnaseq.mind.uci.edu/green/ad\\_plx/gene\\_search.php](https://rnaseq.mind.uci.edu/green/ad_plx/gene_search.php).  $n = 4$  per group for all analyses. Error bars indicate SEM.

2.9A). All common genes were upregulated and the vast majority are microglia-associated, reflecting the microgliosis occurring in 5xfAD mice. The elevation levels averaged 1-fold-change higher across all homeostatic microglial genes, consistent with the observed increase in microglial numbers (Fig. 2.2F). Consistent with these genes being predominantly expressed by microglia, their expression was markedly reduced with treatment in either 5xfAD or wild-type mice. We selected a subset of homeostatic microglial genes (*Csf1r*, *Cx3cr1*, *C1qa*, *Hexb*, *Siglech*, and *Spi1*) and displayed the expression (RPKM) values for each of the brain regions (Fig. 2.9B). The expression of these genes was nearly undetectable from PLX5622-treated mice, highlighting their specific expression by microglia and the specificity of PLX5622 on microglial survival. Of note, the expression of homeostatic microglial genes was higher in the 5xfAD + PLX5622 hippocampus than other microdissected brain regions (or wild-type mice), reflecting the population of surviving microglia identified in the subiculum (Fig. 2.5B1). Next, we sought to characterize the gene expression profile of the surviving, plaque-forming microglia in treated 5xfAD animals. To that end, we searched for genes upregulated in 5xfAD brains that were subsequently downregulated with PLX5622 treatment (to select for microglia-expressed genes) but not present in wild-type brains. We identified expression of *Ccl6*, *Clec7a*, *Cst7*, *Ctsd*, *Ctsz*, and *Itgax* as main genes

that follow this expression pattern (Fig. 2.9C), as well as *Asb10*, *B2m*, *Ccl3*, *Ch25h*, *Gpr65*, *Grn*, *Hcar2*, *Hexa*, *Ly9*, *Lyz2*, *Oasl2*, *Pdcd1*, *Plcg2*, and *Trem12*. Notably, several of these genes are known markers of disease-associated microglia<sup>83</sup> (DAM). Consistent with our expectations, these genes were present in PLX5622-treated 5xfAD hippocampus (but not cortex or thalamus), reflecting the population of surviving microglia in this region (see images of subicula in Fig. 2.5A1, B1, which are included in microdissected hippocampi) and providing a gene expression signature of plaque-forming/associated microglia.

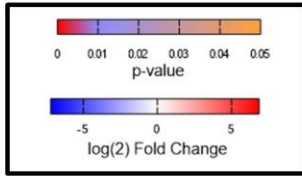
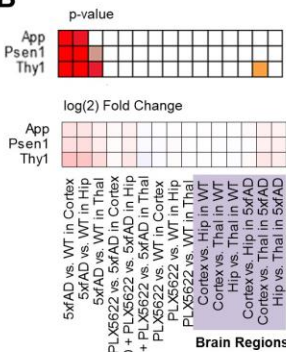
*Microglia mediate the downregulation of synaptic genes in the hippocampus:* We compared the number of differentially expressed genes (adjusted p-values <0.05) induced by AD pathology in each of the three microdissected brain regions (i.e., wild-both cortex and thalamus exhibited fewer changes in gene expression (141 and 107 type vs. 5xfAD) and found that the hippocampus was most impacted (414 genes), while both cortex and thalamus exhibited fewer changes in gene expression (141 and 107 genes respectively; Fig. 2.10A). Transgene expression in 5xfAD mice (consisting of *App*, *Psen1*, and *Thy1*) was increased by ~2-fold over endogenous expression across brain regions (Fig. 2.10B) and was not impacted by treatment, consistent with the protein expression data (Fig. 2.4K, L). Initially focusing on the 414 gene expression changes in the hippocampus induced by pathology, we plotted a heat map of the log(2) fold change for each of the 9 relevant comparisons (5xfAD vs. wild-type, 5xfAD + PLX5622 vs. 5xfAD, and PLX5622 vs. wild-type, each for cortex, hippocampus, and thalamus; Fig. 2.10C). The hippocampus displayed a unique gene expression profile

**A** # of Genes with p < 0.05 Wild-Type Vs. 5xfAD

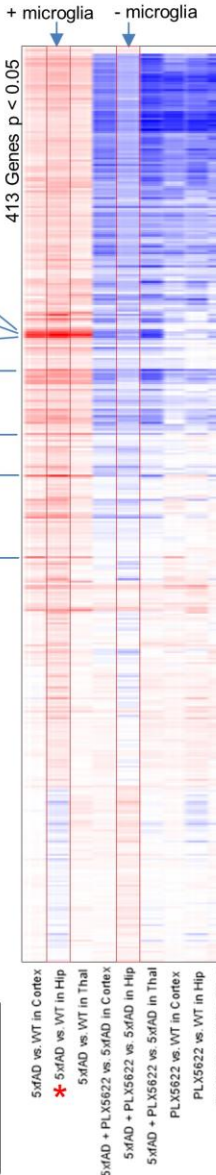


Shown in Figure 8

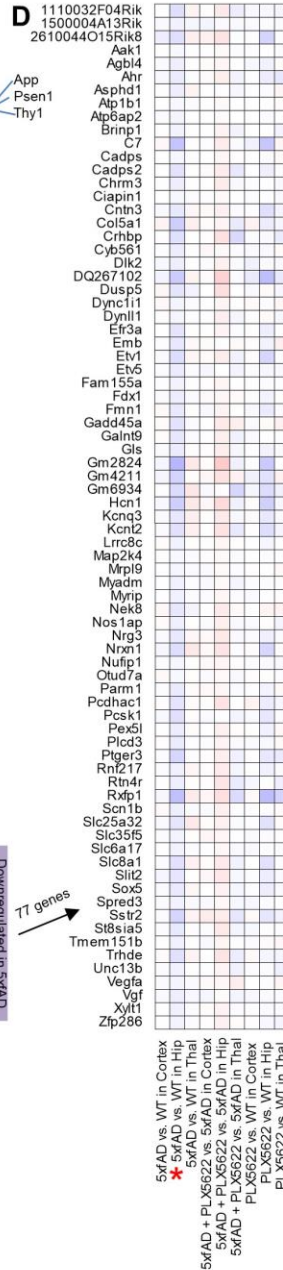
**B**



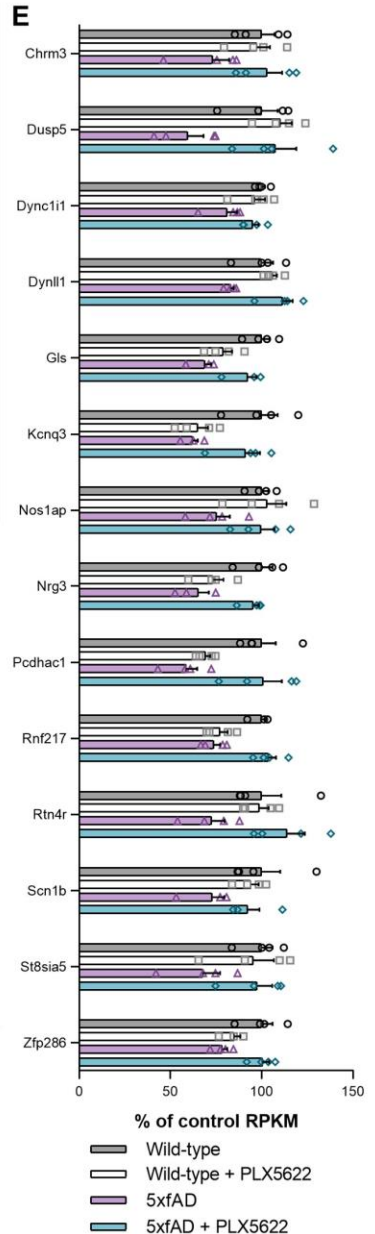
**C** Genes with p < 0.05 WT and 5xfAD Hip



**D**



**E**



**F**

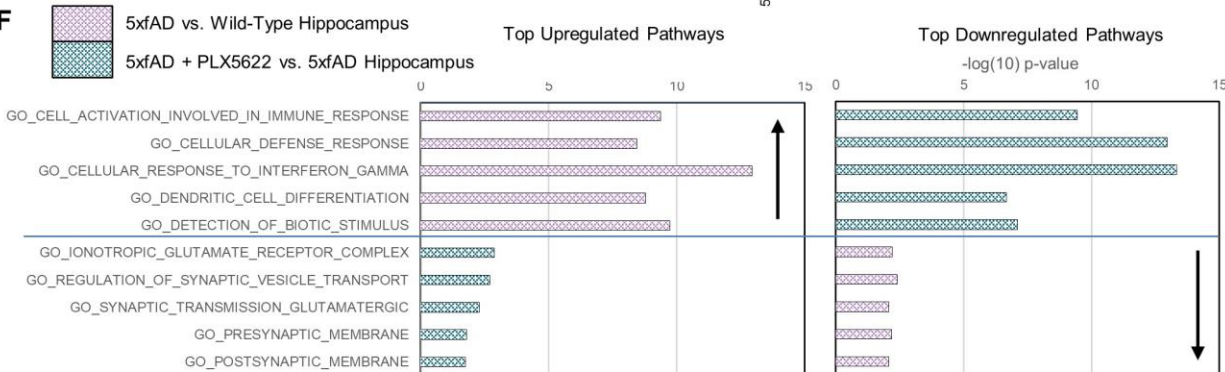


**Figure 2.10: Microglia mediate downregulation of neuronal/plasticity genes in the hippocampus in response to AD pathology.** **A**, Venn diagram showing the number of differentially expressed genes (adjusted  $p < 0.05$ ) for cortex, hippocampus, and thalamus for wild-type (WT) vs. 5xfAD mice. **B**, Heatmap of the p-value and  $\log(2)$  fold change for all 9 comparison groups (5xfAD vs. WT in cortex, hippocampus, or thalamus, 5xfAD + PLX5622 vs. 5xfAD in cortex, hippocampus, or thalamus, and WT + PLX5622 vs. WT in cortex, hippocampus, or thalamus), as well as 3 comparisons between brain regions for both WT and 5xfAD mice, for the transgene components in 5xfAD mice (*App*, *Psen1*, *Thy1*). **C**, Heatmap of all 413 gene expression differences identified in the hippocampus for wild-type vs. 5xfAD, expressed as  $\log(2)$  fold change, and all 9 comparison groups included. Hippocampus for 5xfAD vs. WT and 5xfAD + PLX5622 vs. 5xfAD highlighted by red border, showing that most significant gene expression changes induced by pathology do not occur in the absence of microglia. **D**, Downregulated genes in the hippocampus from (A), displayed as a heatmap of  $\log(2)$  fold change differences for all 9 comparisons, showing that the same genes are not downregulated in the absence of microglia (5xfAD + PLX5622 vs. 5xfAD Hip). **E**, RPKM values plotted on a  $\log(2)$  scale for a subset of plasticity genes from (D). **F**, The top 5 significantly upregulated and downregulated pathways for 5xfAD vs. wild-type hippocampus (red), along with respective  $-\log(10)$  p-values plotted: most upregulated pathways are related to immune function, while downregulated pathways are mainly associated with neuronal and synaptic activity. The same pathways are displayed for the comparison between 5xfAD + PLX5622 vs. 5xfAD hippocampus (yellow), showing that the absence of microglia prevents the upregulation of immune pathways and the downregulation of synaptic pathways. Expression difference denoted by \*.  $\log(2)$  fold change and p-values indicated by respective scale bar.  $n = 4$  per group for all analyses. Error bars indicate SEM.

relative to the cortex and thalamus and included a unique subset of downregulated genes. Of note, only 1 downregulated gene was identified in the cortex and none were detected in the thalamus. Furthermore, all gene expression changes (either upregulated or downregulated) appeared to be fully reversed in the hippocampus of treated 5xfAD mice, with fold-changes in 5xfAD + PLX5622 vs. 5xfAD hippocampus being equal and opposite to those induced in the 5xfAD mice (highlighted by red border). Of the 414 identified genes, 77 were down-regulated in the 5xfAD hippocampus (Fig. 2.10C, and individual genes plotted in D). Notably, these genes were primarily synaptic- and neuronal-associated genes such as *Dlk2*, *Dync111*, *Gls*, *Kcnq3*, *Nrg3*, and *Scn1b*. Importantly, the absence of microglia prevented the AD-pathology induced downregulation of neuron-associated genes (Fig. 2.10E), highlighting that microglia in the 5xfAD brain drive the downregulation of plasticity-related genes in the hippocampus. Enrichment analyses of the hippocampus revealed an upregulation in immune function-

associated pathways in 5xfAD vs. wild-type, and accordingly, these pathways were all highly significantly downregulated with PLX5622 treatment (Fig. 2.10F). Analyses of downregulated pathways in 5xfAD vs. wild-type hippocampi revealed that the most highly significant pathways were related to neuronal functioning, such as glutamate receptors, synaptic vesicles, and neuronal membranes (Fig. 2.10F). Importantly, many of these pathways were upregulated – or more accurately, never downregulated – with the absence of microglia (Fig. 2.10F), indicating that microglia influence neuronal gene expression pathways in response to AD pathology.

*Neither AD pathology nor treatment/absence of microglia grossly modulate AD-related gene expression:* Although we confirmed that the absence of microglia/treatment with PLX5622 did not alter the amount of A $\beta$  produced, we wanted to explore the impact of pathology and microglia on genes associated with APP processing, A $\beta$  clearance and metabolism, and AD in general (Fig. 2.4M). The only significant changes in gene expression in 5xfAD mice compared to wild-type were the upregulation of the transgenes (*App* and *Psen1*; as expected due to overexpression), and *ApoE*, all of which were not altered by the absence of microglia, and the downregulation of myeloid-expressed *Trem2*, *Ctsb*, *Ctsc*, and *Ctsd* in the absence of microglia, as expected. Comparisons of changes in expression between brain regions showed regional differences in *Ache*, *ApoE*, *Ptk2b*, *Sorl1*, and *Sort1*. Thus, both AD pathology and the absence of microglia have minimal effects on AD-related genes, and importantly, we observe no alterations in gene expression or protein production in the absence of microglia that could account for reduced plaque formation.

## Repopulation of microglia seed plaques

While microglia can be indefinitely depleted via the continued administration of CSF1R inhibitors, the microglial compartment can also be repopulated upon CSF1R inhibitor withdrawal<sup>36,133,228</sup>. To further prove that microglia are responsible for plaque formation, we sought to examine the effects of microglial repopulation in 5xfAD mice after 10 weeks of PLX5622 treatment. We treated a cohort of 1.5-month-old 5xfAD mice with PLX5622 (1200 ppm in chow) to eliminate microglia until 4 months of age, then CSF1R inhibitor-formulated chow was removed to stimulate microglial repopulation and the brains were examined 1 month later (Fig. 2.11A). Microglia repopulated all areas of the brain in both wild-type and 5xfAD mice (Fig. 2.11B), although overall densities were lower than the untreated mice in cortical regions (Fig. 2.11C, D; quantified in F). As demonstrated previously, untreated 5xfAD mice exhibit cortical plaques at 4 months of age, but 5xfAD mice devoid of microglia show reduced plaque formation (Fig. 2.3C, F, L). Furthermore, from our extended cohort of 5xfAD mice devoid of microglia, we know that plaque formation is severely diminished in treated 5xfAD animals, even by 7 months of age (Fig. 2.3E, H). However, examination of microglia-repopulated 5xfAD brains revealed the appearance of robust plaque pathology (Fig. 2.11D) with plaque numbers being equal to the untreated 5xfAD mice (Fig. 2.11G), although average plaque volumes were smaller (Fig. 2.11H). Notably, vascular pathology was still present in the repopulated brains (Fig. 2.11D), showing that the reintroduction of microglia does not reverse the vascular deposition of A $\beta$ , at least within this one-month timeframe. Repopulating microglia associate with the new plaques but do not appear to react to the vascular deposits (Fig. 2.11E). Moreover, GFAP<sup>+</sup> astrocytes associated with plaques in

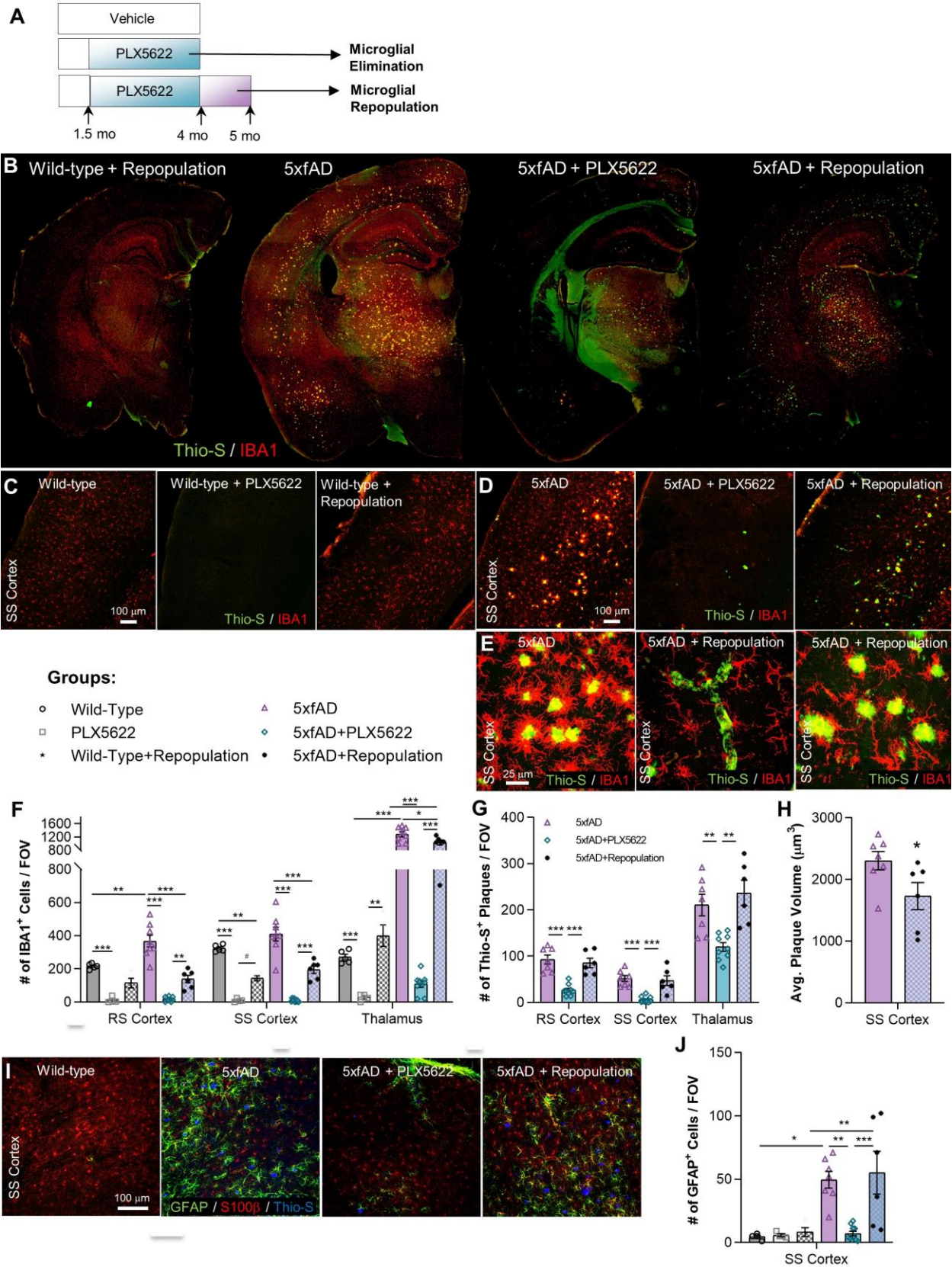


**Figure 2.11: Microglia seed plaques.** All analyses listed in respective order for retrosplenial (RS) cortex, somatosensory (SS) cortex, and thalamus. **A**, Experimental design: 1.5-month-old wild-type (WT) and 5xfAD mice were administered PLX5622 (1200 ppm in chow) until 4 months of age to eliminate microglia and PLX5622 diet was subsequently withdrawn for 1 month to allow microglial repopulation. **B**, Representative hemisphere stitches of sections stained for dense core plaques (Thio-S in green) and immunolabeled for microglia (IBA1 in red). **C-E**, Cortical images of dense-core plaque staining (Thio-S in green) and microglia immunolabeling (IBA1 in red). **F**, Quantification of IBA1<sup>+</sup> cell number revealed an increase in the 5xfAD group compared to WT ( $p=0.001$ , NS,  $p<0.001$ ). PLX5622-treatment reduced microglial numbers in both WT ( $p<0.001$ ,  $p<0.001$ ,  $p<0.001$ ) and 5xfAD animals ( $p<0.001$ ,  $p<0.001$ ,  $p<0.001$ ). Repopulated groups showed an increase in microglial number compared to PLX5622-treated groups in both WT (NS,  $p=0.054$ ,  $p=0.008$ ) and 5xfAD animals ( $p=0.006$ ,  $p<0.001$ ,  $p<0.001$ ). Microglial numbers in repopulated groups of WT (NS,  $p=0.002$ , NS) and 5xfAD ( $p<0.001$ ,  $p<0.001$ ,  $p=0.027$ ) animals were ~50% of untreated mice in the cortex. Two-way ANOVA with Tukey's post hoc test;  $n = 5$  for Wild-type,  $n = 4$  for PLX5622,  $n = 4$  for Wild-type + Repopulation,  $n = 8$  for 5xfAD,  $n = 9$  for 5xfAD + PLX5622,  $n = 6$  for 5xfAD + Repopulation. **G**, Thio-S<sup>+</sup> plaque number was significantly reduced in 5xfAD + PLX5622 mice compared to the 5xfAD group ( $p<0.001$ ,  $p<0.001$ ,  $p=0.007$ ). Compared to 5xfAD animals devoid of microglia, the 5xfAD + Repopulation group showed significantly elevated plaque numbers ( $p<0.001$ ,  $p<0.001$ ,  $p=0.001$ ). Repopulation in 5xfAD mice restored plaque numbers to that of untreated 5xfAD mice (NS, NS, NS). NS, not significant. One-way ANOVA with Tukey's post hoc test;  $n = 7$  for 5xfAD,  $n = 9$  for 5xfAD + PLX5622,  $n = 6$  for 5xfAD + Repopulation. **H**, Cortical plaque volume was reduced by ~20% with microglia repopulation in 5xfAD mice compared to untreated 5xfAD mice ( $p=0.048$ ). Two-tailed independent t-test;  $n = 7$  for 5xfAD,  $n = 6$  for 5xfAD + Repopulation. **I**, Confocal images of cortical sections stained for dense-core plaques (Thio-S in blue) and immunolabeled for astrocytes with GFAP (in green) and S100 $\beta$  (in red). **J**, Quantification of the number of GFAP<sup>+</sup> astrocytes in the SS cortex. GFAP number was increased in 5xfAD animals relative to untreated mice ( $p=0.010$ ) and PLX5622 treatment in 5xfAD mice normalized GFAP cell number ( $p=0.002$ ). Microglia repopulation in 5xfAD animals restored astrocyte reactivity ( $p<0.001$ ), and increased GFAP cell number relative to WT repopulated mice ( $p=0.009$ ). Two-way ANOVA with Tukey's post hoc test;  $n = 4$  for Wild-type,  $n = 4$  for PLX5622,  $n = 4$  for Wild-type + Repopulation,  $n = 7$  for 5xfAD,  $n = 10$  for 5xfAD + PLX5622,  $n = 6$  for 5xfAD + Repopulation. Statistical significance is denoted by \* $p<0.05$ , \*\* $p<0.01$ , and \*\*\* $p<0.001$ . Error bars indicate SEM.

both control and repopulated 5xfAD brains (Fig. 2.11I, J), but were absent in 5xfAD brains devoid of microglia. Thus, the reintroduction of microglia in the 5xfAD brain via CSF1R inhibitor withdrawal coincides with a full restoration of plaque pathology and directly implicate the reappearance of microglia in the brain with the seeding and formation of plaques.

## DISCUSSION

In this study, we sought to investigate the role of microglia throughout the onset and development of AD pathology in 5xfAD mice, requiring the sustained depletion of

microglia from the adult mouse brain for a period of ~6 months. While various methods of microglial ablation are available, the extent/duration of microglial depletion and the technical requirements necessary to achieve sustained microglial elimination prohibit the use of most depletion paradigms. For example, the CX3CR1<sup>cre<sup>ER</sup></sup> x DTR<sup>ff</sup> mouse model relies on administration of diphtheria toxin, which not only induces a cytokine storm, but also limits microglial elimination to 5 days<sup>120</sup>. The CD11b-HSVTK model requires intracerebroventricular infusion of ganciclovir in order to produce substantial microglial depletion, which in turn induces BBB damage and myelotoxicity, resulting in increased mortality following 4 weeks of ganciclovir treatment<sup>104</sup>. Clodronate liposome administration is also reported to deplete microglia, however, this effect is short-lived and requires intrahippocampal infusion, as clodronate liposomes are incapable of crossing the BBB<sup>121</sup>. Previously, we discovered that microglia are critically dependent upon CSF1R signaling for their survival<sup>133</sup> and that CSF1R inhibitors serve as effective tools to achieve microglial depletion. In contrast to other methods, CSF1R inhibitors provide the following advantages: 1) their administration is non-invasive, 2) they do not rely on other pharmacological drivers such as ganciclovir or tamoxifen, 3) they do not induce an inflammatory response (cytokine storm) from the surviving cells, 4) they have highly selective effects on microglia, 5) they can be formulated to control for peripheral myeloid effects on microglial responses, and 6) they can be used clinically, and therefore, experimental findings are potentially translatable. Most importantly, CSF1R inhibition is the only currently available method capable of achieving sustained long-term microglial elimination. Using PLX5622, we were able to eliminate >95% of microglia from the brains of 5xAD mice prior to and during the formation of AD

pathology, even up to 6 months of duration, and elucidate their roles in plaque formation. Data presented here show that long-term PLX5622-mediated microglial depletion is highly robust, sustainable, and specific to the microglial compartment. These findings are demonstrated by extensive gene expression analyses, a lack of behavioral/cognitive impairments, and unaffected circulating immune cell numbers. Together, these data demonstrate that PLX5622 is a useful compound for investigating microglial dynamics.

The genetics of familial AD indicate that altered APP processing and plaque accumulation are critical for disease etiology<sup>229</sup>. In sporadic AD, plaques appear in the brain prior to any other overt pathologies<sup>199</sup> and precede cognitive deterioration and disease progression<sup>230-232</sup>. AD appears to be precipitated by the formation and development of plaques in the brain, and therefore, identifying the underlying biology of plaque formation is crucial to understanding and preventing disease onset. Genome-wide association studies have identified several genes associated with an increased risk for developing sporadic AD. Many of these risk variants are highly enriched in myeloid cells<sup>201</sup>, indicating that myeloid biology appears to be a large contributor to the development of disease. Microglia are the resident myeloid cell of the CNS, and their activated presence surrounding plaques is a prominent feature of AD pathology. While microglia are phagocytes, in the later stages of disease, studies indicate that these cells do not clear A $\beta$  or modulate plaque numbers/sizes in the brain<sup>104,115,132</sup>. Instead, evidence indicates that they play a role in synaptic damage and neuronal loss<sup>132,198,233</sup>. Examination of human brains (non-demented, high pathology non-demented, and Alzheimer's disease subjects), as well as mouse models of AD, reveal the accumulation

of A $\beta$  aggregates within the lysosomes of microglia unassociated with plaques. Thus, we hypothesized that neuronally-derived A $\beta$  is internalized/aggregated within microglia, and that this material contributes to the initial formation of plaques. In a prior study, we evaluated the contributions of microglia in an advanced stage of AD, by eliminating microglia in aged (*i.e.*, 10-month-old) 5xfAD mice that had developed extensive plaque-related pathologies. We found that the elimination of microglia prevented synaptic and neuronal loss, without affecting plaque deposition or A $\beta$  levels in the brain<sup>132</sup>. Subsequent studies confirmed the critical roles of microglia to neuronal loss<sup>234</sup>, highlighting the deleterious actions of chronically activated microglia in the advanced stages of AD. In this study, we sought to identify whether microglia play a role in the initial deposition of plaques, via sustained treatment with PLX5622 prior to and during the period of plaque formation in the 5xfAD mouse model of AD. Here, we find that plaque formation is prevented in the absence of microglia, even over extended periods of time. While some plaques form in specific brain areas with treatment, we find that these few remaining plaques are associated with a small subset of microglia initially resistant to CSF1R-inhibition. These microglia are most apparent in the thalamus, retrosplenial cortex, and subiculum. Once formed, these plaques persist thereafter, even long after plaque-associated microglia are eliminated. Thus, our work demonstrates that plaque onset relies on the presence and activity of microglia. Additionally, as some microglia survive CSF1R inhibitor treatment, this approach also allows for the exploration of these remaining cells in plaque structure and maintenance. Insights into the roles of microglia in plaque biology have been explored via the study of the myeloid gene *Trem2*, in which coding mutations, presumed to be loss of function,

are associated with increased risk of sporadic AD<sup>235-237</sup>. Recently, it was demonstrated that perturbation of *Trem2* signaling impaired the association of microglia with plaques<sup>91,116,238</sup>, revealing that plaque-associated microglia compact plaque cores and form a barrier that protects surrounding neurites from toxicity<sup>91,116,117</sup>. In line with these studies, we confirm and demonstrate that plaque compaction and barrier formation are natural functions of microglia in disease, rather than functions conferred by the loss of TREM2 function. In addition, we show that microglia are necessary for the development of the plaques. These findings are supported by recent data showing that plaque seeding is accelerated in *Trem2* knockout mice<sup>82</sup>, suggesting that the microglial function involved in the initial formation of plaques is related to TREM2 signaling.

By way of further mechanism for plaque seeding and growth, microglia could be: 1) secreting factors that facilitate A $\beta$  fibrillization<sup>50</sup>, 2) physically forming plaque cores from extracellular A $\beta$  via compaction<sup>239</sup>, or 3) ingesting, aggregating, and modifying extracellular A $\beta$  internally, which is eventually released to seed plaques, in line with *in vitro* data<sup>240</sup>. Indeed, we observe aggregated A $\beta$  within ramified microglia distal to plaques in two different mouse models of AD (Fig. 2.1A-F), as well as the human brain (Fig. 2.1K-O). This observation is seemingly contrary to the idea that the source of internalized microglial A $\beta$  is plaque-derived. In accordance, we find that plaque growth ceases in the absence of microglia, suggesting a mechanism by which microglia deliver A $\beta$  to the plaque seed/core. These data suggest that following the uptake of freely available A $\beta$ , microglia subsequently deposit aggregated A $\beta$  into the extracellular space, thus contributing to the formation of plaques.

Together, these results demonstrate that plaque formation does not result from impaired microglial clearance, but rather requires the action(s) of microglia – an observation that may explain the overrepresentation of microglia-expressed genes in AD genome-wide association studies. In line with this, modulation of ApoE4 signaling prior to the period of plaque deposition alters A $\beta$  accumulation, whereas intervening after the emergence of plaques has no effect<sup>225,241</sup>. Notably, the manipulation of ApoE in AD mouse models phenocopies the absence of microglia (i.e. CAA instead of plaques<sup>242-244</sup>). Hence, it appears that the presence of microglia is necessary and integral for the formation of plaques, similar to elevated brain A $\beta$ 42/A $\beta$ 40 ratios<sup>245,246</sup> and the presence of ApoE, in disease<sup>243</sup>. Of particular note, in the absence of microglia, A $\beta$  accumulates not in the parenchymal space, but instead within cortical blood vessels as CAA, suggesting that microglia may play a role in shuttling A $\beta$  away from the vasculature. Thus, it could be possible that microglia protect against CAA via the formation of parenchymal plaques. As 5xfAD mice overexpress APP/A $\beta$ , it is unknown whether the experimentally observed accumulation of A $\beta$  in blood vessels is physiologically relevant. It is not detected in untreated 5xfAD mice containing microglia nor wild-type mice devoid of microglia. Interestingly, this phenotype is akin to A $\beta$  immunotherapy studies in mice and humans, in which clearance of parenchymal plaques is accompanied by A $\beta$  deposition in blood vessels<sup>247-249</sup>. Since low CNS exposure of PLX3397 (~1 $\mu$ M) does not modulate microglia, plaques, or induce CAA, we conclude that the appearance of CAA is not due to peripheral effects of the drug, but is in fact dependent on microglial elimination.

To further delineate microglial roles, we performed gene expression analyses of wild-type and 5xfAD mice in cortex, hippocampus, and thalamus, in both microglia-intact

animals and mice lacking microglia for the entirety of their adult lives. Notably, we find hippocampal gene expression is greatly influenced by the presence of AD pathology relative to the cortex and thalamus, despite abundant plaque load in all these regions. Differential gene analysis revealed that nearly all significantly altered genes, in 5xfAD compared to WT mice, were associated with microgliosis in the cortex and thalamus, while the hippocampus displayed reductions in gene expression associated with neuronal and synaptic function. The absence of microglia prevented many of these changes in 5xfAD mice, despite the continued presence of hippocampal plaques, due to a small population of surviving myeloid cells in the subiculum. Although plaque-associated microglia may protect against local neurite damage, the presence of microglia is also required for the reduction in expression of synaptic and neuronal genes in the hippocampus associated with AD. Notably, the absence of microglia is not associated with detectable alterations in immune- and synapse-related genes, suggesting that microglia mediate most AD pathology-induced changes in gene expression. Therefore, microglia appear to have detrimental and beneficial roles in a preclinical model of AD. Whether these effects are stratified into separate populations (i.e., protective effects of plaque-associated microglia vs. harmful effects of non-plaque associated microglia, as recently suggested<sup>83</sup>) needs to be determined. In support of discrete microglial populations mediating dichotomous effects, we show that the elimination of 88% of non-plaque associated microglia and presence of ~50% of plaque-associated microglia in 5xfAD mice with existing pathology using our CSF1R inhibitor treatment paradigm resulted in the prevention of both synaptic and neuronal loss<sup>132</sup>.

These findings highlight detrimental functions of non-plaque-associated microglia and beneficial roles of plaque-associated microglia.

In conclusion, we have designed and created a specific CSF1R inhibitor, PLX5622, that allows for the sustained and specific elimination of microglia. This novel method of microglial depletion provided us with the means to eliminate microglia for the duration of AD pathogenesis. Ultimately, these data demonstrate that microglial elimination is associated with the prevention of plaque formation and the downregulation of hippocampal neuronal genes that occur in a preclinical mouse model of AD. These results indicate that microglia appear to contribute to multiple facets of AD etiology – microglia appear crucial to the initial appearance and structure of plaques, and following plaque formation, promote a chronic inflammatory state modulating neuronal gene expression changes in response to A $\beta$ /AD pathology.

## CHAPTER THREE

### Evaluating microglial ApoE as a contributor to plaque formation

#### INTRODUCTION

In chapter two, we show that an absence of microglia before and during the normal period of plaque development prevents cortical parenchymal plaque formation, and instead, shifts A $\beta$  deposition to the vasculature. Modulation of ApoE signaling, the strongest identified genetic risk factor for the development of AD, bears a striking similarity to this phenotype<sup>242,244,250-252</sup>. The brains of mice with knocked-in human ApoE3 or ApoE4 show a dramatic reduction in parenchymal plaque deposits, and a shift in pathology to the vasculature<sup>242,244</sup>, whereas complete knockout of ApoE signaling inhibits plaque formation<sup>118,243,253</sup>. Additionally, reductions in ApoE signaling prior to the period of plaque deposition prevents A $\beta$  accumulation, whereas its reduction after the emergence of plaques had no effect<sup>225,241</sup>. These observations resemble the effects of microglial elimination in AD – the data in chapter two demonstrate that the elimination of microglia prior to plaque onset also prevents plaque formation, whereas the elimination of microglia subsequent to plaque onset bears no effect on plaque burden<sup>132</sup>. Together, these data highlight potential overlapping pathways between microglia-eliminated AD brains and mouse models modulating ApoE expression that could underlie plaque pathogenesis.

While predominantly expressed by astrocytes<sup>254</sup>, ApoE expression can be induced in microglia in disease states<sup>81,83,119,255</sup>, including data from chapter one that shows a ~20% contribution of microglia to the total pool of measured ApoE transcripts in AD (Fig.

1.6A<sup>132</sup>). In the AD brain, ApoE expression is highly enriched in plaque-associated microglia<sup>82,83,119</sup> and dense core A $\beta$  deposits<sup>82</sup>. Given the phenotypic parallels between pathology in contexts of both microglial or ApoE loss, we set out to understand whether microglial ApoE plays a crucial role in the seeding of plaques. To that end, we selectively knocked-out ApoE from microglia/myeloid cells in 5xfAD mice, allowing us to determine the contribution of microglial ApoE to plaque formation. We find that in the absence of microglial ApoE signaling, plaque numbers and volumes in the subiculum of 5xfAD mice are reduced relative to ApoE-intact 5xfAD animals, identifying ApoE signaling as a driver of plaque formation.

## **MATERIALS AND METHODS**

**Compounds:** PLX5622 was formulated in AIN-76A standard chow by Research Diets Inc. at 1200 ppm.

**Animal Treatments:** All rodent experiments were performed in accordance with animal protocols approved by the Institutional Animal Care and Use Committee at the University of California, Irvine. B6.129S6-*ApoE*<sup>tm1.1Mae</sup>/MazzJ (*ApoE*<sup>fl/fl</sup>; stock no. 028530) and FVB-Tg(Csf1r-icre)1Jwp/J (*CSF1R-Cre*<sup>+/-</sup>; stock no. 021024) animals were obtained from Jackson Laboratory and backcrossed 5 generations to yield congenic B6 offspring. *ApoE*<sup>fl/fl</sup>/*CSF1R-Cre*<sup>+/-</sup> mice were subsequently bred with 5xfAD<sup>+/-</sup> animals to generate experimental animals. All rodent experiments were performed in accordance with animal protocols approved by the Institutional Animal Care and Use Committee at the University of California, Irvine. The 5xfAD<sup>174</sup> mouse

model has been previously described in detail. At the end of treatments, mice were euthanized via CO<sub>2</sub> inhalation and transcardially perfused with 1X phosphate buffered saline (PBS). For all studies, brains were removed, and hemispheres separated along the midline. Brain halves were either flash frozen for subsequent biochemical analysis or drop-fixed in 4% paraformaldehyde (PFA (Thermo Fisher Scientific, Waltham, MA)) for immunohistochemical analysis. Fixed half brains were sliced at 40 µm using a Leica SM2000R freezing microtome.

**Confocal Microscopy:** Immunofluorescent labeling was performed on mouse and human brain sections following a standard indirect technique as previously described<sup>180</sup>. Mice were perfused with PBS prior to tissue fixation, followed by tissue sectioning to produce 40 µm thick floating sections. Primary antibodies and dilutions used are as follows: anti-ionized calcium-binding adapter molecule 1 (IBA1; 1:1000; Wako, Osaka, Japan), anti-Apolipoprotein E (ApoE; 1:100; Abcam), and anti-gial fibrillary protein (GFAP; 1:1000; Abcam). Thioflavin-S (Thio-S; Sigma-Aldrich) staining was carried out as previously described<sup>181</sup>. Total microglia and plaque counts/volumes were obtained by imaging comparable sections of tissue from each animal at the 20X objective, at multiple z-planes, followed by automated analyses using Bitplane Imaris 7.5 spots or surfaces modules, respectively.

**Statistics:** Every reported *n* is the number of biologically independent replicates. Immunohistological data were analyzed using a two-tailed independent-samples t-test (5xfAD vs. 5xfAD + PLX5622 or 5xApoE vs. 5xApoECC) in GraphPad Prism Version 7

(La Jolla, CA). Symbols denote significant differences between groups: \* $p < 0.05$ , \*\* $p < 0.01$ , and \*\*\* $p < 0.001$ . Statistical trends are accepted at  $p < 0.10$  (#). Data are presented as raw means and standard error of the mean (SEM).

## RESULTS

### Microglial ApoE facilitates plaque formation in 5xfAD mice:

Previous reports describe the coaggregation of ApoE with A $\beta$  fibrils in both plaques and vascular pathology<sup>82,242</sup>. Consistent with this, ApoE immunoreactivity was apparent within dense core plaques, but also in cellular processes surrounding the cores (Fig.

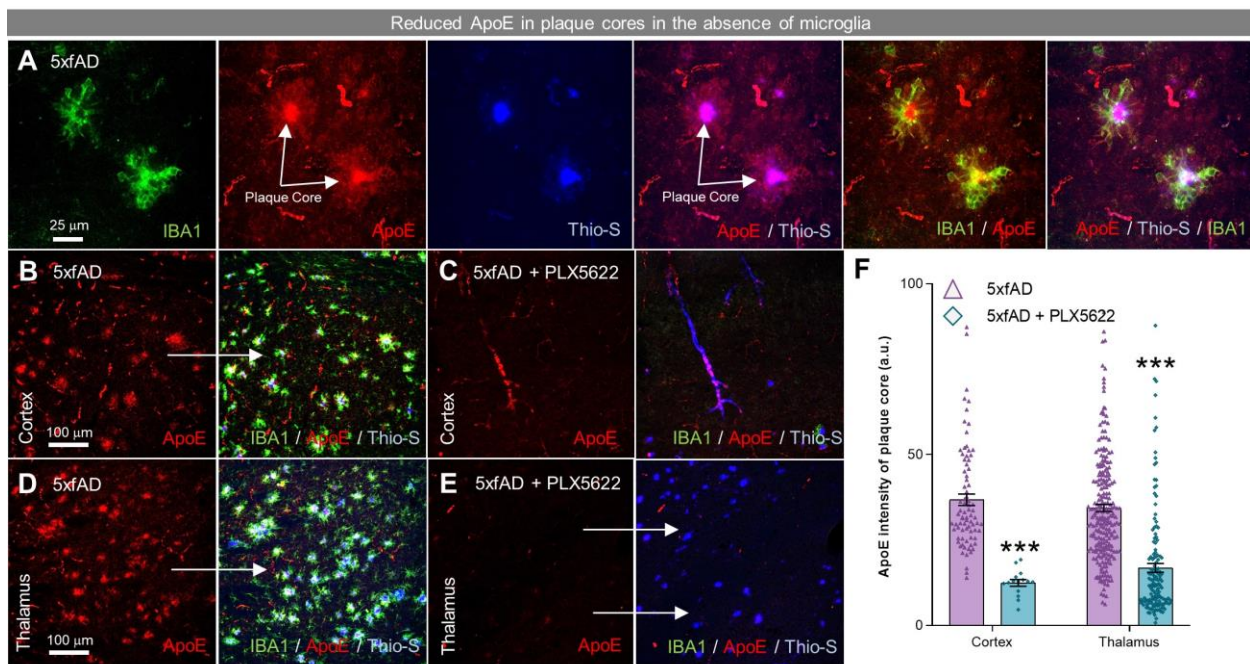


**Figure 3.1: ApoE immunoreactivity is absent from plaques and microglia with PLX5622 treatment.** **A**, Immunolabeling of tissue from 7-month-old 5xfAD animals for microglia (IBA1 in green), ApoE (in red), and stained for dense-core deposits (Thio-S in blue), showing high immunoreactivity of ApoE in plaque cores and microglia. **B-E**, Representative images of the cortex (**B, C**) and thalamus (**D, E**) from 7-month-old 5xfAD animals treated with control diet or PLX5622 immunolabeled for ApoE (in red) and microglia (IBA1 in green), and stained for dense-core deposits (Thio-S in blue). **F**, ApoE immunoreactivity is reduced in plaque cores of treated 5xfAD animals relative to untreated 5xfAD mice in the cortex ( $p < 0.001$ ) and thalamus ( $p < 0.001$ ). Two-tailed independent t-test;  $n = 7-10$  for 5xfAD,  $n = 7$  for 5xfAD+ PLX5622. Statistical significance is denoted by \* $p < 0.05$ , \*\* $p < 0.01$ , and \*\*\* $p < 0.001$ . Error bars indicate SEM.

3.1A). In this study, colocalization of ApoE with the microglia/myeloid marker IBA1 revealed that these ApoE<sup>+</sup> processes were indeed microglial (Fig. 3.1A). These data provide evidence that microglia surrounding plaques contain ApoE, potentially indicating a unique role for microglial-expressed apoE in the immune response to AD pathology<sup>80</sup>. Examination of ApoE immunoreactivity in microglia-devoid 5xfAD mice showed a strong reduction in ApoE<sup>+</sup> staining in microglial processes surrounding dense core plaques, as expected, as well as in the plaque cores themselves. We quantified ApoE immunoreactivity in Thio-S<sup>+</sup> dense-core plaques in the cortex (Fig. 3.1B, C) and thalamus (Fig. 3.1D, E), and found a 50-70% reduction in plaque core ApoE (Fig. 3.1F). Thus, microglia surrounding fibrillar plaques appear to be a significant source of plaque-associated ApoE, consistent with recent findings showing an upregulation of ApoE in specifically plaque-proximal microglia<sup>82,119</sup>.

To further investigate the role of microglial ApoE signaling in facilitating plaque formation in AD, we generated a mouse model in which ApoE expression is specifically and constitutively excised from microglia/myeloid cells (*i.e.*, under the CSF1R promoter) in 5xfAD animals via a Cre-lox system (5xApoECC; Fig. 3.2A). To evaluate the efficiency with which Cre recombines loxP sites under the CSF1R promoter, we crossed a CSF1R-cre animal to a *Rosa26*<sup>YFP</sup> reporter mouse, generating offspring that express YFP in microglial progeny and found a ~76% recombination efficiency as measured by %IBA1<sup>+</sup> cells expressing YFP (Fig. 3.2H), highlighting the efficiency of cre recombination of the floxed *ApoE* alleles. Immunohistochemical analysis of 4-month-old 5xApoE and 5xApoECC animals revealed that ApoE expression is predominantly restricted to GFAP<sup>+</sup> astrocytes in both groups (Fig. 3.2C, D), suggesting that significant

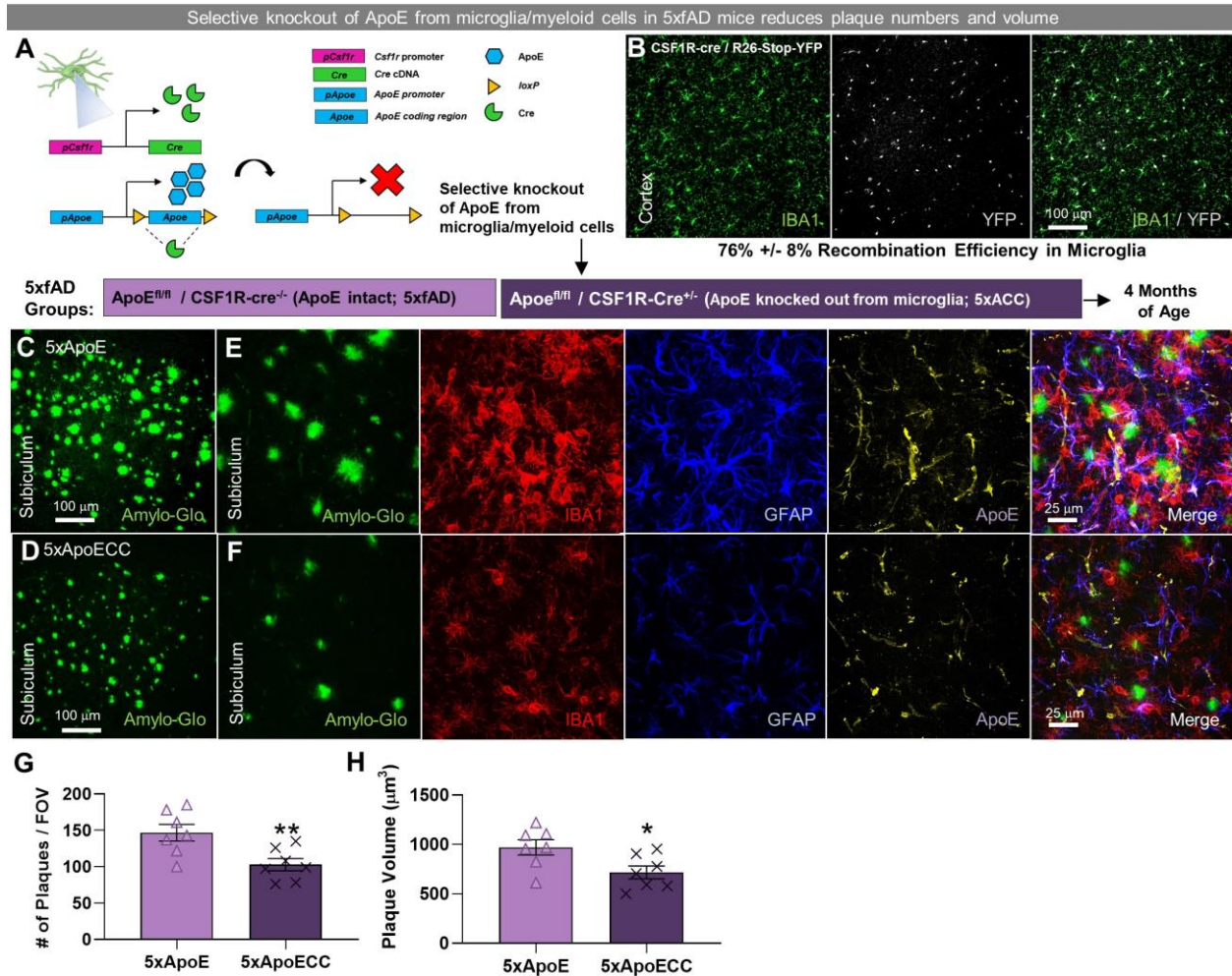


**Figure 3.2: Microglial ApoE contributes to plaque formation.** **A**, Schematic of 5xfAD<sup>+/+</sup>/ApoE<sup>fl/fl</sup>/CSF1R-cre<sup>+/-</sup> (5xApoeECC) mouse model of microglial knockout of ApoE in 5xfAD mice and experimental design. **B**, Cortical image of a CSF1R-cre<sup>+/+</sup> animal crossed to a Rosa26-YFP reporter line, demonstrating a 76% recombination efficiency in microglia. **C**, **D**, Images of subicula stained for dense-core plaques (Amylo-Glo in green). **E**, **F**, Zoomed images of 5xApoe and 5xApoeECC animals stained for dense-core plaques (Amylo-Glo in green), microglia (IBA1 in red), astrocytes (GFAP in blue) and ApoE (in yellow). **G**, **H**, Quantification of Amylo-Glo staining reveals a reduction in plaque number ( $p=0.009$ ) and volume ( $p=0.027$ ), respectively, with knockout of microglial ApoE in 5xfAD mice. Two-tailed independent t-test;  $n = 7$  for 5xApoe,  $n = 7$  for 5xApoeECC. Statistical significance is denoted by \* $p<0.05$ , \*\* $p<0.01$ , and \*\*\* $p<0.001$ . Error bars indicate SEM.

upregulation of microglial ApoE occurs later in the disease process, as shown by our initial immunohistochemical assays for ApoE in 7-month-old animals (Fig. 3.1A) and recent reports<sup>82,119</sup>. However, analysis of dense core plaques in the subiculum of 4-month-old 5xApoeECC mice (Fig. 3.2C-F) revealed a ~30% reduction in both plaque number (Fig. 3.2G) and volume (Fig. 3.2H) relative to 5xApoe controls. Collectively,

these findings provide further evidence that microglial activity facilitates the formation of plaques in AD and that this process is mediated in part by microglia-specific production of ApoE.

## **DISCUSSION**

Our previous work has established that the absence of microglia in 5xfAD results in diminished plaque formation and altered pathological deposition (i.e., shifting from the parenchyma to vasculature). To expand upon these findings, we next sought to determine the mechanism underlying this observation. In line with data from chapter one (i.e., microglia elimination subsequent to plaque deposition) and results from chapter two (i.e., microglial ablation prior to plaque onset), modulation of ApoE signaling after the emergence of plaques has no effect, whereas intervening prior to the period of plaque deposition altered A $\beta$  accumulation<sup>225,241</sup>. Notably, the manipulation of ApoE in AD mouse models phenocopies the absence of microglia (i.e., appearance of CAA instead of plaques<sup>242-244,250</sup>). In the extended absence of microglia in 5xfAD mice, we find a lack of ApoE within plaque cores, suggesting a shared pathway between microglia, ApoE, and A $\beta$  that contributes to plaque formation. In line with these findings, a recent study demonstrated that plaque-associated microglia upregulate ApoE expression<sup>82,83</sup> and contribute to the coaggregation and accumulation of ApoE in plaques<sup>82</sup>. Moreover, it was shown that microglia take up ApoE-A $\beta$  complexes via TREM2<sup>256</sup>, hypothesizing that ApoE facilitates A $\beta$  uptake and that microglial clearance of A $\beta$  protects against plaque deposition. However, we contend that ApoE-A $\beta$  complexes are an important convergence point by which A $\beta$  is internalized by microglia,

ultimately resulting in plaque seeding. In support of this, ApoE knock-out models exhibit reduced A $\beta$  pathology/plaques - not enhanced plaque burden - providing further evidence that plaque formation occurs in an ApoE-dependent fashion. Here, we extend these findings further by investigating a pathophysiological convergence between ApoE and microglia that contributes to plaque formation, given the pathological similarities between microglia- and ApoE-null mice. To explore this further, we selectively excised *ApoE* from myeloid cells in 5xfAD mice, revealing reductions in plaque number and volume without fully preventing the formation of plaques, as observed in the cohort of 5xfAD mice depleted of microglia for six months in chapter two. While ApoE expression is primarily astrocytic in 5xACC animals, microglia are reported to regulate astrocyte activation in AD<sup>64</sup>, which may play a role in the observed reduction in plaque burden. Thus, our data provide evidence that microglia-derived *ApoE* plays an important role in plaque formation but does not represent the single mechanism by which microglia promote the formation of A $\beta$  plaque pathology.

## DISSERTATION CONCLUDING REMARKS

Currently, treatment options for AD are limited to symptomatic relief, rather than targeting initiating factors that drive disease onset and progression. For this reason, no AD treatment has proven effective at altering the course of disease-related pathology or cognitive decline. The lack of disease-modifying therapies presumably stems from the underlying and causative disease mechanisms in AD remaining elusive, despite numerous attempts to identify such mechanisms. Due to long-standing support of the amyloid cascade hypothesis, A $\beta$ -targeting therapies aimed at reducing the production or increasing the clearance of A $\beta$  have been the object of several clinical trials. However, these compounds have all failed in the clinic, indicating that A $\beta$  is not the pathogenic factor driving cognitive decline in AD. Although a possible pathogenetic role of A $\beta$  cannot be completely ruled out at present, the breadth of evidence accumulated to date points to a waning of the amyloid cascade hypothesis, leading to renewed efforts of the scientific community to identify the true culprit(s) of Alzheimer's disease. Recently, neuroinflammation, of which a chronic form is observed in AD, has gained considerable research interest, stemming from GWAS findings that highlight variants in myeloid genes as a significant risk factor for AD development. Thus, it is only recently that research has begun to understand and appreciate the multitude of roles myeloid cells play within AD, including their contribution to disease pathology.

In the CNS, microglia are the resident myeloid cell that perform immune surveillance and supportive functions to maintain CNS homeostasis. From development to adulthood, microglia are crucial in shaping neuronal connectivity through refinement of extraneuronal synapses and neurons, thereby establishing and preserving a functional

network, as well as supporting neuronal health through the release of neurotrophic factors. In addition to their roles in the healthy brain, microglia have been shown to exert dichotomous and differential functions in the AD brain, including A $\beta$  degradation and seeding, neurotoxicity, and synaptic degeneration. Thus, the ways in which microglial function changes across the spectra of disease progression (*i.e.*, preceding overt pathology, early pathogenesis, and advanced pathology) that ultimately culminates in the development of AD remains elusive. As neuroinflammatory processes mediated by microglia are complex and multifaceted, much consideration is required regarding the modulation and management of this process. In support of this and prior to my admittance into graduate school, we demonstrated that microglial depletion in a model of hippocampal neuronal lesion resulted in diverging effects depending upon insult phase; acute microglial responses were crucial for beneficial post-lesion outcomes, whereas chronic microglial activation exacerbated neuronal loss and cognitive functioning. Thus, for my dissertation, I sought to investigate the various roles of microglia over the spectrum of the most prevalent neurodegenerative disease, AD.

In the first chapter of my dissertation, I determined that microglia in the AD brain are dependent on CSF1R signaling for their survival, and through this, was able to ascertain the effects of one-month of microglia depletion on AD pathology dynamics under severe/advanced pathology conditions. Using CSF1R inhibitors to eliminate microglia for one month in 10-month-old 5xfAD mice, I found a recovery of contextual memory, a reversal of dendritic spine loss, and prevention of neuronal loss, and yet no changes on A $\beta$  levels or plaque deposition. These data highlight the largely detrimental roles of microglia in the aged AD brain, predominantly carried out by plaque-distal microglia. To

expand upon these findings, I next set out to explore the contribution(s) of microglia to plaque formation in the initial stages of the disease, which is described in the second chapter of my dissertation. Importantly, this requires prolonged depletion of microglia throughout the plaque-forming period, which is only achievable using CSF1R inhibitors. To that end, I administered PLX5622 to 5xfAD mice at 1.5 months of age to deplete microglia for ~6 months. With the elimination of microglia, we uncovered critical roles of these cells in plaque formation and growth, as well as modulating hippocampal neuronal gene expression in response to A $\beta$  pathology. Thus, contrary to the current body of literature pointing to microglial dysfunction as a driving factor in plaque onset, it appears that plaque formation is a physiological activity of microglia and may be the benign product of a deeper pathological process. However, subsequent to plaque formation, microglia mitigated toxicity to nearby neurons by compacting A $\beta$  fibrils into dense deposits, highlighting the contrasting roles of microglia in early AD. Collectively, these results point to microglia as critical and causative in the development and progression of multiple facets of AD. Based on the findings of diminished plaque formation, I hypothesized that microglial functions in plaque formation are dependent on ApoE, given the parallels between pathology in microglia- and ApoE-null mice. To that end, I created a mouse model that expresses floxed *Apoe* alleles under a transgenic CSF1R promoter, effectively knocking out ApoE expression from myeloid cells without affecting the endogenous CSF1R locus. In line with my hypothesis, knockout of the *Apoe* gene from microglia/myeloid cells reduced plaque numbers and volumes, indicating that microglial ApoE is at least partially involved in the formation of plaques in 5xfAD mice. However, as A $\beta$  plaques were observed in 5xfAD animals lacking microglial ApoE

signaling, this suggests that other cellular sources of ApoE or other signaling pathways altogether contribute to plaque formation in AD.

Collectively, these data strengthen our understanding of microglial influences on neuronal health and protein aggregate clearance the AD brain, reveal diverging, disease/pathology-dependent functions of these cells, and identify a unique pathway involved in microglia-mediated plaque pathogenesis. These findings highlight the significance of microglia in the development of AD, and with hope, will accelerate the development of disease-modifying therapies that target and modulate microglial function.

## REFERENCES

- 1 Hebert, S. E., Scherr, P. A., Bienias, J. L., Bennett, D. A. & Evans, D. A. Alzheimer disease in the US population: prevalence estimates using the 2000 census. *Arch Neurol* **60**, 1119-1122 (2003).
- 2 Hebert, L. E., Weuve, J., Scherr, P. A. & Evans, D. A. Alzheimer disease in the United States (2010–2050) estimated using the 2010 census. *Neurology* **80**, 1778-1783 (2013).
- 3 Hardy, J. & Selkoe, D. J. The Amyloid Hypothesis of Alzheimer's Disease: Progress and Problems on the Road to Therapeutics. *Science* **297**, 353-356 (2002).
- 4 Karch, C. M., Cruchaga, C. & Goate, A. M. Alzheimer's disease genetics: from the bench to the clinic. *Neuron* **83**, 11-26, doi:10.1016/j.neuron.2014.05.041 (2014).
- 5 Musiek, E. S. & Holtzman, D. M. Three dimensions of the amyloid hypothesis: time, space and 'wingmen'. *Nat Neurosci* **18**, 800-806, doi:10.1038/nn.4018 (2015).
- 6 Jack, C. R., Jr. *et al.* Introduction to the recommendations from the National Institute on Aging-Alzheimer's Association workgroups on diagnostic guidelines for Alzheimer's disease. *Alzheimers Dement* **7**, 257-262, doi:10.1016/j.jalz.2011.03.004 (2011).
- 7 Nelson, P. T., Braak, H. & Markesbery, W. R. Neuropathology and cognitive impairment in Alzheimer disease: a complex but coherent relationship. *J Neuropathol Exp Neurol* **68**, 1-14, doi:10.1097/NEN.0b013e3181919a48 (2009).
- 8 Mintun, M. A. *et al.* [11C]PIB in a nondemented population: potential antecedent marker of Alzheimer disease. *Neurology* **67**, 446-452 (2006).
- 9 Cummings, J. L., Morstorf, T. & Zhong, K. Alzheimer's disease drug-development pipeline: few candidates, frequent failures. *Alzheimer's Research & Therapy* **6** (2014).
- 10 Lawson, L. J., Perry, V. H. & Gordon, S. Turnover of resident microglia in the normal adult mouse brain. *Neuroscience* **48**, 405-415 (1992).
- 11 Hanisch, U. K. & Kettenmann, H. Microglia: active sensor and versatile effector cells in the normal and pathologic brain. *Nat Neurosci* **10**, 1387-1394, doi:10.1038/nn1997 (2007).
- 12 Graeber, M. B. & Streit, W. J. Microglia: biology and pathology. *Acta Neuropathol* **119**, 89-105, doi:10.1007/s00401-009-0622-0 (2010).
- 13 Streit, W. J., Sammons, N. W., Kuhns, A. J. & Sparks, D. L. Dystrophic microglia in the aging human brain. *Glia* **45**, 208-212, doi:10.1002/glia.10319 (2004).
- 14 Akiyama, H. *et al.* Inflammation and Alzheimer's disease. *Neurobiol Aging* **21**, 383-421 (2000).
- 15 Hoarau, J. J. *et al.* Activation and control of CNS innate immune responses in health and diseases: a balancing act finely tuned by neuroimmune regulators (NIReg). *CNS Neurol Disord Drug Targets* **10**, 25-43 (2011).
- 16 Polazzi, E. & Monti, B. Microglia and neuroprotection: from in vitro studies to therapeutic applications. *Prog Neurobiol* **92**, 293-315, doi:10.1016/j.pneurobio.2010.06.009 (2010).

- 17 Perry, V. H., Nicoll, J. A. R. & Holmes, C. Microglia in neurodegenerative disease. *Nature Reviews Neurology* **6**, 193–201 (2010).
- 18 Nimmerjahn, A., Kirchhoff, F. & F., H. Resting Microglial Cells Are Highly Dynamic Surveillants of Brain Parenchyma in Vivo. *Science* **308**, 1314-1318 (2005).
- 19 Town, T., Nikolic, V. & Tan, J. The microglial "activation" continuum: from innate to adaptive responses. *Journal of neuroinflammation* **2**, 24, doi:10.1186/1742-2094-2-24 (2005).
- 20 Paolicelli, R. C. *et al.* Synaptic Pruning by Microglia Is Necessary for Normal Brain Development. *Science* **333**, 1456-1458 (2011).
- 21 Sierra, A. *et al.* Microglia shape adult hippocampal neurogenesis through apoptosis-coupled phagocytosis. *Cell Stem Cell* **7**, 483-495, doi:10.1016/j.stem.2010.08.014 (2010).
- 22 Tremblay, M. E., Lowery, R. L. & Majewska, A. K. Microglial interactions with synapses are modulated by visual experience. *PLoS Biol* **8**, e1000527, doi:10.1371/journal.pbio.1000527 (2010).
- 23 Wake, H., Moorhouse, A. J., Jinno, S., Kohsaka, S. & Nabekura, J. Resting microglia directly monitor the functional state of synapses in vivo and determine the fate of ischemic terminals. *J Neurosci* **29**, 3974-3980, doi:10.1523/JNEUROSCI.4363-08.2009 (2009).
- 24 Stevens, B. *et al.* The classical complement cascade mediates CNS synapse elimination. *Cell* **131**, 1164-1178, doi:10.1016/j.cell.2007.10.036 (2007).
- 25 Gordon, S. & Taylor, P. R. Monocyte and macrophage heterogeneity. *Nat Rev Immunol* **5**, 953-964, doi:10.1038/nri1733 (2005).
- 26 Varol, C., Mildner, A. & Jung, S. Macrophages: development and tissue specialization. *Annu Rev Immunol* **33**, 643-675, doi:10.1146/annurev-immunol-032414-112220 (2015).
- 27 Lemke, G. & Rothlin, C. V. Immunobiology of the TAM receptors. *Nat Rev Immunol* **8**, 327-336, doi:10.1038/nri2303 (2008).
- 28 Nimmerjahn, F. & Ravetch, J. V. Fcγ receptors as regulators of immune responses. *Nat Rev Immunol* **8**, 34-47, doi:10.1038/nri2206 (2008).
- 29 Ricklin, D., Hajishengallis, G., Yang, K. & Lambris, J. D. Complement: a key system for immune surveillance and homeostasis. *Nat Immunol* **11**, 785-797, doi:10.1038/ni.1923 (2010).
- 30 Flynn, G., Maru, S., Loughlin, J., Romero, I. A. & Male, D. Regulation of chemokine receptor expression in human microglia and astrocytes. *Journal of Neuroimmunology* **136**, 84-93, doi:10.1016/s0165-5728(03)00009-2 (2003).
- 31 Blinzinger, K. & Kreutzberg, G. Displacement of synaptic terminals from regenerating motoneurons by microglial cells. *Zeitschrift fur Zellforschung und mikroskopische Anatomie* **85**, 145-157 (1968).
- 32 Sipe, G. O. *et al.* Microglial P2Y<sub>12</sub> is necessary for synaptic plasticity in mouse visual cortex. *Nat Commun* **7**, 10905, doi:10.1038/ncomms10905 (2016).
- 33 Ji, K., Akgul, G., Wollmuth, L. P. & Tsirka, S. E. Microglia Actively Regulate the Number of Functional Synapses. *PLoS One* **8** (2013).

- 34 Schafer, D. P. *et al.* Microglia sculpt postnatal neural circuits in an activity and complement-dependent manner. *Neuron* **74**, 691-705, doi:10.1016/j.neuron.2012.03.026 (2012).
- 35 Rice, R. A. *et al.* Elimination of Microglia Improves Functional Outcomes Following Extensive Neuronal Loss in the Hippocampus. *J Neurosci* **35**, 9977-9989, doi:10.1523/JNEUROSCI.0336-15.2015 (2015).
- 36 Rice, R. A. *et al.* Microglial repopulation resolves inflammation and promotes brain recovery after injury. *Glia* **65**, 931-944 (2017).
- 37 Malik, M. *et al.* Genetics ignite focus on microglial inflammation in Alzheimer's disease. *Mol Neurodegener* **10**, 52, doi:10.1186/s13024-015-0048-1 (2015).
- 38 Tosto, G. & Reitz, C. Genome-wide association studies in Alzheimer's disease: a review. *Curr Neurol Neurosci Rep* **13**, 381, doi:10.1007/s11910-013-0381-0 (2013).
- 39 Huang, K. L. *et al.* A common haplotype lowers PU.1 expression in myeloid cells and delays onset of Alzheimer's disease. *Nat Neurosci* **20**, 1052-1061, doi:10.1038/nn.4587 (2017).
- 40 Griciuc, A. *et al.* Alzheimer's disease risk gene CD33 inhibits microglial uptake of amyloid beta. *Neuron* **78**, 631-643, doi:10.1016/j.neuron.2013.04.014 (2013).
- 41 Sakae, N. *et al.* ABCA7 Deficiency Accelerates Amyloid-beta Generation and Alzheimer's Neuronal Pathology. *J Neurosci* **36**, 3848-3859, doi:10.1523/JNEUROSCI.3757-15.2016 (2016).
- 42 Satoh, K., Abe-Dohmae, S., Yokoyama, S., St George-Hyslop, P. & Fraser, P. E. ATP-binding cassette transporter A7 (ABCA7) loss of function alters Alzheimer amyloid processing. *J Biol Chem* **290**, 24152-24165, doi:10.1074/jbc.M115.655076 (2015).
- 43 Wang, Y. *et al.* TREM2 lipid sensing sustains the microglial response in an Alzheimer's disease model. *Cell* **160**, 1061-1071, doi:10.1016/j.cell.2015.01.049 (2015).
- 44 Jay, T. R. *et al.* TREM2 deficiency eliminates TREM2+ inflammatory macrophages and ameliorates pathology in Alzheimer's disease mouse models. *The Journal of experimental medicine* **212**, 287-295, doi:10.1084/jem.20142322 (2015).
- 45 Jay, T. R. *et al.* Disease progression-dependent effects of TREM2 deficiency in a mouse model of Alzheimer's disease. doi:10.1523/JNEUROSCI.2110-16.2016 (2016).
- 46 Heneka, M. T. *et al.* Focal glial activation coincides with increased BACE1 activation and precedes amyloid plaque deposition in APP[V717I] transgenic mice. *Journal of neuroinflammation* **2**, 22, doi:10.1186/1742-2094-2-22 (2005).
- 47 Wright, A. L. *et al.* Neuroinflammation and neuronal loss precede Abeta plaque deposition in the hAPP-J20 mouse model of Alzheimer's disease. *PLoS One* **8**, e59586, doi:10.1371/journal.pone.0059586 (2013).
- 48 Ferretti, M. T., Bruno, M. A., Ducatenzeiler, A., Klein, W. L. & Cuello, A. C. Intracellular A $\beta$ -oligomers and early inflammation in a model of Alzheimer's disease. *Neurobiol Aging* **33**, 1329-1342 (2012).

- 49 Krstic, D. *et al.* Systemic immune challenges trigger and drive Alzheimer-like neuropathology in mice. *Journal of neuroinflammation* **2**, 151, doi:10.1186/1742-2094-9-151 (2012).
- 50 Venegas, C. *et al.* Microglia-derived ASC specks cross-seed amyloid- $\beta$  in Alzheimer's disease. *Nature* **552**, 355-361, doi:10.1038/nature25158 (2017).
- 51 Hamelin, L. *et al.* Early and protective microglial activation in Alzheimer's disease: a prospective study using 18F-DPA-714 PET imaging. *Brain : a journal of neurology* **139**, 1252-1264, doi:10.1093/brain/aww017 (2016).
- 52 Xanthos, D. N. & Sandkuhler, J. Neurogenic neuroinflammation: inflammatory CNS reactions in response to neuronal activity. *Nat Rev Neurosci* **15**, 43-53, doi:10.1038/nrn3617 (2014).
- 53 Maderna, P. & Godson, C. Phagocytosis of apoptotic cells and the resolution of inflammation. *Biochimica et Biophysica Acta (BBA) - Molecular Basis of Disease* **1639**, 141-151, doi:10.1016/j.bbadis.2003.09.004 (2003).
- 54 Shastri, A., Bonifati, D. M. & Kishore, U. Innate immunity and neuroinflammation. *Mediators Inflamm* **2013**, 342931, doi:10.1155/2013/342931 (2013).
- 55 Skaper, S. D., Facci, L., Zusso, M. & Giusti, P. An Inflammation-Centric View of Neurological Disease: Beyond the Neuron. *Front Cell Neurosci* **12**, 72, doi:10.3389/fncel.2018.00072 (2018).
- 56 Ransohoff, R. M. & Perry, V. H. Microglial physiology: unique stimuli, specialized responses. *Annu Rev Immunol* **27**, 119-145, doi:10.1146/annurev.immunol.021908.132528 (2009).
- 57 Glass, C. K., Saijo, K., Winner, B., Marchetto, M. C. & Gage, F. H. Mechanisms underlying inflammation in neurodegeneration. *Cell* **140**, 918-934, doi:10.1016/j.cell.2010.02.016 (2010).
- 58 Paresce, D. M., Ghosh, R. N. & Maxfield, F. R. Microglial Cells Internalize Aggregates of the Alzheimer's Disease Amyloid-B Protein Via a Scavenger Receptor. *Neuron* **17**, 553-565 (1996).
- 59 Stewart, C. R. *et al.* CD36 ligands promote sterile inflammation through assembly of a Toll-like receptor 4 and 6 heterodimer. *Nat Immunol* **11**, 155-161, doi:10.1038/ni.1836 (2010).
- 60 Liu, Y. *et al.* LPS receptor (CD14): a receptor for phagocytosis of Alzheimer's amyloid peptide. *Brain : a journal of neurology* **128**, 1778-1789, doi:10.1093/brain/awh531 (2005).
- 61 Garg, A. D. *et al.* Immunogenic cell death, DAMPs and anticancer therapeutics: an emerging amalgamation. *Biochim Biophys Acta* **1805**, 53-71, doi:10.1016/j.bbcan.2009.08.003 (2010).
- 62 Krysko, D. V. *et al.* Emerging role of damage-associated molecular patterns derived from mitochondria in inflammation. *Trends Immunol* **32**, 157-164, doi:10.1016/j.it.2011.01.005 (2011).
- 63 Lull, M. E. & Block, M. L. Microglial activation and chronic neurodegeneration. *Neurotherapeutics* **7**, 354-365, doi:10.1016/j.nurt.2010.05.014 (2010).
- 64 Liddel, S. A. *et al.* Neurotoxic reactive astrocytes are induced by activated microglia. *Nature* **541**, 481-487, doi:10.1038/nature21029 (2017).

- 65 Heneka, M. T. *et al.* NLRP3 is activated in Alzheimer's disease and contributes to pathology in APP/PS1 mice. *Nature* **493**, 674-678, doi:10.1038/nature11729 (2013).
- 66 Gustin, A. *et al.* NLRP3 Inflammasome Is Expressed and Functional in Mouse Brain Microglia but Not in Astrocytes. *PLoS One* **10**, e0130624, doi:10.1371/journal.pone.0130624 (2015).
- 67 Eikelenboom, P. *et al.* The significance of neuroinflammation in understanding Alzheimer's disease. *J Neural Transm (Vienna)* **113**, 1685-1695, doi:10.1007/s00702-006-0575-6 (2006).
- 68 Heneka, M. T., Kummer, M. P. & Latz, E. Innate immune activation in neurodegenerative disease. *Nat Rev Immunol* **14**, 463-477, doi:10.1038/nri3705 (2014).
- 69 Ingelsson, M. *et al.* Early A $\beta$  accumulation and progressive synaptic loss, gliosis, and tangle formation in AD brain. *Neurology* **62**, 925-931 (2004).
- 70 Sarlus, H. & Heneka, M. T. Microglia in Alzheimer's disease. *The Journal of clinical investigation* **127**, 3240-3249, doi:10.1172/JCI90606 (2017).
- 71 Morris, G. L., Clark, I. A. & Vissel, B. Inconsistencies and Controversies Surrounding the Amyloid Hypothesis of Alzheimer's Disease. *Acta Neuropathologica Communications* **2** (2014).
- 72 Ries, M. & Sastre, M. Mechanisms of Abeta Clearance and Degradation by Glial Cells. *Front Aging Neurosci* **8**, 160, doi:10.3389/fnagi.2016.00160 (2016).
- 73 Farris, W. *et al.* Insulin-degrading enzyme regulates the levels of insulin, amyloid beta-protein, and the beta-amyloid precursor protein intracellular domain in vivo. *Proc Natl Acad Sci U S A* **100**, 4162-4167, doi:10.1073/pnas.0230450100 (2003).
- 74 Bernstein, H. G. *et al.* Regional and cellular distribution patterns of insulin-degrading enzyme in the adult human brain and pituitary. *J Chem Neuroanat* **35**, 216-224, doi:10.1016/j.jchemneu.2007.12.001 (2008).
- 75 Halle, A. *et al.* The NALP3 inflammasome is involved in the innate immune response to amyloid-beta. *Nat Immunol* **9**, 857-865, doi:10.1038/ni.1636 (2008).
- 76 Rock, K. L. *et al.* Inhibitors of the Proteasome Block the Degradation of Most Cell Proteins and the Generation of Peptides Presented on MHC Class I Molecules. *Cell* **78**, 761-771 (1994).
- 77 Zhao, X. & Yang, J. Amyloid-beta peptide is a substrate of the human 20S proteasome. *ACS Chem Neurosci* **1**, 655-660, doi:10.1021/cn100067e (2010).
- 78 Caccamo, A., Majumder, S., Richardson, A., Strong, R. & Oddo, S. Molecular interplay between mammalian target of rapamycin (mTOR), amyloid-beta, and Tau: effects on cognitive impairments. *J Biol Chem* **285**, 13107-13120, doi:10.1074/jbc.M110.100420 (2010).
- 79 Corder, E. H. *et al.* Gene Dose of Apolipoprotein E Type 4 Allele and the Risk for Alzheimer's Disease in Late Onset Families. *Science* **261**, 921-923, doi:10.1126/science.8346443 (1993).
- 80 Uchihara, T. *et al.* ApoE immunoreactivity and microglial cells in Alzheimer's disease brain. *Neurosci Lett* **195**, 5-8 (1995).

- 81 Butovsky, O. *et al.* Targeting miR-155 restores abnormal microglia and attenuates disease in SOD1 mice. *Ann Neurol* **77**, 75-99, doi:10.1002/ana.24304 (2015).
- 82 Parhizkar, S. *et al.* Loss of TREM2 function increases amyloid seeding but reduces plaque-associated ApoE. *Nat Neurosci*, doi:10.1038/s41593-018-0296-9 (2019).
- 83 Keren-Shaul, H. *et al.* A Unique Microglia Type Associated with Restricting Development of Alzheimer's Disease. *Cell* **169**, 1276-1290 e1217, doi:10.1016/j.cell.2017.05.018 (2017).
- 84 Wildsmith, K. R., Holley, M., Savage, J. C., Skerrett, R. & Landreth, G. E. Evidence for impaired amyloid  $\beta$  clearance in Alzheimer's disease. *Alzheimer's Research & Therapy* **5** (2013).
- 85 Mandrekar, S. *et al.* Microglia mediate the clearance of soluble A $\beta$  through fluid phase macropinocytosis. *J Neurosci* **29**, 4252-4262, doi:10.1523/JNEUROSCI.5572-08.2009 (2009).
- 86 Lee, C. Y. & Landreth, G. E. The role of microglia in amyloid clearance from the AD brain. *J Neural Transm (Vienna)* **117**, 949-960, doi:10.1007/s00702-010-0433-4 (2010).
- 87 El Khoury, J. B. *et al.* CD36 mediates the innate host response to beta-amyloid. *The Journal of experimental medicine* **197**, 1657-1666, doi:10.1084/jem.20021546 (2003).
- 88 Tahara, K. *et al.* Role of toll-like receptor signalling in A $\beta$  uptake and clearance. *Brain : a journal of neurology* **129**, 3006-3019 (2006).
- 89 Jones, R. S., Minogue, A. M., Connor, T. J. & Lynch, M. A. Amyloid-beta-induced astrocytic phagocytosis is mediated by CD36, CD47 and RAGE. *J Neuroimmune Pharmacol* **8**, 301-311, doi:10.1007/s11481-012-9427-3 (2013).
- 90 Wilcock, D. M. *et al.* Passive amyloid immunotherapy clears amyloid and transiently activates microglia in a transgenic mouse model of amyloid deposition. *J Neurosci* **24**, 6144-6151, doi:10.1523/JNEUROSCI.1090-04.2004 (2004).
- 91 Wang, Y. *et al.* TREM2-mediated early microglial response limits diffusion and toxicity of amyloid plaques. *The Journal of experimental medicine* **213**, 667-675, doi:10.1084/jem.20151948 (2016).
- 92 Yang, L. *et al.* LRP1 modulates the microglial immune response via regulation of JNK and NF-kappaB signaling pathways. *Journal of neuroinflammation* **13**, 304, doi:10.1186/s12974-016-0772-7 (2016).
- 93 Pan, X. D. *et al.* Microglial phagocytosis induced by fibrillar  $\beta$ -amyloid is attenuated by oligomeric  $\beta$ -amyloid: implications for Alzheimer's disease. *Mol Neurodegener* **6**, 45, doi:10.1186/1750-1326-6-45 (2011).
- 94 Hellwig, S. *et al.* Forebrain microglia from wild-type but not adult 5xFAD mice prevent amyloid-beta plaque formation in organotypic hippocampal slice cultures. *Sci Rep* **5**, 14624, doi:10.1038/srep14624 (2015).
- 95 Koenigsnecht-Talboo, J. & Landreth, G. E. Microglial phagocytosis induced by fibrillar beta-amyloid and IgGs are differentially regulated by proinflammatory cytokines. *The Journal of neuroscience : the official journal of the Society for Neuroscience* **25**, 8240-8249, doi:10.1523/JNEUROSCI.1808-05.2005 (2005).

- 96 Li, R. *et al.* Estrogen enhances uptake of amyloid beta-protein by microglia derived from the human cortex. *J Neurochem* **75**, 1447-1454 (2000).
- 97 Paresce, D. M., Chung, H. & Maxfield, F. R. Slow Degradation of Aggregates of the Alzheimer's Disease Amyloid b-Protein by Microglial Cells. *J Biol Chem* **272**, 29390-29397 (1997).
- 98 Webster, S. D. *et al.* Complement component C1q modulates the phagocytosis of A $\beta$  by microglia. *Exp Neurol* **161**, 127-138, doi:10.1006/exnr.1999.7260 (2000).
- 99 Bolmont, T. *et al.* Dynamics of the microglial/amyloid interaction indicate a role in plaque maintenance. *J Neurosci* **28**, 4283-4292, doi:10.1523/JNEUROSCI.4814-07.2008 (2008).
- 100 Meyer-Luehmann, M. *et al.* Rapid appearance and local toxicity of amyloid-beta plaques in a mouse model of Alzheimer's disease. *Nature* **451**, 720-724, doi:10.1038/nature06616 (2008).
- 101 Stalder, M., Deller, T., Staufenbiel, M. & Jucker, M. 3D-Reconstruction of microglia and amyloid in APP23 transgenic mice: no evidence of intracellular amyloid. *Neurobiol Aging* **22**, 427-434 (2001).
- 102 Claassen, I., Van Rooijen, N. & Claassen, E. A new method for removal of mononuclear phagocytes from heterogeneous cell populations in vitro, using the liposome-mediated macrophage 'suicide' technique. *J Immunol Methods* **134**, 153-161 (1990).
- 103 Gowing, G., Vallieres, L. & Julien, J. P. Mouse model for ablation of proliferating microglia in acute CNS injuries. *Glia* **53**, 331-337, doi:10.1002/glia.20288 (2006).
- 104 Grathwohl, S. A. *et al.* Formation and maintenance of Alzheimer's disease beta-amyloid plaques in the absence of microglia. *Nature neuroscience* **12**, 1361-1363, doi:10.1038/nn.2432 (2009).
- 105 Chakrabarty, P. *et al.* IL-10 alters immunoproteostasis in APP mice, increasing plaque burden and worsening cognitive behavior. *Neuron* **85**, 519-533, doi:10.1016/j.neuron.2014.11.020 (2015).
- 106 Johansson, J. U. *et al.* Prostaglandin signaling suppresses beneficial microglial function in Alzheimer's disease models. *The Journal of clinical investigation* **125**, 350-364, doi:10.1172/JCI77487 (2015).
- 107 Kan, M. J. *et al.* Arginine deprivation and immune suppression in a mouse model of Alzheimer's disease. *J Neurosci* **35**, 5969-5982, doi:10.1523/JNEUROSCI.4668-14.2015 (2015).
- 108 DiCarlo, G., Wilcock, D., Henderson, D., Gordon, M. & Morgan, D. Intrahippocampal LPS injections reduce A $\beta$  load in APP+PS1 transgenic mice. *Neurobiol Aging* **22**, 1007-1012 (2001).
- 109 Shaftel, S. S. *et al.* Sustained hippocampal IL-1 beta overexpression mediates chronic neuroinflammation and ameliorates Alzheimer plaque pathology. *The Journal of clinical investigation* **117**, 1595-1604, doi:10.1172/JCI31450 (2007).
- 110 Fu, A. K. *et al.* IL-33 ameliorates Alzheimer's disease-like pathology and cognitive decline. *Proc Natl Acad Sci U S A*, doi:10.1073/pnas.1604032113 (2016).
- 111 Cramer, P. E. *et al.* ApoE-Directed Therapeutics Rapidly Clear  $\beta$ -Amyloid and Reverse Deficits in AD Mouse Models. *Science* **335**, 1503-1506 (2012).

- 112 Iaccarino, H. F. *et al.* Gamma frequency entrainment attenuates amyloid load  
and modifies microglia. *Nature* **540**, 230-235, doi:10.1038/nature20587 (2016).
- 113 Leinenga, G. & Götz, J. Scanning ultrasound removes amyloid- $\beta$  and restores  
memory in an Alzheimer's disease mouse model. *Science translational medicine*  
**7** (2015).
- 114 Martorell, A. J. *et al.* Multi-sensory Gamma Stimulation Ameliorates Alzheimer's-  
Associated Pathology and Improves Cognition. *Cell* **177**, 256-271 e222,  
doi:10.1016/j.cell.2019.02.014 (2019).
- 115 Jankowsky, J. L. *et al.* Persistent amyloidosis following suppression of Abeta  
production in a transgenic model of Alzheimer disease. *PLoS medicine* **2**, e355,  
doi:10.1371/journal.pmed.0020355 (2005).
- 116 Yuan, P. *et al.* TREM2 Haplodeficiency in Mice and Humans Impairs the  
Microglia Barrier Function Leading to Decreased Amyloid Compaction and  
Severe Axonal Dystrophy. *Neuron* **90**, 724-739,  
doi:10.1016/j.neuron.2016.05.003 (2016).
- 117 Condello, C., Yuan, P., Schain, A. & Grutzendler, J. Microglia constitute a barrier  
that prevents neurotoxic protofibrillar A $\beta$ 42 hotspots around plaques. *Nat*  
*Commun* **6**, 6176, doi:10.1038/ncomms7176 (2015).
- 118 Ulrich, J. D. *et al.* ApoE facilitates the microglial response to amyloid plaque  
pathology. *The Journal of experimental medicine* **215**, 1047-1058,  
doi:10.1084/jem.20171265 (2018).
- 119 Krasemann, S. *et al.* The TREM2-APOE Pathway Drives the Transcriptional  
Phenotype of Dysfunctional Microglia in Neurodegenerative Diseases. *Immunity*  
**47**, 566-581 e569, doi:10.1016/j.immuni.2017.08.008 (2017).
- 120 Bruttger, J. *et al.* Genetic Cell Ablation Reveals Clusters of Local Self-Renewing  
Microglia in the Mammalian Central Nervous System. *Immunity* **43**, 92-106,  
doi:10.1016/j.immuni.2015.06.012 (2015).
- 121 Faustino, J. V. *et al.* Microglial cells contribute to endogenous brain defenses  
after acute neonatal focal stroke. *J Neurosci* **31**, 12992-13001,  
doi:10.1523/JNEUROSCI.2102-11.2011 (2011).
- 122 Dai, X. M. *et al.* Targeted disruption of the mouse colony-stimulating factor 1  
receptor gene results in osteopetrosis, mononuclear phagocyte deficiency,  
increased primitive progenitor cell frequencies, and reproductive defects. *Blood*  
**99**, 111-120 (2002).
- 123 Erlich, B., Zhu, L., Etgen, A. M., Dobrenis, K. & Pollard, J. W. Absence of colony  
stimulation factor-1 receptor results in loss of microglia, disrupted brain  
development and olfactory deficits. *PLoS One* **6**, e26317,  
doi:10.1371/journal.pone.0026317 (2011).
- 124 Ginhoux, F. *et al.* Fate Mapping Analysis Reveals That Adult Microglia Derive  
from Primitive Macrophages. *Science* **330**, 841-845 (2010).
- 125 Wang, Y. *et al.* IL-34 is a tissue-restricted ligand of CSF1R required for the  
development of Langerhans cells and microglia. *Nat Immunol* **13**, 753-760,  
doi:10.1038/ni.2360 (2012).
- 126 Luo, J. *et al.* Colony-stimulating factor 1 receptor (CSF1R) signaling in injured  
neurons facilitates protection and survival. *The Journal of experimental medicine*  
**210**, 157-172, doi:10.1084/jem.20120412 (2013).

- 127 Cecchini, M. G. *et al.* Role of colony stimulating factor-1 in the establishment and regulation of tissue macrophages during postnatal development of the mouse. *Development (Cambridge, England)* **120**, 1357-1372 (1994).
- 128 Jenkins, S. J. *et al.* IL-4 directly signals tissue-resident macrophages to proliferate beyond homeostatic levels controlled by CSF-1. *The Journal of experimental medicine* **210**, 2477-2491, doi:10.1084/jem.20121999 (2013).
- 129 Wegiel, J. *et al.* Reduced number and altered morphology of microglial cells in colony stimulating factor-1-deficient osteopetrotic op/op mice. *Brain Res* **804**, 135-139 (1998).
- 130 Konno, T. *et al.* Clinical and genetic characterization of adult-onset leukoencephalopathy with axonal spheroids and pigmented glia associated with CSF1R mutation. *Eur J Neurol* **24**, 37-45, doi:10.1111/ene.13125 (2017).
- 131 Pridans, C., Sauter, K. A., Baer, K., Kissel, H. & Hume, D. A. CSF1R mutations in hereditary diffuse leukoencephalopathy with spheroids are loss of function. *Sci Rep* **3**, 3013, doi:10.1038/srep03013 (2013).
- 132 Spangenberg, E. E. *et al.* Eliminating microglia in Alzheimer's mice prevents neuronal loss without modulating amyloid-beta pathology. *Brain : a journal of neurology* **139**, 1265-1281, doi:10.1093/brain/aww016 (2016).
- 133 Elmore, M. R. *et al.* Colony-stimulating factor 1 receptor signaling is necessary for microglia viability, unmasking a microglia progenitor cell in the adult brain. *Neuron* **82**, 380-397, doi:10.1016/j.neuron.2014.02.040 (2014).
- 134 Valdearcos, M. *et al.* Microglia dictate the impact of saturated fat consumption on hypothalamic inflammation and neuronal function. *Cell reports* **9**, 2124-2138, doi:10.1016/j.celrep.2014.11.018 (2014).
- 135 Klein, D. *et al.* Targeting the colony stimulating factor 1 receptor alleviates two forms of Charcot-Marie-Tooth disease in mice. *Brain : a journal of neurology* **138**, 3193-3205, doi:10.1093/brain/awv240 (2015).
- 136 Schreiner, B. *et al.* Astrocyte Depletion Impairs Redox Homeostasis and Triggers Neuronal Loss in the Adult CNS. *Cell reports* **12**, 1377-1384, doi:10.1016/j.celrep.2015.07.051 (2015).
- 137 Asai, H. *et al.* Depletion of microglia and inhibition of exosome synthesis halt tau propagation. *Nat Neurosci* **18**, 1584-1593, doi:10.1038/nn.4132 (2015).
- 138 De, I. *et al.* CSF1 overexpression has pleiotropic effects on microglia in vivo. *Glia* **62**, 1955-1967, doi:10.1002/glia.22717 (2014).
- 139 Dagher, N. N. *et al.* Colony-stimulating factor 1 receptor inhibition prevents microglial plaque association and improves cognition in 3xTg-AD mice. *Journal of neuroinflammation* **12**, 139, doi:10.1186/s12974-015-0366-9 (2015).
- 140 Fillit, H. *et al.* Elevated circulating tumor necrosis factor levels in Alzheimer's disease. *Neurosci Lett* **129**, 318-320 (1991).
- 141 Ishizuka, K. *et al.* Identification of monocyte chemoattractant protein-1 in senile plaques and reactive microglia of Alzheimer's disease. *Psychiatry Clin Neurosci* **51**, 135-138 (1997).
- 142 McGeer, E. G. & McGeer, P. L. Brain inflammation in Alzheimer disease and the therapeutic implications. *Curr Pharm Des* **5**, 821-836 (1999).
- 143 Dandrea, M. R., Reiser, P. A., Gumula, N. A., Hertzog, B. M. & Andrade-Gordon, P. Application of triple immunohistochemistry to characterize amyloid plaque-

- associated inflammation in brains with Alzheimer's disease. *Biotech Histochem* **76**, 97-106 (2001).
- 144 Cagnin, A. *et al.* In-vivo measurement of activated microglia in dementia. *Lancet* **358**, 461-467, doi:10.1016/S0140-6736(01)05625-2 (2001).
- 145 Kitazawa, M., Oddo, S., Yamasaki, T. R., Green, K. N. & LaFerla, F. M. Lipopolysaccharide-induced inflammation exacerbates tau pathology by a cyclin-dependent kinase 5-mediated pathway in a transgenic model of Alzheimer's disease. *J Neurosci* **25**, 8843-8853, doi:10.1523/JNEUROSCI.2868-05.2005 (2005).
- 146 Rozemuller, J. M., Eikelenboom, P. & Stam, F. C. Role of microglia in plaque formation in senile dementia of the Alzheimer type. An immunohistochemical study. *Virchows Arch B Cell Pathol Incl Mol Pathol* **51**, 247-254 (1986).
- 147 Dickson, D. W. *et al.* Alzheimer's disease. A double-labeling immunohistochemical study of senile plaques. *Am J Pathol* **132**, 86-101 (1988).
- 148 Mattiace, L. A., Davies, P., Yen, S. H. & Dickson, D. W. Microglia in cerebellar plaques in Alzheimer's disease. *Acta Neuropathol* **80**, 493-498 (1990).
- 149 Akiyama, H. *et al.* Cell mediators of inflammation in the Alzheimer disease brain. *Alzheimer disease and associated disorders* **14 Suppl 1**, S47-53 (2000).
- 150 Meda, L. *et al.* Activation of microglial cells by beta-amyloid protein and interferon-gamma. *Nature* **374**, 647-650, doi:10.1038/374647a0 (1995).
- 151 Akama, K. T. & Van Eldik, L. J. Beta-amyloid stimulation of inducible nitric-oxide synthase in astrocytes is interleukin-1beta- and tumor necrosis factor-alpha (TNFalpha)-dependent, and involves a TNFalpha receptor-associated factor- and NFkappaB-inducing kinase-dependent signaling mechanism. *J Biol Chem* **275**, 7918-7924 (2000).
- 152 Cacquevel, M., Lebourrier, N., Cheenne, S. & Vivien, D. Cytokines in neuroinflammation and Alzheimer's disease. *Curr Drug Targets* **5**, 529-534 (2004).
- 153 Centonze, D. *et al.* Inflammation triggers synaptic alteration and degeneration in experimental autoimmune encephalomyelitis. *The Journal of neuroscience : the official journal of the Society for Neuroscience* **29**, 3442-3452, doi:10.1523/JNEUROSCI.5804-08.2009 (2009).
- 154 Hauss-Wegrzyniak, B., Lynch, M. A., Vraniak, P. D. & Wenk, G. L. Chronic brain inflammation results in cell loss in the entorhinal cortex and impaired LTP in perforant path-granule cell synapses. *Exp Neurol* **176**, 336-341 (2002).
- 155 Ziehn, M. O., Avedisian, A. A., Tiwari-Woodruff, S. & Voskuhl, R. R. Hippocampal CA1 atrophy and synaptic loss during experimental autoimmune encephalomyelitis, EAE. *Lab Invest* **90**, 774-786, doi:10.1038/labinvest.2010.6 (2010).
- 156 Kitazawa, M. *et al.* Blocking IL-1 signaling rescues cognition, attenuates tau pathology, and restores neuronal beta-catenin pathway function in an Alzheimer's disease model. *Journal of immunology* **187**, 6539-6549, doi:10.4049/jimmunol.1100620 (2011).
- 157 Spires-Jones, T. L. *et al.* Impaired spine stability underlies plaque-related spine loss in an Alzheimer's disease mouse model. *Am J Pathol* **171**, 1304-1311, doi:10.2353/ajpath.2007.070055 (2007).

- 158 Dong, H., Martin, M. V., Chambers, S. & Csernansky, J. G. Spatial relationship between synapse loss and beta-amyloid deposition in Tg2576 mice. *The Journal of comparative neurology* **500**, 311-321, doi:10.1002/cne.21176 (2007).
- 159 Grutzendler, J. & Gan, W. B. Long-term two-photon transcranial imaging of synaptic structures in the living brain. *CSH protocols* **2007**, pdb prot4766, doi:10.1101/pdb.prot4766 (2007).
- 160 Scheff, S. W., Price, D. A., Schmitt, F. A. & Mufson, E. J. Hippocampal synaptic loss in early Alzheimer's disease and mild cognitive impairment. *Neurobiol Aging* **27**, 1372-1384, doi:10.1016/j.neurobiolaging.2005.09.012 (2006).
- 161 Robinson, J. L. *et al.* Perforant path synaptic loss correlates with cognitive impairment and Alzheimer's disease in the oldest-old. *Brain : a journal of neurology*, doi:10.1093/brain/awu190 (2014).
- 162 Medway, C. & Morgan, K. Review: The genetics of Alzheimer's disease; putting flesh on the bones. *Neuropathology and applied neurobiology* **40**, 97-105, doi:10.1111/nan.12101 (2014).
- 163 Srivatsan, S., Swiecki, M., Otero, K., Cella, M. & Shaw, A. S. CD2-associated protein regulates plasmacytoid dendritic cell migration, but is dispensable for their development and cytokine production. *Journal of immunology* **191**, 5933-5940, doi:10.4049/jimmunol.1300454 (2013).
- 164 Bradshaw, E. M. *et al.* CD33 Alzheimer's disease locus: altered monocyte function and amyloid biology. *Nat Neurosci* **16**, 848-850, doi:10.1038/nn.3435 (2013).
- 165 Butovsky, O. *et al.* Identification of a unique TGF-beta-dependent molecular and functional signature in microglia. *Nat Neurosci* **17**, 131-143, doi:10.1038/nn.3599 (2014).
- 166 Crehan, H., Hardy, J. & Pocock, J. Blockage of CR1 prevents activation of rodent microglia. *Neurobiology of disease* **54**, 139-149, doi:10.1016/j.nbd.2013.02.003 (2013).
- 167 Ando, K. *et al.* Clathrin adaptor CALM/PICALM is associated with neurofibrillary tangles and is cleaved in Alzheimer's brains. *Acta Neuropathol* **125**, 861-878, doi:10.1007/s00401-013-1111-z (2013).
- 168 Kim, W. S. *et al.* Deletion of Abca7 increases cerebral amyloid-beta accumulation in the J20 mouse model of Alzheimer's disease. *J Neurosci* **33**, 4387-4394, doi:10.1523/JNEUROSCI.4165-12.2013 (2013).
- 169 Guerreiro, R. *et al.* TREM2 variants in Alzheimer's disease. *The New England journal of medicine* **368**, 117-127, doi:10.1056/NEJMoa1211851 (2013).
- 170 Xu, Q., Li, Y., Cyrus, C., Sanan, D. A. & Cordell, B. Isolation and characterization of apolipoproteins from murine microglia. Identification of a low density lipoprotein-like apolipoprotein J-rich but E-poor spherical particle. *J Biol Chem* **275**, 31770-31777, doi:10.1074/jbc.M002796200 (2000).
- 171 Mok, S. *et al.* Inhibition of CSF1 Receptor Improves the Anti-tumor Efficacy of Adoptive Cell Transfer Immunotherapy. *Cancer research*, doi:10.1158/0008-5472.CAN-13-1816 (2013).
- 172 Kim, T. S. *et al.* Increased KIT inhibition enhances therapeutic efficacy in gastrointestinal stromal tumor. *Clin Cancer Res* **20**, 2350-2362, doi:10.1158/1078-0432.CCR-13-3033 (2014).

- 173 Chitu, V. *et al.* PSTPIP2 deficiency in mice causes osteopenia and increased differentiation of multipotent myeloid precursors into osteoclasts. *Blood* **120**, 3126-3135, doi:10.1182/blood-2012-04-425595 (2012).
- 174 Oakley, H. *et al.* Intraneuronal beta-amyloid aggregates, neurodegeneration, and neuron loss in transgenic mice with five familial Alzheimer's disease mutations: potential factors in amyloid plaque formation. *J Neurosci* **26**, 10129-10140, doi:10.1523/JNEUROSCI.1202-06.2006 (2006).
- 175 Buskila, Y., Crowe, S. E. & Ellis-Davies, G. C. Synaptic deficits in layer 5 neurons precede overt structural decay in 5xFAD mice. *Neuroscience* **254**, 152-159, doi:10.1016/j.neuroscience.2013.09.016 (2013).
- 176 Eimer, W. A. & Vassar, R. Neuron loss in the 5XFAD mouse model of Alzheimer's disease correlates with intraneuronal Abeta42 accumulation and Caspase-3 activation. *Mol Neurodegener* **8**, 2, doi:10.1186/1750-1326-8-2 (2013).
- 177 Jawhar, S., Trawicka, A., Jenneckens, C., Bayer, T. A. & Wirths, O. Motor deficits, neuron loss, and reduced anxiety coinciding with axonal degeneration and intraneuronal Abeta aggregation in the 5XFAD mouse model of Alzheimer's disease. *Neurobiol Aging* **33**, 196 e129-140, doi:10.1016/j.neurobiolaging.2010.05.027 (2012).
- 178 Crowe, S. E. & Ellis-Davies, G. C. Spine pruning in 5xFAD mice starts on basal dendrites of layer 5 pyramidal neurons. *Brain structure & function* **219**, 571-580, doi:10.1007/s00429-013-0518-6 (2014).
- 179 Rodriguez-Ortiz, C. J. *et al.* Neuronal-specific overexpression of a mutant valosin-containing protein associated with IBMPFD promotes aberrant ubiquitin and TDP-43 accumulation and cognitive dysfunction in transgenic mice. *Am J Pathol* **183**, 504-515, doi:10.1016/j.ajpath.2013.04.014 (2013).
- 180 Neely, K. M., Green, K. N. & LaFerla, F. M. Presenilin is necessary for efficient proteolysis through the autophagy-lysosome system in a gamma-secretase-independent manner. *J Neurosci* **31**, 2781-2791, doi:10.1523/JNEUROSCI.5156-10.2010 (2011).
- 181 Rice, R. A., Berchtold, N. C., Cotman, C. W. & Green, K. N. Age-related downregulation of the CaV3.1 T-type calcium channel as a mediator of amyloid beta production. *Neurobiol Aging* **35**, 1002-1011, doi:10.1016/j.neurobiolaging.2013.10.090 (2014).
- 182 Peters, A. & Kaiserman-Abramof, I. R. The small pyramidal neuron of the rat cerebral cortex. The perikaryon, dendrites and spines. *The American journal of anatomy* **127**, 321-355, doi:10.1002/aja.1001270402 (1970).
- 183 Myczek, K., Yeung, S. T., Castello, N., Baglietto-Vargas, D. & LaFerla, F. M. Hippocampal adaptive response following extensive neuronal loss in an inducible transgenic mouse model. *PLoS One* **9**, e106009, doi:10.1371/journal.pone.0106009 (2014).
- 184 Elmore, M. R., Lee, R. J., West, B. L. & Green, K. N. Characterizing Newly Repopulated Microglia in the Adult Mouse: Impacts on Animal Behavior, Cell Morphology, and Neuroinflammation. *PLoS One* **10**, doi:10.1371/journal.pone.0122912 (2015).

- 185 Naj, A. C. *et al.* Common variants at MS4A4/MS4A6E, CD2AP, CD33 and  
EPHA1 are associated with late-onset Alzheimer's disease. *Nature genetics* **43**,  
436-441, doi:10.1038/ng.801 (2011).
- 186 Chapuis, J. *et al.* Increased expression of BIN1 mediates Alzheimer genetic risk  
by modulating tau pathology. *Molecular psychiatry*, doi:10.1038/mp.2013.1  
(2013).
- 187 Seshadri, S. *et al.* Genome-wide analysis of genetic loci associated with  
Alzheimer disease. *JAMA : the journal of the American Medical Association* **303**,  
1832-1840, doi:10.1001/jama.2010.574 (2010).
- 188 Lambert, J. C. *et al.* Genome-wide association study identifies variants at CLU  
and CR1 associated with Alzheimer's disease. *Nature genetics* **41**, 1094-1099,  
doi:10.1038/ng.439 (2009).
- 189 Coniglio, S. J. *et al.* Microglial stimulation of glioblastoma invasion involves  
epidermal growth factor receptor (EGFR) and colony stimulating factor 1 receptor  
(CSF-1R) signaling. *Molecular medicine* **18**, 519-527,  
doi:10.2119/molmed.2011.00217 (2012).
- 190 Guillot-Sestier, M. V. *et al.* IL10 deficiency rebalances innate immunity to mitigate  
Alzheimer-like pathology. *Neuron* **85**, 534-548, doi:10.1016/j.neuron.2014.12.068  
(2015).
- 191 Boissonneault, V. *et al.* Powerful beneficial effects of macrophage colony-  
stimulating factor on beta-amyloid deposition and cognitive impairment in  
Alzheimer's disease. *Brain : a journal of neurology* **132**, 1078-1092,  
doi:10.1093/brain/awn331 (2009).
- 192 Leinenga, G. & Gotz, J. Scanning ultrasound removes amyloid-beta and restores  
memory in an Alzheimer's disease mouse model. *Science translational medicine*  
**7**, 278ra233, doi:10.1126/scitranslmed.aaa2512 (2015).
- 193 Gabbita, S. P. *et al.* Early intervention with a small molecule inhibitor for tumor  
necrosis factor-alpha prevents cognitive deficits in a triple transgenic mouse  
model of Alzheimer's disease. *Journal of neuroinflammation* **9**, 99,  
doi:10.1186/1742-2094-9-99 (2012).
- 194 Kiyota, T. *et al.* CNS expression of anti-inflammatory cytokine interleukin-4  
attenuates Alzheimer's disease-like pathogenesis in APP+PS1 bigenic mice.  
*FASEB journal : official publication of the Federation of American Societies for  
Experimental Biology* **24**, 3093-3102, doi:10.1096/fj.10-155317 (2010).
- 195 Parachikova, A., Vasilevko, V., Cribbs, D. H., LaFerla, F. M. & Green, K. N.  
Reductions in amyloid-beta-derived neuroinflammation, with minocycline, restore  
cognition but do not significantly affect tau hyperphosphorylation. *J Alzheimers  
Dis* **21**, 527-542, doi:10.3233/JAD-2010-100204 (2010).
- 196 Yamanaka, M. *et al.* PPARgamma/RXRalpha-induced and CD36-mediated  
microglial amyloid-beta phagocytosis results in cognitive improvement in amyloid  
precursor protein/presenilin 1 mice. *J Neurosci* **32**, 17321-17331,  
doi:10.1523/JNEUROSCI.1569-12.2012 (2012).
- 197 Costello, D. A., Carney, D. G. & Lynch, M. A. alpha-TLR2 antibody attenuates  
the Abeta-mediated inflammatory response in microglia through enhanced  
expression of SIGIRR. *Brain, behavior, and immunity* **46**, 70-79,  
doi:10.1016/j.bbi.2015.01.005 (2015).

- 198 Fuhrmann, M. *et al.* Microglial Cx3cr1 knockout prevents neuron loss in a mouse model of Alzheimer's disease. *Nat Neurosci* **13**, 411-413, doi:10.1038/nn.2511 (2010).
- 199 Jack, C. R., Jr. *et al.* Tracking pathophysiological processes in Alzheimer's disease: an updated hypothetical model of dynamic biomarkers. *Lancet Neurol* **12**, 207-216, doi:10.1016/S1474-4422(12)70291-0 (2013).
- 200 Hardy, J. The amyloid hypothesis for Alzheimer's disease: a critical reappraisal. *J Neurochem* **110**, 1129-1134, doi:10.1111/j.1471-4159.2009.06181.x (2009).
- 201 Karch, C. M. & Goate, A. M. Alzheimer's disease risk genes and mechanisms of disease pathogenesis. *Biol Psychiatry* **77**, 43-51, doi:10.1016/j.biopsych.2014.05.006 (2015).
- 202 Huang, K.-I. *et al.* A common haplotype lowers SPI1 (PU.1) expression in myeloid cells and delays age at onset for Alzheimer's disease. *bioRxiv*, doi:10.1101/110957 (2017).
- 203 Jiang, Q. *et al.* ApoE promotes the proteolytic degradation of Abeta. *Neuron* **58**, 681-693, doi:10.1016/j.neuron.2008.04.010 (2008).
- 204 Hickman, S. E., Allison, E. K. & El Khoury, J. Microglial dysfunction and defective beta-amyloid clearance pathways in aging Alzheimer's disease mice. *The Journal of neuroscience : the official journal of the Society for Neuroscience* **28**, 8354-8360, doi:10.1523/JNEUROSCI.0616-08.2008 (2008).
- 205 Daria, A. *et al.* Young microglia restore amyloid plaque clearance of aged microglia. *EMBO J*, doi:10.15252/embj.201694591 (2016).
- 206 Grathwohl, S. A. *et al.* Formation and maintenance of Alzheimer's disease beta-amyloid plaques in the absence of microglia. *Nature neuroscience* **12**, 1361-1363, doi:10.1038/nn.2432 (2009).
- 207 Tap, W. D. *et al.* Structure-Guided Blockade of CSF1R Kinase in Tenosynovial Giant-Cell Tumor. *The New England journal of medicine* **373**, 428-437, doi:10.1056/NEJMoa1411366 (2015).
- 208 Oddo, S. *et al.* Triple-Transgenic Model of Alzheimer's Disease with Plaques and Tangles. *Neuron* **39**, 409-421, doi:10.1016/s0896-6273(03)00434-3 (2003).
- 209 Green, K. N., Khashwji, H., Estrada, T. & Laferla, F. M. ST101 induces a novel 17 kDa APP cleavage that precludes Abeta generation in vivo. *Ann Neurol* **69**, 831-844, doi:10.1002/ana.22325 (2011).
- 210 Dobin, A. *et al.* STAR: ultrafast universal RNA-seq aligner. *Bioinformatics* **29**, 15-21, doi:10.1093/bioinformatics/bts635 (2013).
- 211 Liao, Y., Smyth, G. K. & Shi, W. The Subread aligner: fast, accurate and scalable read mapping by seed-and-vote. *Nucleic Acids Res* **41**, e108, doi:10.1093/nar/gkt214 (2013).
- 212 R Core Team. *R: A Language and Environment for Statistical Computing*, <Available online at <http://www.R-project.org/>> (2017).
- 213 Robinson, M. D., McCarthy, D. J. & Smyth, G. K. edgeR: a Bioconductor package for differential expression analysis of digital gene expression data. *Bioinformatics* **26**, 139-140, doi:10.1093/bioinformatics/btp616 (2010).
- 214 Ritchie, M. E. *et al.* limma powers differential expression analyses for RNA-sequencing and microarray studies. *Nucleic Acids Res* **43**, e47, doi:10.1093/nar/gkv007 (2015).

- 215 Olmos-Alonso, A. *et al.* Pharmacological targeting of CSF1R inhibits microglial proliferation and prevents the progression of Alzheimer's-like pathology. *Brain : a journal of neurology* **139**, 891-907, doi:10.1093/brain/awv379 (2016).
- 216 Su, Y. & Chang, P. Acidic pH promotes the formation of toxic fibrils from b-amyloid peptide. *Brain Research* **893**, 287 (2001).
- 217 Tseng, B. P. *et al.* Deposition of Monomeric, Not Oligomeric, A $\beta$  Mediates Growth of Alzheimer's Disease Amyloid Plaques in Human Brain Preparations. *Biochemistry* **38**, 10424 (1999).
- 218 Hu, X. *et al.* Amyloid seeds formed by cellular uptake, concentration, and aggregation of the amyloid-beta peptide. *Proc Natl Acad Sci U S A* **106**, 20324-20329, doi:10.1073/pnas.0911281106 (2009).
- 219 Sole-Domenech, S., Cruz, D. L., Capetillo-Zarate, E. & Maxfield, F. R. The endocytic pathway in microglia during health, aging and Alzheimer's disease. *Ageing Res Rev*, doi:10.1016/j.arr.2016.07.002 (2016).
- 220 Kaye, R. *et al.* Fibril specific, conformation dependent antibodies recognize a generic epitope common to amyloid fibrils and fibrillar oligomers that is absent in prefibrillar oligomers. *Mol Neurodegener* **2**, 18, doi:10.1186/1750-1326-2-18 (2007).
- 221 Kaye, R. *et al.* Common structure of soluble amyloid oligomers implies common mechanism of pathogenesis. *Science* **300**, 486-489, doi:10.1126/science.1079469 (2003).
- 222 Harigaya, Y. *et al.* Amyloid beta protein starting pyroglutamate at position 3 is a major component of the amyloid deposits in the Alzheimer's disease brain. *Biochem Biophys Res Commun* **276**, 422-427, doi:10.1006/bbrc.2000.3490 (2000).
- 223 Cummings, B. J. *et al.* Aggregation of the amyloid precursor protein within degenerating neurons and dystrophic neurites in Alzheimer's disease. *Neuroscience* **48**, 763-777 (1992).
- 224 Gowrishankar, S. *et al.* Massive accumulation of luminal protease-deficient axonal lysosomes at Alzheimer's disease amyloid plaques. *Proc Natl Acad Sci U S A* **112**, E3699-3708 (2015).
- 225 Huynh, T. V. *et al.* Age-Dependent Effects of apoE Reduction Using Antisense Oligonucleotides in a Model of beta-amyloidosis. *Neuron* **96**, 1013-1023 e1014, doi:10.1016/j.neuron.2017.11.014 (2017).
- 226 Condello, C., Yuan, P., Schain, A. & Grutzendler, J. Microglia constitute a barrier that prevents neurotoxic protofibrillar Abeta42 hotspots around plaques. *Nature communications* **6**, 6176, doi:10.1038/ncomms7176 (2015).
- 227 Najafi, A. R. *et al.* A limited capacity for microglial repopulation in the adult brain. *Glia*, doi:10.1002/glia.23477 (2018).
- 228 Elmore, M. R. P. *et al.* Replacement of microglia in the aged brain reverses cognitive, synaptic, and neuronal deficits in mice. *Ageing Cell*, e12832, doi:10.1111/ace1.12832 (2018).
- 229 Bateman, R. J. *et al.* Autosomal-dominant Alzheimer's disease: a review and proposal for the prevention of Alzheimer's disease. *Alzheimers Res Ther* **3**, 1, doi:10.1186/alzrt59 (2011).

- 230 Morris, J. C. *et al.* Pittsburgh compound B imaging and prediction of progression from cognitive normality to symptomatic Alzheimer disease. *Arch Neurol* **66**, 1469-1475, doi:10.1001/archneurol.2009.269 (2009).
- 231 Vlassenko, A. G., Benzinger, T. L. & Morris, J. C. PET amyloid-beta imaging in preclinical Alzheimer's disease. *Biochim Biophys Acta* **1822**, 370-379, doi:10.1016/j.bbadis.2011.11.005 (2012).
- 232 Vlassenko, A. G. *et al.* Imaging and cerebrospinal fluid biomarkers in early preclinical Alzheimer disease. *Ann Neurol* **80**, 379-387, doi:10.1002/ana.24719 (2016).
- 233 Hong, S. *et al.* Complement and microglia mediate early synapse loss in Alzheimer mouse models. *Science* (2016).
- 234 Park, J. *et al.* A 3D human triculture system modeling neurodegeneration and neuroinflammation in Alzheimer's disease. *Nature neuroscience* **21**, 941-951, doi:10.1038/s41593-018-0175-4 (2018).
- 235 Giraldo, M. *et al.* Variants in triggering receptor expressed on myeloid cells 2 are associated with both behavioral variant frontotemporal lobar degeneration and Alzheimer's disease. *Neurobiol Aging* **34**, 2077.e2011-2078, doi:10.1016/j.neurobiolaging.2013.02.016 (2013).
- 236 Gonzalez Murcia, J. D. *et al.* Assessment of TREM2 rs75932628 association with Alzheimer's disease in a population-based sample: the Cache County Study. *Neurobiol Aging* **34**, 2889.e2811-2883, doi:10.1016/j.neurobiolaging.2013.06.004 (2013).
- 237 Roussos, P. *et al.* The triggering receptor expressed on myeloid cells 2 (TREM2) is associated with enhanced inflammation, neuropathological lesions and increased risk for Alzheimer's dementia. *Alzheimers Dement* **11**, 1163-1170, doi:10.1016/j.jalz.2014.10.013 (2015).
- 238 Ulrich, J. D. *et al.* Altered microglial response to A $\beta$  plaques in APPPS1-21 mice heterozygous for TREM2. *Mol Neurodegener* **9**, 20, doi:10.1186/1750-1326-9-20 (2014).
- 239 Baik, S. H., Kang, S., Son, S. M. & Mook-Jung, I. Microglia contributes to plaque growth by cell death due to uptake of amyloid beta in the brain of Alzheimer's disease mouse model. *Glia* **64**, 2274-2290, doi:10.1002/glia.23074 (2016).
- 240 Chung, H., Brazil, M. I., Soe, T. T. & Maxfield, F. R. Uptake, degradation, and release of fibrillar and soluble forms of Alzheimer's amyloid beta-peptide by microglial cells. *J Biol Chem* **274**, 32301-32308 (1999).
- 241 Liu, C. C. *et al.* ApoE4 Accelerates Early Seeding of Amyloid Pathology. *Neuron* **96**, 1024-1032 e1023, doi:10.1016/j.neuron.2017.11.013 (2017).
- 242 Liao, F. *et al.* Murine versus human apolipoprotein E4: differential facilitation of and co-localization in cerebral amyloid angiopathy and amyloid plaques in APP transgenic mouse models. *Acta Neuropathol Commun* **3**, 70, doi:10.1186/s40478-015-0250-y (2015).
- 243 Bales, K. R. *et al.* Apolipoprotein E is essential for amyloid deposition in the APP(V717F) transgenic mouse model of Alzheimer's disease. *Proc Natl Acad Sci U S A* **96**, 15233-15238 (1999).
- 244 Fryer, J. D. *et al.* Human apolipoprotein E4 alters the amyloid-beta 40:42 ratio and promotes the formation of cerebral amyloid angiopathy in an amyloid

- precursor protein transgenic model. *J Neurosci* **25**, 2803-2810, doi:10.1523/JNEUROSCI.5170-04.2005 (2005).
- 245 Duering, M., Grimm, M. O., Grimm, H. S., Schroder, J. & Hartmann, T. Mean age of onset in familial Alzheimer's disease is determined by amyloid beta 42. *Neurobiol Aging* **26**, 785-788, doi:10.1016/j.neurobiolaging.2004.08.002 (2005).
- 246 Kim, J. *et al.* Abeta40 inhibits amyloid deposition in vivo. *J Neurosci* **27**, 627-633, doi:10.1523/JNEUROSCI.4849-06.2007 (2007).
- 247 Sevigny, J. *et al.* The antibody aducanumab reduces Abeta plaques in Alzheimer's disease. *Nature* **537**, 50-56, doi:10.1038/nature19323 (2016).
- 248 Boche, D. *et al.* Consequence of Abeta immunization on the vasculature of human Alzheimer's disease brain. *Brain : a journal of neurology* **131**, 3299-3310, doi:10.1093/brain/awn261 (2008).
- 249 Pfeifer, M. *et al.* Cerebral hemorrhage after passive anti-Abeta immunotherapy. *Science* **298**, 1379, doi:10.1126/science.1078259 (2002).
- 250 Fryer, J. D. *et al.* Apolipoprotein E markedly facilitates age-dependent cerebral amyloid angiopathy and spontaneous hemorrhage in amyloid precursor protein transgenic mice. *J Neurosci* **23**, 7889-7896 (2003).
- 251 Kim, J. *et al.* Haploinsufficiency of human APOE reduces amyloid deposition in a mouse model of amyloid-beta amyloidosis. *J Neurosci* **31**, 18007-18012, doi:10.1523/JNEUROSCI.3773-11.2011 (2011).
- 252 Oddo, S., Caccamo, A., Cheng, D. & LaFerla, F. M. Genetically altering Abeta distribution from the brain to the vasculature ameliorates tau pathology. *Brain pathology (Zurich, Switzerland)* **19**, 421-430, doi:10.1111/j.1750-3639.2008.00194.x (2009).
- 253 Bales, K. R. *et al.* Lack of apolipoprotein E dramatically reduces amyloid  $\beta$ -peptide deposition. *Nature genetics* **17**, 263-264, doi:doi:10.1038/ng1197-263 (1997).
- 254 Boyles, J. K., Pitas, R. E., Wilson, E., Mahley, R. W. & Taylor, J. M. Apolipoprotein E associated with astrocytic glia of the central nervous system and with nonmyelinating glia of the peripheral nervous system. *The Journal of clinical investigation* **76**, 1501-1513, doi:10.1172/jci112130 (1985).
- 255 Chiu, I. M. *et al.* A neurodegeneration-specific gene-expression signature of acutely isolated microglia from an amyotrophic lateral sclerosis mouse model. *Cell reports* **4**, 385-401, doi:10.1016/j.celrep.2013.06.018 (2013).
- 256 Yeh, F. L., Wang, Y., Tom, I., Gonzalez, L. C. & Sheng, M. TREM2 Binds to Apolipoproteins, Including APOE and CLU/APOJ, and Thereby Facilitates Uptake of Amyloid-Beta by Microglia. *Neuron* **91**, 328-340, doi:10.1016/j.neuron.2016.06.015 (2016).